UCSF
UC San Francisco Electronic Theses and Dissertations

Title
Targeting Ras in Cancer: Mutation-Specific Dependencies in Oncogenic Signaling

Permalink
https://escholarship.org/uc/item/5wd3q3kr

Author
Pitt, Cameron L.W.

Publication Date
2015

Peer reviewed|Thesis/dissertation

eScholarship.org Powered by the California Digital Library
University of California

TARGETING RAS IN CANCER: MUTATION-SPECIFIC DEPENDENCIES IN ONCOGENIC SIGNALING

by

Cameron Pitt

DISSERTATION

Submitted in partial satisfaction of the requirements for the degree of

DOCTOR OF PHILOSOPHY

in

Biomedical Sciences

in the

GRADUATE DIVISION

of the

UNIVERSITY OF CALIFORNIA, SAN FRANCISCO

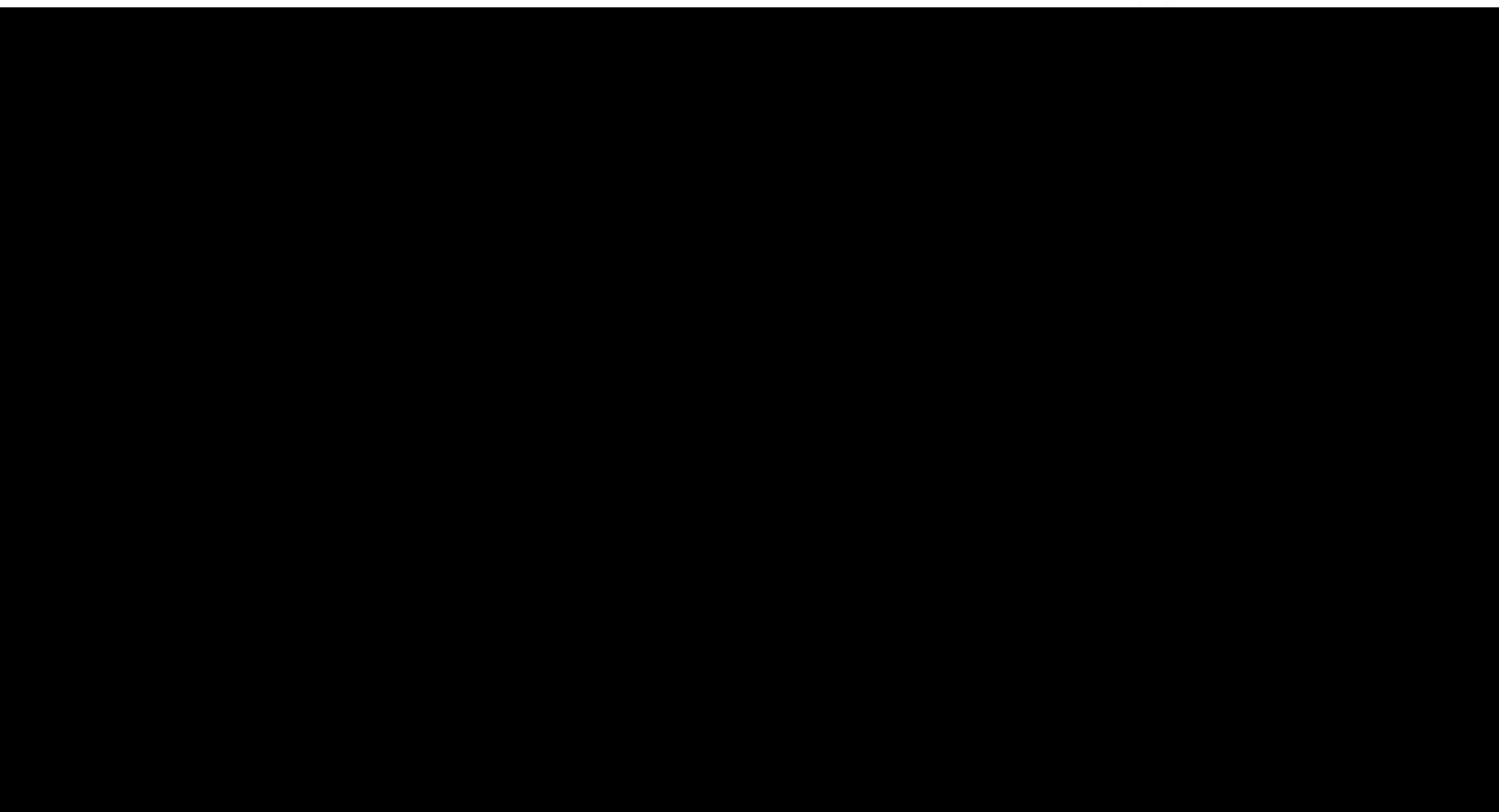

Copyright 2015 by

Cameron Pitt

ACKNOWLEDGEMENTS

I would not have been able to produce this body of work and achieve this point in my scientific career without the support of many people. I will not list them all here but I fully acknowledge that every step that I take forward is an opportunity to pay honor to the many who endured greater struggles to pave a way before me. I can only hope to do justice to all of those who have put me on their back. My successes are a constant reminder of my duty to lift someone else as I continue forward. I am truly indebted for this one.

DECLARATION

The studies described in this dissertation were performed under the supervision of Dr. Frank McCormick at the Helen Diller Family Comprehensive Cancer Center at the University of California, San Francisco, from April 2011 to May 2015. This work was supported in part by the National Science Foundation Graduate Research Fellowship Program, NSF Grant No. 1144247. Also thanks to financial support from the UCSF Discovery Fellows Program.

Chapters one, four and five contain portions of material that I contributed to the following articles:

Pitt C, Afghani S, Bindu L, Alexander P, Stephen AG, McCormick F. Oncogenic KRAS mutants retain dependence on nucleotide exchange and link EGFR-PLC positive feedback signaling to MAPK activation. In submission.

Nan X, Meyer T, Collison EA, Lin LJ, Pitt C, Galeas J, Lewis S, Gray JW, McCormick F, Chu S. Ras-GTP Dimers Activate the Mitogen-Activated Protein Kinase (MAPK) Pathway. In submission.

ABSTRACT

Ras mutations drive approximately one third of human cancers by aberrant regulation of the mitogen-activated protein kinase (MAPK) signaling cascade and other effector pathways. While oncogenic Ras mutations are commonly viewed as sufficient for constitutive GTP-loading, it is unclear whether these mutant forms display differences in reliance on upstream and downstream growth signals for activity. Use of mouse embryonic fibroblasts (MEFs) devoid of the H-, N- and KRAS alleles, and rescued by single Ras isoforms, has provided a model for comparison of the requirements for growth factor signaling amongst oncogenic Ras mutants. In MEFs expressing KRAS G12C, G12V or G12D, growth factors increase GTP loading, in a Sos-dependent manner. In contrast, Q61L and Q61R mutants show little, if any, increase in GTP-loading. These differences reflect differences in intrinsic GTPase rates. Growth factors activate phospholipase C (PLC) in addition to SOS, resulting in PKC activation and mobilization of calcium. PKC increases GTP-loading on G12 mutant KRAS proteins through SOS1 and activates MAPK signaling downstream from Ras. However, different KRAS mutants vary dramatically in their requirement for PLC signaling to activate the MAPK pathway. Downstream of PLC, the calcium-regulated chloride channel TMEM16A (ANO1) completes an autocrine EGFR feedback loop that modulates the MAPK response to calcium flux in a KRAS mutation-dependent manner. The discovery that specific Ras mutants may be more susceptible to EGFR and PLC inhibition or downstream modulation of calcium signaling may provide a potent therapeutic strategy for certain Ras-driven cancers.

CONTENTS

Title.....i

Acknowledgements.....iii

Declaration.....iv

Abstract.....v

Contents.....vi

List of Tables.....ix

List of Figures.....x

CHAPTER 1: INTRODUCTION.....1

1.1 RAS ONCOGENES IN CANCER.....2

1.2 RAS PROCESSING AND LOCALIZATION.....4

1.3 INTRACTIONS BETWEEN WILD TYPE AND ONCOGENIC RAS SIGNALING.....5

1.4 DIFFERENTIAL SIGNALING BETWEEN ONCOGENIC RAS VARIANTS.....6

1.5 EGFR AND GROWTH FACTOR SIGNALING.....7

1.6 MAPK PATHWAY SIGNALING DOWNSTREAM OF EGFR AND RAS.....7

1.7 AIMS OF THIS STUDY.....8

CHAPTER 2. MATERIALS AND METHODS.....11

2.1 REAGENTS.....12

2.2 LENTIVIRAL VECTORS AND TRANSDUCTIONS.....12

2.3 ANTIBODIES.....13

2.4 CELL LINES AND CULTURE CONDITIONS.....13

2.5 NRAS PROTEIN PURIFICATION.....14

2.6 MASS SPECTROMETRY.....14

2.7 IN VITRO RAS PRENYLATION ASSAYS 15
2.8 PROTEIN CRYSTALIZATION SCREENING 15
2.9 TRANSFECTIONS 16
2.10 IMMUNOBLOT ANALYSIS 16
2.11 RAS ACTIVATION ASSAY 17
2.12 CELL PROLIFERATION ANALYSIS 17
2.13 QUANTITATIVE REAL TIME PCR 17
2.14 GENE EXPRESSION ANALYSIS 18
2.15 IMMUNOPRECIPITATION 18
2.16 SUPERRESOLUTION IMAGING AND DIMERIZATION ANALYSIS 19
2.17 MEASUREMENT OF GTP HYROLYSIS RATES 19

CHAPTER 3: DISRUPTING NRAS PRENYLATION USING CYSTEINE TETHERING 20

3.1 INTRODUCTION 21
3.2 RESULTS 22
3.2.i. Mass spectrometry (MS) screening detects tethering compound hits 22
3.2.ii. Farnesylation of the NRAS CAAX-box cysteine is blocked by a subset of MS hits 23
3.2.iii. Compounds display varied levels of cytotoxicity in a Ras-dependent MEF model 24
3.2.iv. Optimization and scale-up of 3E10 labeling of NRAS yields protein suitable for crystallization studies 25
3.3 DISCUSSION 26

CHAPTER 4: POTENTIAL MECHANISMS FOR WILD TYPE SUPPRESSION OF ONCOGENIC RAS SIGNALING……...34

4.1 INTRODUCTION 35
4.2 RESULTS 36
4.2.i. TIRF-PALM imaging of KRAS G12D plasma membrane organization in a Rasless

background..... 36
4.2.ii. Wild type KRAS displays a minor disruption of oncogenic KRAS clustering in the plasma membrane 37
4.2.iii. Comparison of wild type to oncogenic (G12V) expression profiles across isoforms displays isoform-independent differences in gene regulation.....38
4.2.iv. Oncogenic allele-specific differential regulation of KRAS effector genes…….…50
4.3 DISCUSSION 51

CHAPTER 5: ONCOGENIC KRAS MUTANTS RETAIN DEPENDENCE ON NUCLEOTIDE EXCHANGE AND LINK EGFR-PLC POSITIVE FEEDBACK SIGNALING TO MAPK ACTIVATION. 59

5.1 INTRODUCTION 60
5.2 RESULTS..... 62
5.2.i. Oncogenic KRAS mutants respond to growth factors…….... 62
5.2.ii. GTP-loading of mutant KRAS in response to receptor tyrosine kinase signaling is SOS1-mediated..... 65
5.2.iii. Phorbol esters increase MAPK output by activating GTP-loading on mutant KRAS and by downstream signaling 66
5.2.iv. KRAS 4B variants display a differential requirement for PLC in MAPK activation……...67
5.2.v. Requirement for PLC in phorbol ester-induced CRAF-MAPK signaling complexes differs between oncogenic KRAS mutants……..……..68
5.2.vi. Activation of PLC-responsive channel TMEM16A triggers MEK-ERK signaling in an EGFR-dependent manner……..……..69
5.3 DISCUSSION 71

BIBLIOGRAPHY……..87

LIST OF TABLES

Table 1.1 Ras isoform comparisons……2

Table 4.1 PI3K array gene table……39

Table 4.2 MAPK array gene table……44

LIST OF FIGURES

Figure 1.1. Diagram of modifications in the C-terminal hypervariable regions of the major Ras isoforms……10

Figure 3.1. Screening approach using compounds tethering the NRAS CAAX box……28

Figure 3.2. Inhibition of in vitro farnesylation by a subset of tethering compounds……...29

Figure 3.3. GGTase assays reveal lead compounds for stable NRAS CAAX targeting……...30

Figure 3.4. Initial testing of compounds in MEFs displays correlation with *in vitro* compound efficacy and low off-target toxicity……..31

Figure 3.5. Mass spectra of binding conditions for near 100% 3E10-labeling of NRAS……...32

Figure 3.6. $NRAS^{G12V,C181S}$-3E10 protein crystals……33

Figure 4.1. Proposed Ras dimerization model for MAPK signaling following Ras activation...52

Figure 4.2. Superresolution imaging comparison of KRAS G12D membrane organization and clustering in MEFs before and after loss of wild type alleles……53

Figure 4.3. Loss of wild type KRAS alleles affects stimulation-dependent signaling of KRAS G12D transgenic MEFs……..54

Figure 4.4. Stimulation-responsive expression changes of PI3K and MAPK pathway genes across Ras isoforms in wild type and oncogenic forms……..55

Figure 4.5. Oncogenic and wild type Ras produce significant differences in regulation of PI3K and MAPK pathway genes whether starved or stimulated……56

Figure 4.6. PI3K array genes showing over 2-fold differential expression between wild type and G12D or G12V KRAS4B MEFs……...57

Figure 4.7. MAPK array genes showing over 2-fold differential expression between wild type and G12D or G12V KRAS4B MEFs……58

Figure 5.1. Generating MEF lines for comparison of Ras variants without background……75

Figure 5.2. Comparing effects of EGFR-Ras signaling inhibitors by KRAS genotype……76

Figure 5.3. MEF lines display Ras-dependent EGFR-MAPK signaling responses……77

Figure 5.4. Oncogenic KRAS mutants display differences in their persisting dependency on EGFR signaling for GTP loading and MAPK signaling……78

Figure 5.5. GTP loading of oncogenic KRAS in response to growth factors is SOS1-mediated……79

Figure 5.6. Phorbol esters amplify MAPK signaling upstream and downstream of oncogenic KRAS……80

Figure 5.7. KRAS mutants display different levels of dependence on PLC signaling for MAPK output……81

Figure 5.8. KRAS mutants display different levels of dependence on PLC activity for MAPK output downstream of PKC signaling……82

Figure 5.9. Human PDAC cell lines display KRAS mutation status-dependent differences in MAPK sensitivity to PLC inhibition……83

Figure 5.10. Calcium-responsive TMEM16A activity connects the PLC response to EGFR-induced KRAS dependent MAPK signaling……84

Figure 5.11. Human cancer cell lines display a KRAS genotype-specific EGFR dependence in MAPK activation with increasing doses of TMEM16A activator……85

Figure 5.12. Positive feeback mechanism for oncogenic signaling……86

CHAPTER 1.

INTRODUCTION

1.1 RAS ONCOGENES IN CANCER

Though Ras has been recognized as a target in cancer for over 35 years, Ras-driven cancers remain among the most difficult to treat due to insensitivity to available targeted therapies in cancer signaling. Ras, encoded by the three major genes *KRAS, NRAS and HRAS*, has the highest frequency of mutation of any oncogene. Ras proteins are critical switches in mitogenic signaling[1]. When in the active GTP-bound state, Ras proteins bind signaling effectors at the plasma membrane, resulting in their activation[2-5]. Of the three major Ras isoforms, the *KRAS* gene is most commonly mutated, a tumor-driving event occurring in over 25% of human cancers[6, 7]. Specific distinctions between the Ras isoforms are cataloged in Table 1.1[8-30].

Table 1.1. Ras isoform comparisons

	KRas4A	KRas4B	HRas	NRas
Mutation frequency				
Lung	16%	16%	1%	1%
Small Intestine	18%	18%	0%	0%
Large Intenstine	35%	35%	0%	4%
Bladder/Urinary	5%	5%	10%	1%
Skin	2%	2%	7%	6%
Kidney	1%	1%	0%	1%
Prostate	8%	8%	6%	1%
Esophagus	3%	3%	1%	0%
Pancreas	58%	58%	0%	2%
Breast	2%	2%	1%	1%
Thyroid	2%	2%	4%	6%
Ovary	14%	14%	0%	2%
Hematopoietic	5%	5%	0%	11%
Expression in normal tissues	Highest in gut, lung, thymus Lowest in skin and skeletal muscle	Highest in gut, lung, thymus Lowest in skin and skeletal muscle	Highest in brain, muscle, skin Lowest in liver	Highest in testis and thymus

Post-transcriptional processing	Prenylation (FTase or GGTase) [C186] Proteolysis Carboxylmethylation Palmitoylation [C180] Depalmitoylation	Prenylation (FTase or GGTase) [C185] Proteolysis Carboxylmethylation	Prenylation (FTase only) [C186] Proteolysis Carboxylmethylation Palmitoylation [C181 and/or C184] Depalmitoylation	Prenylation (FTase or GGTase) [C186] Proteolysis Carboxylmethylation Palmitoylation [C181] Depalmitoylation
Modifications				
Phosphorylation	Not known	Phosphoyrlated by PKC at Ser181.	Not known	Not known
Acetylation	Not known	Acetylated at Lys104	Not known	Not known
Ubiquination	Monoubiquitinated at Lys147	Monoubiquitinated at Lys147	Diubiquitinated, site unknown	Diubiquitinated, site unknown
Primary subcellular localization sites	Endomembranes, Plasma Membrane	Plasma Membrane, Cytosol, Cytoskeletal Matrix	Endomembranes, Plasma Membrane	Endomembranes, Plasma Membrane, Mitochondria
Relative affinities and activity levels of GEFs:				
SOS (Plasma membrane and endosomes)	+	+	+++	++
Ras-GRP1 (Golgi)	Not Observed	Not Observed	+++	+++
Ras-GRP2	Not Observed	Not Observed	+++	+++
Ras-GRF1 (ER)	Not Observed	Not Observed	+++	Not observed
Ras-GRF2	+	+	+++	+
CAL_DAGII	=	=	=	=
CAL-DAGIII	+	+	+++	++

Activation and/or affinity levels	
+++	Highest
++	Moderate
+	Least
=	Equivalent

Activating mutations impair the small GTPases' ability to perform their role in hydrolyzing GTP and this loss of the brake causes the proteins to accumulate in the active signaling form. This impairment is fundamental for initiating and maintaining tumor progression. Despite extensive efforts, small molecules have not been identified which block effector binding or restore GTPase activating protein (GAP) sensitivity, though some have recently been found which block interaction of Ras with the guanine nucleotide exchange factor (GEF), SOS, which activates Ras at the plasma membrane[31]. Though proteins in the Ras family signal through the same effector molecules, each isoform displays unique preferential coupling to cancer types[32]. Due to their biochemical properties, it has proven extremely difficult to find small molecule therapeutics that target the function of these proteins directly[33]. Since membrane localization is required for the activation and downstream signaling of Ras proteins[34], this has been targeted as a potential method of inhibition in cancer. The membrane localization of Ras also provides an avenue for signaling diversity and selective inhibition, as the C-terminus, which interacts with the membrane, is the only site of significant sequence variability in the protein[Fig. 1.1].

1.2 RAS PROCESSING AND LOCALIZATION

The translation products of genes in the Ras family are cytosolic and subjected to at least three steps of post-translational modification that result in their membrane localization. The CAAX box, making up the last four amino acids of all Ras proteins, is irreversibly farnesylated by thioether linkage of a 15-carbon isoprenoid chain to the cysteine before proteolytic removal of the final three amino acids and carboxymethylation of the prenylcysteine at the endoplasmic reticulum (ER) and Golgi. NRAS, HRAS and splice-variant 4A of KRAS are subsequently modified by palmitoylation at proximal cysteines in the C-terminal for plasma membrane (PM) localization[11, 35] while the highly basic polylysine motif of KRAS4B contributes to its stability in the PM. Little is certain about the functional significance of the differences in hypervariable domain sequences

between the Ras isoforms. Palmitoylation and acetylation of NRAS, HRAS and KRAS4A cycles these isoforms between endomembranes and the plasma membrane[35]. Further, modifications at the two palmitoylation sites on HRAS display distinct consequences on trafficking and protein signaling[36]. KRAS4B may be phosphorylated by protein kinase C (PKC) at S181 in the polylysine motif to lessen the positive charge leading to dissociation and targeting to intracellular membranes[37]. Signaling output may vary significantly dependent on the membrane compartmentalization and spatial distribution of Ras[38]. Ras proteins are not solely present on the ER and Golgi membranes for processing but, the highest local concentration of active GTP bound HRAS and NRAS in cancer cells is detected on the Golgi[39]. This suggests that, at least in HRAS- and NRAS-driven malignancies, signaling for oncogenic transformation does not solely originate from the PM. Considering that activated KRAS is predominantly observed at the PM, this is likely one mechanism for differential signaling among Ras isoforms. The varied membrane distributions of the Ras isoforms around the cell yields differences in access to the “on” and “off” switches, GEFs and GAPs, as well as downstream effectors that may be concentrated in particular membrane compartments.

1.3 INTERACTIONS BETWEEN WILD TYPE AND ONCOGENIC RAS SIGNALING

Tumors driven by oncogenic Ras often show loss of heterozygosity, suggesting that the wild type allele may suppress optimal growth[40]. Accordingly, addition of wild-type Ras to oncogenic Ras-transformed cells in culture can suppress growth[41]. The strongest suppression phenotypes are elicited when wild type Ras is co-expressed with mutant Ras of the cognate isoform, while weaker suppressive effects are observed from alternative wild type Ras isoforms that are present[42]. Considering the potential for WT inhibition of oncogenic Ras signaling by dimerization, these findings support a preference for self-dimerization among molecules of the

same isoform. The weak suppression from wild type Ras of alternative isoforms to the one mutated is potentially due to mild competition for scaffolding or effector molecules.

1.4 DIFFERENTIAL SIGNALING BETWEEN ONCOGENIC RAS VARIANTS

KRAS is most frequently point mutated at glycine 12 of the P-loop, producing an amino acid switch to aspartic acid, valine, cysteine or other products in minor frequencies. Interestingly, particular mutations are linked to certain tissue types[43]. Similarly, mutation of *NRAS* or, more rarely, *HRAS* are also linked to tissue type, though mutation of the catalytic residue glutamine 61 is very common (62% of *NRAS*, 36% of *HRAS* and 2% of *KRAS* mutations) in these genes[43]. The majority of glutamine 61 mutations produce an amino acid switch to histidine, leucine or arginine[43]. The variation in distribution of missense mutations observed in each cancer type implies significant functional differences in the signaling outputs of Ras variants.

Although oncogenic Ras mutants have long been viewed as constitutively active, differences in stability of the mutants in the GTP-bound state are linked to differences in oncogenic potential and patient survival[44, 45]. Mechanistically, mutation at G12 blocks entry of the arginine finger of GTPase activating proteins (GAPs), rendering these Ras variants insensitive to GAP-mediated inactivation and left with varied residual intrinsic GTPase activity[28]. Mutation at Q61 disrupts the transition state for GTP hydrolysis producing a constant “on state” [46]. Though it has be thought that oncogenesis by either of these mechanisms nullifies the role of recruitment of Ras guanine-nucleotide exchange factors (GEFs) in growth factor-induced Ras activation, definitive investigation of residual and alternative effects of upstream signals on Ras mutant proteins has been obscured by the persistent activities of the remaining wild type allele and other Ras isoforms. Moreover, potential differences in oncogenic signaling between the various Ras mutants

may be hidden by secondary genetic alterations particular to the cell lines or tumor samples under comparison.

1.5 EGFR AND GROWTH FACTOR SIGNALING

The ERBB family of growth factor receptors plays a major role in normal cellular growth, while often implicated in cancer signaling and feedback mechanisms in drug resistance. In normal cell signaling, ERBB receptors are activated under the spatiotemporal control of growth factor ligands secreted by neighboring cells or released by autocrine shedding[47]. Signaling of these receptor tyrosine kinases (RTKs) is dysregulated by genetic mutation, amplification or autocrine overexpression observed in brain, breast, head and neck, colorectal and lung tumors[47, 48]. All mechanisms of RTK activation act by driving intracellular signal transduction independent of ligand input, though some mechanisms my allow for further hyperactivation with ligand binding.

The EGFR pathway is has been identified to play a critical role in support of other oncogenic drivers, gaining additional roles in resistance once downstream signaling is impaired by targeted inhibitors. This is particularly relevant in cancer types where KRAS is a common driver. Pancreatic and colorectal tumors driven by oncogenic KRAS have been shown to retain dependence on upstream RTK signals (e.g. EGFR) for positive feedback signaling and activation of phosphoinositide 3-kinase (PI3K) effectors[49]. These studies display the importance of recognizing the key roles of growth factor receptors in varied cancer contexts, even where ostensibly self-sufficient oncogenic players are activated.

1.6 MAPK PATHWAY SIGNALING DOWNSTREAM OF EGFR AND RAS

The mitogen-activated protein kinase (MAPK) pathway is an essential signaling cascade activated by the ERBB family of RTKs for cell growth and mobility[50]. These RTKs are connected

to the MAPK pathway through the membrane recruitment of guanine nucleotide exchange factors (GEFs) for Ras activation. The fundamental GEF in Ras activation, son of sevenless (SOS), is bound by Grb2 in the cytosol and brought to the phosphorylated intracellular residues of activated RTKs, stimulating the exchange of GDP for GTP on proximal Ras proteins[51]. Following Ras activation, A-, B- or the most common C-Raf (Raf1) is recruited to the plasma membrane where it can be activated by protein kinase C (PKC) or p21-activated kinase 1 (PAK1) through phosphorylation at S338 and by protein phosphatase 2A (PP2A)-mediated dephosphorylation[52]. Active Raf is able to phosphorylate MEK1/2 which then phosphorylates ERK1/2 to complete the signaling cascade. Once activated, pERK enters the nucleus to activate a transcription factor network that promotes cell cycle progression, survival and mobility. Sustained MAPK signaling is most often the cause of developmental disorders and cancer[53].

The major effector proteins bound by GTP-loaded Ras are Raf, PI3K and RalGDS. Though PI3K and RalGDS can be activated by Ras-independent mechanisms in growth factor signaling, Ras is required to couple upstream signals to Raf and downstream MAPK activation[54, 55]. Furthermore, it has been shown that only constitutive activation of Raf, MEK and ERK kinases downstream of Ras can bypass the requirement for Ras proteins in proliferative signaling[56]. As all evidence has indicated that the MAPK cascade is essential for the growth effects of Ras in cancer, we focused on this pathway to read out the differences in output between Ras variants.

1.7 AIMS OF THIS STUDY

In this study we focus on the most commonly mutated cancer drivers *KRAS* and *NRAS*. We demonstrate that these proteins are susceptible to specific targeting by their CAAX box cysteines for blockade of prenylation, the essential first step in localization for signaling. We provide evidence for another step in the membrane organization of KRAS, where monomeric

activation is insufficient for signaling. We closely analyze the requirements of particular mutant KRAS alleles and potential mechanisms by which wild type KRAS may suppress signaling.

Significant differences can be observed between KRAS mutants at the levels of nucleotide exchange and connection of CRAF activation to downstream MAPK components. Phospholipase C (PLC) upregulates MAPK signaling by generating diacylglycerol (DAG) and inositol trisphosphate (IP3), activating PKC and calcium signaling. MAPK output downstream of mutant KRAS proteins displays differences in sensitivity to perturbation of PLC signaling. Using the "Rasless" MEF model to probe for unique dependencies of KRAS variants, we display that upstream receptor tyrosine kinase (RTK) signaling and the requirement for a second signal following GTP loading of KRAS can be exploited to target MAPK hyperactivation in KRAS-driven cells characterized by particular mutation. Furthermore, PLC-Ca^{2+} signaling to ion channels potentiates the MAPK signal from KRAS variants in a differentially RTK-dependent manner.

Though the Ras pathway has been extensively studied, we have little insight into the distinct signaling differences generated by Ras mutations commonly observed in human oncogenesis. Without direct inhibitors, clinical blockade of Ras-driven cancers depends on the ability to identify druggable downstream effectors and mediators of their tumorigenic effects. *KRAS* is the most commonly activated oncogene in human tumors. We have found that the most common *KRAS* mutations do not abrogate the need for upstream growth factor signaling and nucleotide exchange in their activation. Additionally, we show that particular KRAS variants display a requirement for PLC signaling in generating MAPK signaling responses. These findings expose opportunities to exploit the particular dependencies of cancers characterized by a specific Ras mutation.

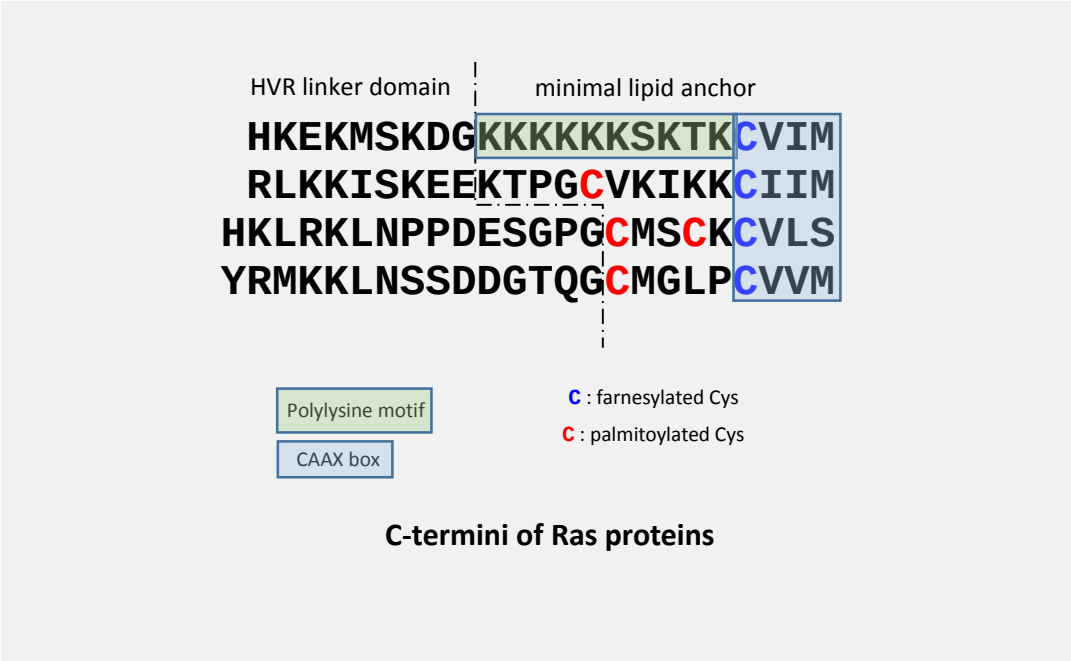

Figure 1.1. Diagram of modifications in the C-terminal hypervariable regions of the major Ras isoforms.

CHAPTER 2.

MATERIALS AND METHODS

2.1 REAGENTS

Epidermal growth factor (EGF) recombinant human protein and fibroblast growth factor (FGF)-basic recombinant mouse protein were from *Life Technologies* (Carlsbad, CA). IGF-1 was from *Sigma-Aldrich* (St. Louis, MO). PLC inhibitor U73122 (1-(6-((17β-3-methoxyestra-1,3,5(10)-trien-17-yl)amino)hexyl)-1H-pyrrole-2,5-dione), phorbol ester PMA (Phorbol-12-Myristate-13-Acetate) and inactive analog of m-3M3FBS, o-3M3FBS (2,4,6-Trimethyl-N-[2-(trifluoromethyl)phenyl]benzenesulfonamide) were from *Santa Cruz Biotechnology* (Santa Cruz, CA). PLC activator m-3M3FBS (N-(3-Trifluoromethylphenyl)-2,4,6-trimethylbenzenesulfonamide) and inactive analog of U73122, U73343 (((17β)-3-Methoxyestra-1,3,5[10]-trien-17-yl)amino]hexyl]-2,5-pyrrolidinedione) and TMEM16A inhibitor T16Ainh-A01 (2-[(5-Ethyl-1,6-dihydro-4-methyl-6-oxo-2-pyrimidinyl)thio]-N-[4-(4-methoxyphenyl)-2-thiazolyl]-acetamide) were from *Sigma-Aldrich* (St. Louis, MO). TMEM16A activator Eact (3,4,5-trimethoxy-N-(2-methoxyethyl)-N-(4-phenylthiazol-2-yl)benzamide) was from *EMD Millipore* (Billerica, MA). EGFR inhibitor erlotinib and PI3K inhibitor BKM120 were from *Selleck Chemicals* (Houston, TX). MEK inhibitor U0126 was from *Promega* (Madison, WI).

2.2 LENTIVIRAL VECTORS AND TRANSDUCTIONS

All Ras cDNAs used in this study were subcloned into the Gateway destination vector pLenti-puro-TetO-CMV-DEST (*Addgene* Plasmid 17293). The human KRAS4B cDNA sequence was used for all KRAS lines, unless specified as KRAS4A. KRAS mutations were introduced using the GeneArt® Site-Directed Mutagenesis PLUS System (*Life Technologies*) with custom mutagenesis primers. Lentiviruses were generated by cotransfection of the corresponding lentiviral vector with a three-plasmid packaging system into 293FT cells using the standard protocol for Lipofectamine 2000 (*Life Technologies*). Viral supernatants were filtered from the 293FT cells at 48 and 72 h post-transfection, polybrene (*Millipore*) was added for a final concentration of 8 ug/mL and the

mixes were directly added to Rasless cells in 6-well plates containing 50K cells per well. Plates were spun at 800 x g for 2 h at room temperature then incubated at 37°C overnight before washing out virus and replacing with fresh media. After puromycin selection and expansion of the stably transduced MEF pools, RNA was collected using the RNeasy Plus Mini Kit with on-column DNAse treatment and cDNA was produced using the RT² First Strand Kit (*Qiagen*). cDNA from each MEF line was used as template for PCR amplification and sequencing with Ras-specific primers to confirm Ras genotypes.

2.3 ANTIBODIES

Antibodies used for western blotting in this study are: pan-Ras (*Millipore* #05-1072), KRAS (*Sigma* # WH0003845M1), NRAS (*Santa Cruz* # sc-31), pERK (*Cell Signaling* # 9106, mouse & # 9101, rabbit), ERK (*Cell Signaling* #9102), pMEK (*Cell Signaling* # 9154), pCRAF S338 (*Cell Signaling* # 9427), pCRAF S259 (*Cell Signaling* # 9421), CRAF (*Abcam* # ab18761), pPLCγ1 (*Cell Signaling* # 8713), PLCγ1 (*Cell Signaling* # 2822), pEGFR Y1068 (*Cell Signaling* # 2234), pEGFR Y1173 (*Cell Signaling* # 4407), EGFR (*Cell Signaling* # 2232), pMARCKS (*Cell Signaling* # 2741), pan-pPKC (*Cell Signaling* # 9371), TMEM16A (*Santa Cruz* # sc-135235), KSR1 (*Santa Cruz* # sc-25416), PP2A subunit A (*Abcam* # ab33537), SOS1 (*BD* # 610095), and β-tubulin (*Sigma* #T8328).

2.4 CELL LINES AND CULTURE CONDITIONS

$KRAS^{lox}$ ($HRAS^{-/-}$;$NRAS^{-/-}$;$KRAS^{lox/lox}$;$RERT^{ert/ert}$) mouse embryonic fibroblasts (MEFs) were provided by the laboratory of Mariano Barbacid (*CNIO*, Madrid, Spain). MEFs and 293FT cells were grown in high-glucose Dulbeco's modified Eagle's medium (DMEM) supplemented with 10% (vol/vol) fetal bovine serum (FBS), 50 U/mL penicillin, and 50 mg/mL streptomycin (*GIBCO*) at 37

°C and 5% (vol/vol) CO_2. Antibiotic selection after retroviral transduction was carried out in 3 ug/mL puromycin (*Sigma*) for 48 h. 4-Hydroxytamoxifen (4-OHT) (Sigma) was used at a final concentration of 600 nM for 12 days to generate “Rasless” MEFs, confirmed by western blot using monoclonal anti-KRAS Clone 3B10-2F2 (*Sigma*). Pancreatic ductal adenocarcinoma (PDAC) cell lines (BxPC3, KP-3, KP-4 and Hs766T) were grown in high-glucose Roswell Park Memorial Institute 1640 (RPMI-1640) supplemented with 15% (vol/vol) FBS, 50 U/mL penicillin, and 50 mg/mL streptomycin (*GIBCO*) at 37 °C and 5% (vol/vol) CO_2. Colorectal cancer cell lines SW43 and LS513 were grown in high-glucose DMEM supplemented with 10% (vol/vol) FBS, 50 U/mL penicillin, and 50 mg/mL streptomycin (*GIBCO*) at 37 °C and 5% (vol/vol) CO_2.

2.5 NRAS PROTEIN PURIFICATION

His-tagged NRAS expressed in *E. coli* was purified by batch affinity with ProBond™ Nickel-chelating resin followed by Superdex-75 FPLC gel filtration for size exclusion. Constructs for expression of His-tagged $NRAS^{C181S}$ and $NRAS^{C186S}$ were also generated using site-directed mutagenesis and Gateway cloning, and proteins were purified similarly for use a controls in the screening process. SDS-Page gel electrophoresis and Coomassie staining was used to confirm protein purity.

2.6 MASS SPECTROMETRY

For mass spec (MS) analysis, a protein concentration of 3 µM was found to be optimal by titration. The protein was incubated with various concentrations of β-mercaptoethanol (β-ME), which serves as a catalyst for the disulfide exchange and controls the stringency of the tethering screen, and 500 µM was found to be optimal for screening. The reaction mixtures were analyzed by MS in a 96-well format to identify molecules that have been covalently tethered to the protein.

2.7 IN VITRO RAS PRENYLATION ASSAYS

Hit compounds were screened in an in vitro farnesylation assays using either purified recombinant farnesyltransferase (FTase) and NBD-GPP (*Jena Biosciences* # LI-014) or purified recombinant geranylgeranyltransferase I (GGTaseI) and NBP-FPP (*Jena Biosciences* # LI-013), with FPLC-purified NRAS or KRAS4B as substrates at 2 µM. NBD-GPP is a fluorescently tagged FPP analog that is efficiently used by FTase with similar kinetics as natural FPP, while NBD-FPP has analogous use by GGTase. Compounds were initially screened at 50 µM in the assays then titrated to as low as 0.5 µM to assess for dose-dependent blockade of modification by either prenylation enzyme. All reactions were run on protein gels, bands were imaged by fluorescence emission at 532 nm with 488 nm excitation, and Coomassie blue staining was used as a loading control.

2.8 PROTEIN CRYSTALIZATION SCREENING

Crystallization trials have were performed using either hanging drop or sitting drop vapor diffusion. The *Qiagen* Pre-Screen Assay was used to identify 15 mg/mL as the starting concentration of purified NRAS for screening of crystallization conditions. *Joint Center for Structural Genomics* (JCSG) Core I-IV screens were used with 200 nL drops set 1:1 (protein:reservoir solution) in 96-well format using a Mosquito® robot (*TTP Labtech*). Tight optimization screens were performed around conditions that yielded small crystals in the JCSG screens. These small crystals were used for the seed bead technique (*Hampton*) and many larger crystals were obtained after a few months. Growth conditions were further optimized but crystals did not diffract with sufficient resolution for structural analysis at the *Advanced Light Source* (*ALS*): Lawrence Berkeley National Labs.

2.9 TRANSFECTIONS

Mammalian expression constructs for WT hSOS1 with a farnesylation tag engineered from the HRAS c-terminus (SOS1-F) and the inactive cytosolic point mutant (SOS1-F*) were provided by the laboratory of Jeroen Roose (*UCSF*). These were transfected using the standard protocol for Lipofectamine 2000 (24 µg plasmid with 60 µL transfection reagent) in 10 cm plates for 28-32 h prior to Raf-RBD pulldowns and western blot analysis. For knockdown of endogenous SOS1, mouse Sos1 siRNA (*Santa Cruz* # sc-36524) was transfected using the standard Lipofectamine 2000 protocol for siRNA (600 pmol siRNA with 30 µL transfection reagent) in 10 cm plates for 48 h prior to Ras activation assays and western blots. For TMEM16A knockdowns, mouse TMEM16A siRNA (*Santa Cruz* # sc-76687) was transfected using the standard Lipofectamine RNAiMAX protocol in 12-well plates for 48 h prior to treatment with compounds modulating TMEM16A activity.

2.10 IMMUNOBLOT ANALYSIS

For immunoblotting, cells were plated in 6- or 12-well plates at densities to reach near-confluency in 24 hours. Cells were treated as indicated and harvested using a TNM buffer (25 mM Tris•HCl/150 mM NaCl/5 mM $MgCl_2$, pH 7.4) containing 10% glycerol, 1% Nonidet P-40 (*Roche*) and supplemented with a cocktail of phosphatase and protease inhibitors (*ThermoFisher*). Collected cell lysates were incubated on ice for 15 min and cleared by centrifugation at 14,000 rpm and 4C for 15 min. Supernatants were collected and assayed with a BCA kit (*ThermoFisher*) to measure the total protein concentrations. Equal amounts of lysate diluted to approximately 1.5 µg/µL per sample were mixed with 4x NuPAGE LDS loading buffer (*Life Technologies*) supplemented with β-mercaptoethanol and heated at 95°C for 5 min. After cooling to room temperature, samples were loaded into a 4-12% Bris-Tris gradient gel (*Life Technologies* # NP0323) and run at 80-120V at room temperature. Protein transfer was performed on an iBlot

transfer system (*Life Technologies*) at 20V for 7 min using a nitrocellulose membrane. Blots were incubated in blocking buffer (*Rockland* # MB-070) for 1 hour at room temperature, primary antibodies diluted in blocking buffer for overnight incubation at 4°C. The next day, the membranes are washed three times for 15 min. each before and after a 45 min. incubation with mouse and/or rabbit Ab-specific secondary antibody conjugates in blocking buffer for imaging on a LICOR Odyssey® system.

2.11 RAS ACTIVATION ASSAY

Raf-1 Ras Binding Domain (Raf-RBD) agarose beads (*Millipore*) were used for pulldown of active GTP-bound KRAS using the standard affinity precipitation/immunoblot protocol with 500 µg of cleared cell lysate per sample with 10 µg of the Ras assay reagent.

2.12 CELL PROLIFERATION ANALYSIS

Cell proliferation was measured by quantifying relative number of viable cells after 48 h under various treatments using the CellTiter 96 Aqueous Non-Radioactive Cell Proliferation Assay (MTS) Assay (*Promega* # G3580). Reagent was added cells treated in triplicate in 96-well format and incubated for 4 hr at 37°C at the end of the treatment period at absorbance was read at 490 nM and 630 nM (for background subtraction) following the manufacturer's instruction. Each condition was normalized to the average of the corresponding DMSO treated wells.

2.13 QUANTITATIVE REAL TIME PCR

For gene expression analysis, MEFs varying by Ras genotype were plated 2 million cells/10 cm dish in duplicate overnight before a 6 h starve in serum-free media or stimulation with 30 ng/mL

EGF, 50 ng/mL IGF-1, 50 ng/mL insulin and 100 ng/mL FGF in 10% FBS media. After either treatment, the cells were lysed in their plates using the standard protocol for Qiagen RNeasy® Mini Plus. 1 µg of each RNA sample was used as template for cDNA synthesis sing the RT^2 First Strand Kit. The cDNA reactions were diluted after genomic DNA elimination, split in two and used for RT^2 Profiler PCR on the Qiagen PI3K (PAMM-058Z) and MAPK (PAMM-061Z) arrays using the Format R protocol.

2.14 GENE EXPRESSION ANALYSIS

Expression analysis was performed to compare transcription profiles between MEF lines and treatments using the SABiosciences™ RT^2 Profiler PCR Array Data Analysis online software for the PI3K and MAPK arrays. Volcano plots were rendered in the program and used to display statistical significance versus fold-change by combining a p-value statistical test with the fold regulation change, enabling identification of genes with both large and small expression changes that are statistically significant ($p < 0.05$).

2.15 IMMUNOPRECIPITATION

Two million cells per treatment were plated in a 10 cm dish 24 h prior to treatment. Cells were treated as indicated and lysed in TNM lysis buffer as previously described. After protein quantification by BCA assay, 500 µg of each sample was diluted to 500 µL and combined with 10 µg of IP antibody: either Ras (Millipore **#** 05-1072) or CRAF (Abcam # ab18761). Antibody mixes were incubated overnight rotating at 4°C. 40 µL of Protein G or Protein A Sepharose beads (GE Healthcare # 17-0618-02 & # 17-5280-04), for Ras and CRAF respectively, were added to the mixes for 1 h. The beads were collected by brief centrifugation at 4°C, washed three times in 500 µL lysis buffer and eluted in 20 µL 2x gel loading buffer at 95°C for 5 min.

2.16 SUPERRESOLUTION IMAGING AND DIMERIZATION ANALYSIS

MEFs stably expressing photoactivatable monomeric Cherry (PAmCherry)-KRAS4B G12D fusion proteins at various levels of density in the membrane were generated by lentiviral transduction of $KRAS^{lox}$ or Rasless MEFs and expansion of single-cell clones. Several clones were assessed by TIRF-PALM imaging to compare the molecular density at the plasma membrane. The fraction of tagged molecules oligomerized at the membrane was quantified using proprietary software [Xiaolin Nan]. PALM analysis of cells, starved vs. mitogen-stimulated prior to fixation, was used to assess whether the GTP-loaded state is required for dimerization.

2.17 MEASUREMENT OF GTP HYDROLYSIS RATES

KRAS4B wild type and [G12C, G12D, G12V, Q61L and Q61R] mutant proteins (2-188) were expressed with a His6 tag in E. Coli. Bacterial pellets were lysed and His-tagged proteins were purified by IMAC chromatography and the His tag was removed by TEV digestion. In order to measure GTP hydrolysis, 5 µg of KRAS-GDP was incubated at 30°C for 15 min in exchange buffer (50 mM Tris-HCl pH7.5, 5mM DTT, 50 mM NaCl and 10 mM EDTA) with 2 µCi of γ-^{32}P-labeled GTP in a total volume of 100 µl. 3 µg of RAS-^{32}P-labeled GTP is incubated at 37°C in 300 µl of hydrolysis buffer supplemented with 1 mM $MgCl_2$. Aliquots were moved and added to 400 µl of pre-chilled stop buffer (5% activated charcoal, 0.2 M HCl, 1 mM NaH_2PO_4 and 20% ethanol). After centrifugation soluble ^{32}P counts were measured by scintillation counting.

CHAPTER 3.

DISRUPTING NRAS PRENYLATION USING CYSTEINE TETHERING

3.1 INTRODUCTION

Thus far, the method that has display the broadest potential in directly inhibiting the signaling capability of Ras is to block the prenylation and proteolysis steps in membrane localization[57, 58]. The outcome of the use of farnesyltransferase inhibitors (FTIs) as therapeutics provides an excellent example of the significance of Ras variability at the C-terminus in modifications for membrane localization. As most studies on the Ras family of proteins were performed with the originally identified isoform, HRAS, FTIs appeared efficacious despite the presence of the functionally redundant protein, geranylgeranyltransferase (GGTase). The difference in the sequence targeted by prenylation proteins, the CAAX box, allows for NRAS and KRAS isoforms to be alternatively prenylated while HRAS is solely prenylated by farnesyltransferase (FTase)[58]. Though *in vivo* studies appeared promising, FTIs have ultimately shown disappointing results in the clinic, where KRAS and NRAS mutations are commonly seen and HRAS mutations are much rarer. Though GGTase inhibitors are in clinical development, dual inhibition of both prenylation enzymes will more than likely provide safety issues in patients, as there are at least 38 prenylated proteins with varied functions in normal cellular functioning.

We devised a strategy to block for specific blockade of the membrane localization of NRAS, and possibly KRAS, with no foreseeable escape route. Specificity may be achieved through modification of the CAAX box cysteine and pharmacological interaction with the hypervariable region (HVR), such that NRAS becomes inaccessible to all prenylation enzymes. The method known as “tethering” is used to identify selective reversible covalent binders of the target cysteine[54]. Tethering is a site-directed ligand discovery strategy that rapidly and reliably identifies small molecule fragments that bind to a specifically targeted site on a protein. The method relies on the formation of a disulfide bond between the ligand and a cysteine residue on the protein of interest. A library of drug-like compounds containing disulfide groups is allowed to

react with a cysteine-containing target protein under partially reducing conditions that promote rapid disulfide exchange. Most of these compounds will show no intrinsic affinity for the protein and therefore the associated disulfide bond to the protein will be easily reduced. However, if the compound has even a modest affinity for another site on the target protein, then the disulfide bond will be entropically stabilized and the equilibrium will lie towards the modified protein. These secondary interactions are what endow the molecule with selectivity for the target. Considering that the different Ras proteins differ greatly in the HVR, there is a strong expectation of finding compounds that are specific for the individual Ras isoforms. This is an important advantage of the site-directed tethering screening method that would be difficult to achieve by other screens or design plans, given that there is no x-ray crystallographic information on the structure of the HVR domains and no existing small molecules are known to interact with them.

Using a tethering approach to identify compounds forming interactions with Ras around the CAAX box cysteine may yield inhibitors of Ras prenylation that can be brought to near 100% labeling efficiency by replacing the thiol group with an irreversible cysteine-reactive electrophile[59]. The interaction can be optimized using information gained from crystallographic studies or an empirical medicinal chemistry approach of iterative rounds of structural modifications followed by testing.

3.2 RESULTS

3.2.i. Mass spectrometry (MS) screening detects tethering compound hits

The method relies on the formation of a disulfide bond between the ligand and a cysteine residue on the protein of interest[Fig. 3.1a]. Briefly, a library of drug-like compounds containing disulfide groups is allowed to react with a cysteine-containing target protein under partially

reducing conditions that promote rapid disulfide exchange. Increasing the concentration of β-ME allows it to compete off weaker binding compounds so that only compounds with higher binding affinity will show up as hits. Most compounds show no intrinsic affinity for the protein and therefore the associated disulfide bond to the protein is easily reduced[Fig. 3.1b]. Secondary interactions, even a modest affinity for another site on the target protein, may provide a sufficient force to push the equilibrium and confer selectivity for the target. Considering that the different Ras isoforms differ greatly in HVR sequences, there is a strong expectation of finding compounds that are isoform-specific.

We screened wild type, C181S palmitoylation mutant and C186S prenylation mutant NRAS with 384 compounds. We found 30 apparent hits. Many of these were moderate hits (<25% labeling), but 16 compounds displayed over 50% labeling[Fig. 3.1c]. None of the hit compounds showed a signal (MW shift) when incubated with either cysteine to serine mutant protein. This suggests that the region around the palmitoylation cysteine in the NRAS HVR might be a site secondary interaction with these compounds. Also, this also confirmed that the compounds were targeting the CAAX box cysteine of NRAS and none of the internal cysteines tether stably.

3.2.ii. Farnesylation of the NRAS CAAX-box cysteine is blocked by a subset of MS hits

Hit compounds were screened in an in vitro farnesylation assay using NBD-GPP and FPLC-purified NRAS and KRAS as substrates. NBD-GPP is a fluorescently tagged FPP analog that is efficiently used by FTase with similar kinetics as natural FPP [60]. While both KRAS4B and NRAS are farnesylated in our *in vitro* assay, we display that the enzymatic modification is less efficient when FTase uses NRAS as a substrate[Fig. 3.2a]. As the only difference in the CAAX box sequences of KRAS4B and NRAS is isoleucine (I) versus valine (V) at the second

"A" residue, it is likely that the terminal methyl group that differentiates I from V better stabilizes FTase activity on the KRAS4B CAAX box cysteine. Sixteen tethering compounds that displayed labeling of NRAS on mass spec were tested at 50 µM for their ability to block *in vitro* farnesylation of NRAS or KRAS4B. Six compounds strongly impaired the modification reaction, though only 2 compounds displayed specificity for NRAS over KRAS4B[Fig. 3.2b]. Three compounds appeared to equally impair farnesylation of either Ras isoform, while one compound displayed a much higher degree activity on KRAS4B[Fig. 3.2b]. All of these compounds displayed some level of dose-dependent inhibition of the prenylation reaction when applied between 50 µM and 500 nM. The average IC50 was between 3.2 and 8 µM[Fig. 3.2c]. However, when the prenylation reaction was carried out with GGTaseI instead of FTase, prenylation was much less efficiently inhibited using all but one compound (3E10)[Fig. 3.3]. This suggest that either GGTaseI displaces the weaker compounds more effectively than FTase or some of our hits target FTase rather than the CAAX box.

3.2.iii. Compounds display varied levels of cytotoxicity in a Ras-dependent MEF model

"Rasless MEFs"[61] that are reconstituted with NRAS undergo proliferation and migration that is dependent on NRAS signaling on cellular membranes. NRAS MEFs or their parental Rasless MEFs were treated for 24 h with DMSO or 50 µM of a hit compound found to have no *in vitro* efficacy as a prenylation inhibitor (3B4), KRAS-specific prenylation inhibitor (5C1), dual KRAS and NRAS prenylation inhibitors (5H5 and 6E8) or NRAS-specific prenylation inhibitor (3E10). This initial testing of our compounds in NRAS-dependent cells displays correlation between *in vitro* compound efficacy and cytotoxicity, with relatively low off-target activity observed on the treated Rasless MEFs[Fig. 3.4].

3.2.iv. Optimization and scale-up of 3E10 labeling of NRAS yields protein suitable for crystallization studies

Gaining atomic resolution of the interaction of lead compounds with the C-terminus of NRAS will grant understanding of the mode of interaction and inform efforts to modify functional groups for improvement of lead affinity and selectivity. As previous crystallization methods have required the use of in situ proteolysis of full-length NRAS, resulting in the loss of the HVR sequence, there is no available structural data for the NRAS C-terminus. We believe that the interaction at the CAAX box cysteine along with non-covalent interactions at proximal sites has potential to stabilize the tail sequence for an ordered structure. Even if there is still a fair amount of disorder, we should be able to obtain useful information on the specific interactions that our molecule makes with the protein. These insights will guide us in the production of more specific inhibitors with higher affinity. If a crystal structure cannot be obtained using our compounds, a more classical approach of iterative medical chemistry will be used to alter functional groups and followed by rounds of testing.

Crystallization studies require large amounts of protein at near 100% purity. We optimized our bacterial NRAS production for yield and purity to generate over 50 mg of protein with no visible contaminant bands on when 50 µg of the concentrate was run on gel and Coomassie-stained. This protein was used to confirm binding with 3E10 using surface plasmon resonance (SPR) on Biacore. The palmitoylation mutant NRAS C181S displayed a binding curve while binding was not quantifiable with the wild type protein (data not shown). For this reason, we focused on optimizing 3E10 binding with the CAAX-cysteine of NRAS C181S using different concentrations of compound and reductant, then analyzing the extent of compound labeling on mass spec. We achieved nearly 100% binding of the protein after overnight incubation with 1mM 3E10 and 250 µM dithiothreitol (DTT)[Fig. 3.5]. With 500 µM 3E10 or 500 µM DTT, there was residual unbound protein. Conversely, with 1 mM 3E10 and no reducing agent, a peak at a

mass consistent with two 3E10 molecules labeling the protein was observed[Fig. 3.5].

With the near 100% 3E10-labeled NRAS C181S in hand, we performed a pilot crystallization screen using the Qiagen Pre-Screen Assay. Precipitation was observed in approximately 50% of the screen of drops using 15 mg/mL protein 1:1 with the varied reservoir solutions. *Joint Center for Structural Genomics* (JCSG) Core I-IV screens were used with 200 nL drops set 1:1 (protein:reservoir solution) in 96-well format using a Mosquito® robot (*TTP Labtech*). It was noticed early on that PEGs, especially of low molecular weight, were producing microcrystals and other precipitate. In this direction, we obtained and similarly screened the *Qiagen* PEGs Suite and PEGs II Suite but did not obtain crystals. Tight optimization screens were performed around conditions that yielded small crystals in the JCSG screens[Fig. 3.6a]. These small crystals were used for the seed bead technique (*Hampton*) and many larger crystals were obtained after a few months[Fig. 3.6b]. To our dismay, these protein crystals did not diffract with sufficient resolution for structural analysis.

3.3 DISCUSSION

As the one essential requirement for all signaling from Ras, membrane localization remains the premier anti-Ras strategy for cancer therapy[62]. Given our current understanding that the failure of FTIs in the clinic was not due to a flawed hypothesis but an underappreciation of a backup mechanism in the large majority of Ras-driven cancers, we must continue in effort to block membrane association however possible. Due to the diversity of functions served by prenylated proteins, it would not be wise to wipe out prenylation across the broad by inhibition of all enzymes performing this modification. Our approach of direct attack on the CAAX-box cysteines of the particular Ras isoforms driving human cancers solves this problem in generating specificity.

Using tethering, we have identified compounds that effectively block the prenylation of the problematic Ras isoforms in FTI-resistance, NRAS and KRAS. These compounds generate isoform specificity by forming interactions with the HVR domains secondary to covalent interactions with the exposed CAAX box cysteines. Though the reducible disulfide bond of the tethering compounds that we have identified as *in vitro* inhibitors makes these molecules not very drug-like, they do display activity in cells that is consistent with their levels of activity on purified Ras proteins. Tethering compounds are made more drug-like by replacement of the disulfide bonded linker when an electrophilic group interact with the target cysteine non-covalently[59, 63]. We have done this effectively targeting the KRAS CAAX box (non-published).

Better understanding of the C-terminal structure of NRAS will allow for better tuning of potential prenylation inhibitors to generate greater affinity and specificity. Though our initial study was unsuccessful in yielding structural data, the conditions used for expression, purification, compound labeling and crystal formation could prove valuable in the work-up process for generation of better diffracting crystals. If this approach does not work, it is possible to identify related compounds that better stabilize the interactions with C-terminus through computationally-driven iterative rounds of medicinal chemistry altering the functional groups for analysis via binding assays prior to further crystallization attempts. The Rasless cell model will provide a valuable tool for assessment of the specific on- and off-target activities of lead compounds as the search continues for isoform-specific prenylation inhibitors. This strategy is most promising considering both efficacy and safety, in that all downstream signaling is lost by blocking localization of the mutated Ras isoform while the wild type Ras isoforms are sparred for normal function.

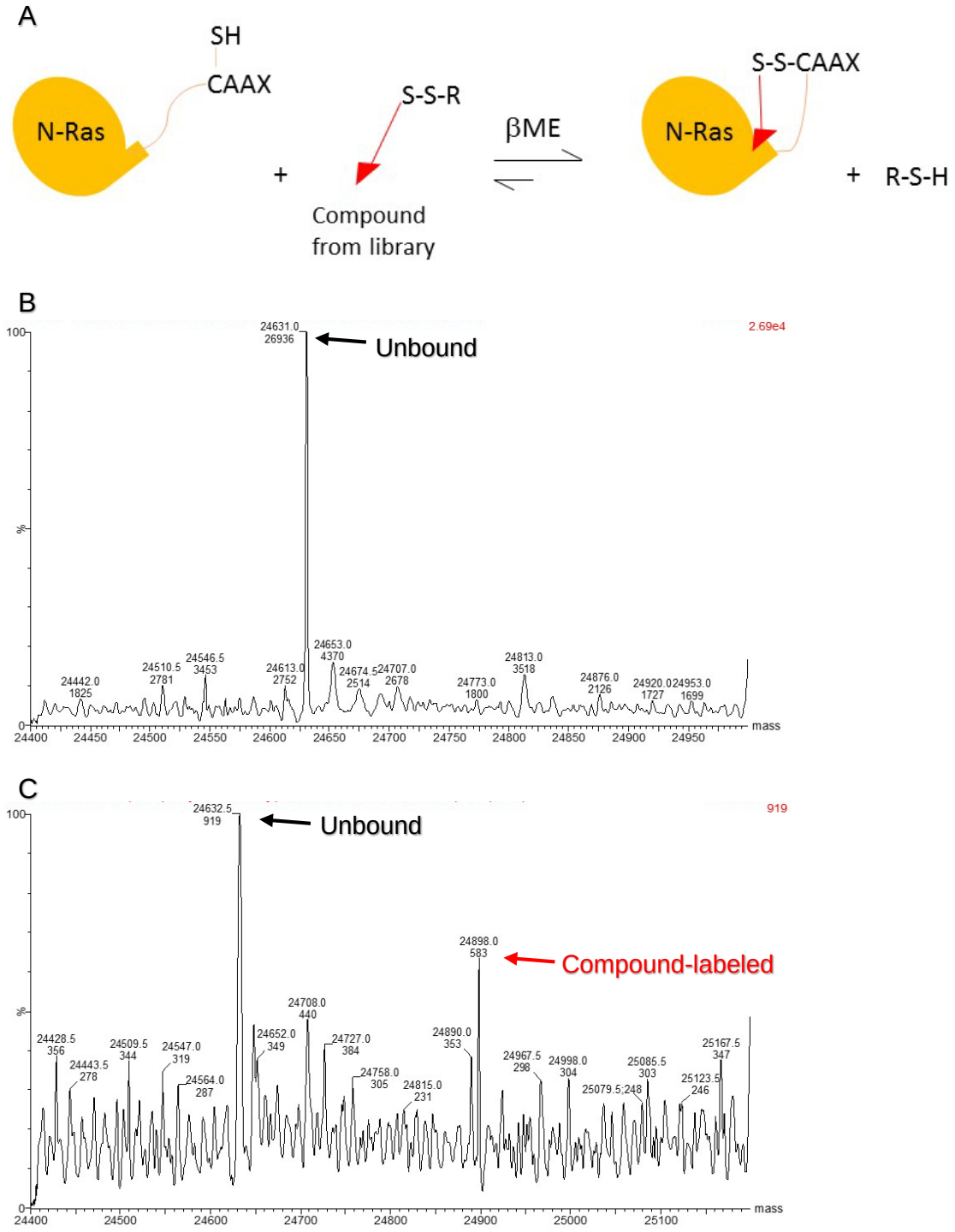

Figure 3.1. Screening approach using compounds tethering the NRAS CAAX box

(A) Schematic diagram of the CAAX-box cysteine tethering reaction used for screening.

(B) Mass spectrum around the molecular weight of NRAS displaying unbound protein.

(C) Mass spectrum for NRAS displaying compound tethering at equilibrium.

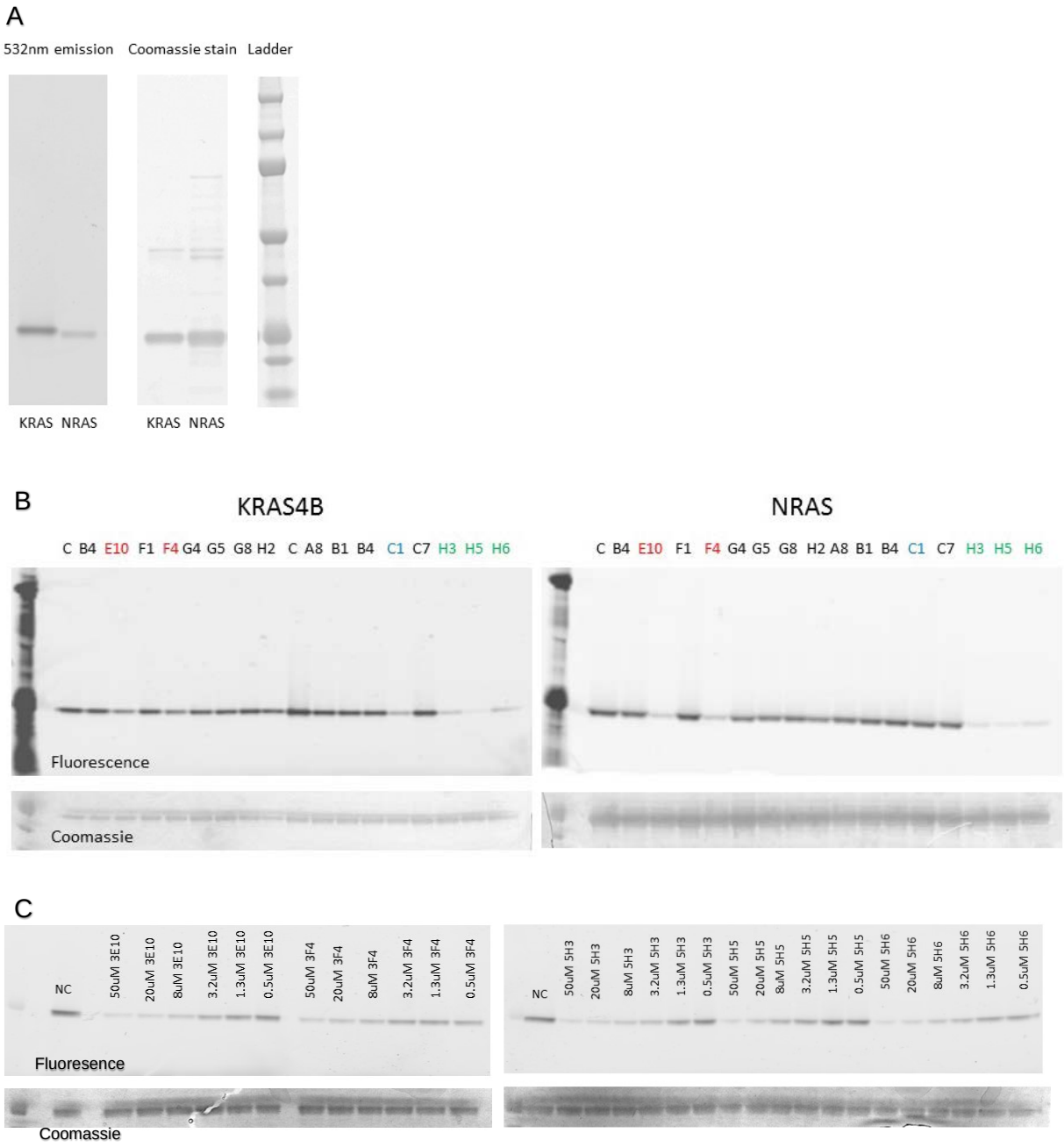

Figure 3.2. Inhibition of in vitro farnesylation by a subset of tethering compounds

(A) *In vitro* farnesylation assay comparing efficiency of FTase modification of KRAS4B^{G12V} or NRAS^{G12V} with fluorescent NBD-GPP. Coomassie staining served as a loading control.

(B) *In vitro* farnesylation assay in the presence or absence (C) of tethering compounds, assessing isoform-specificity for KRAS4B and NRAS. (red: NRAS, blue: KRAS, green: both)

(C) *In vitro* farnesylation assay assessing NRAS prenylation with no compound (NC) or descending concentrations of active tethering compounds.

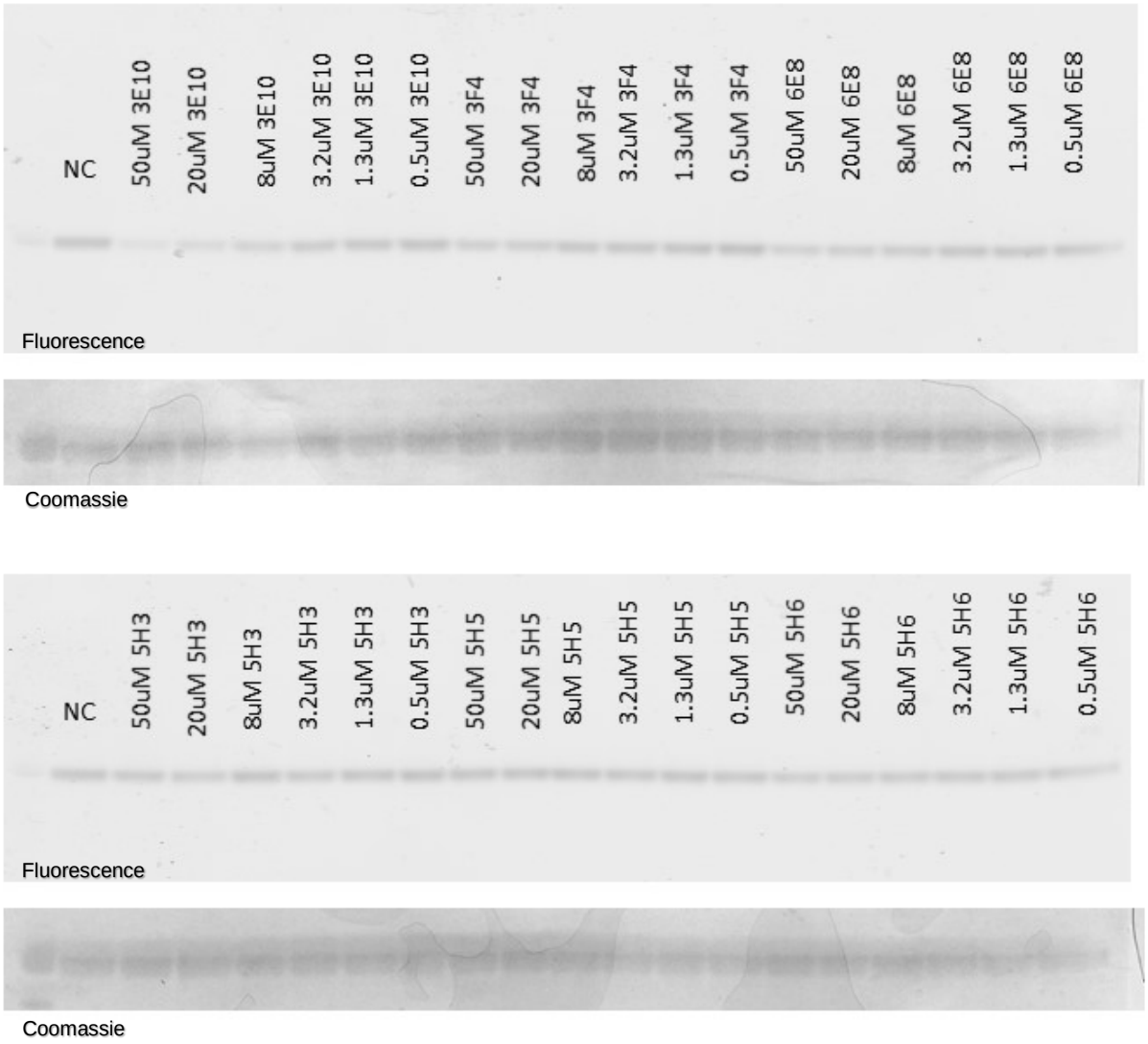

Figure 3.3. GGTase assays reveal lead compounds for stable NRAS CAAX targeting

In vitro geranylgeranylation assay revealing GGTase modification of $NRAS^{G12V}$ using fluorescent NBD-FPP with no compound (NC) or descending concentrations of tethering compounds displaying activity against FTase modification. Coomassie staining served as a control for protein loading.

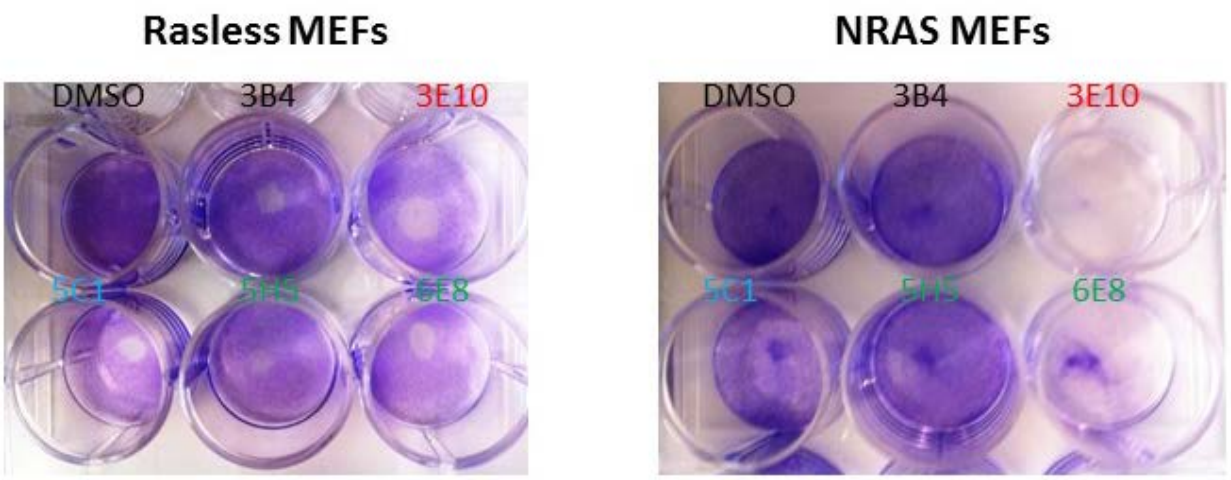

Figure 3.4. Initial testing of compounds in MEFs displays correlation with *in vitro* compound efficacy and low off-target toxicity.

Rasless or NRAS reconstituted MEFs were treated for 24 h with the specified compound or DMSO vehicle control then media was removed for crystal violet staining of live cells.

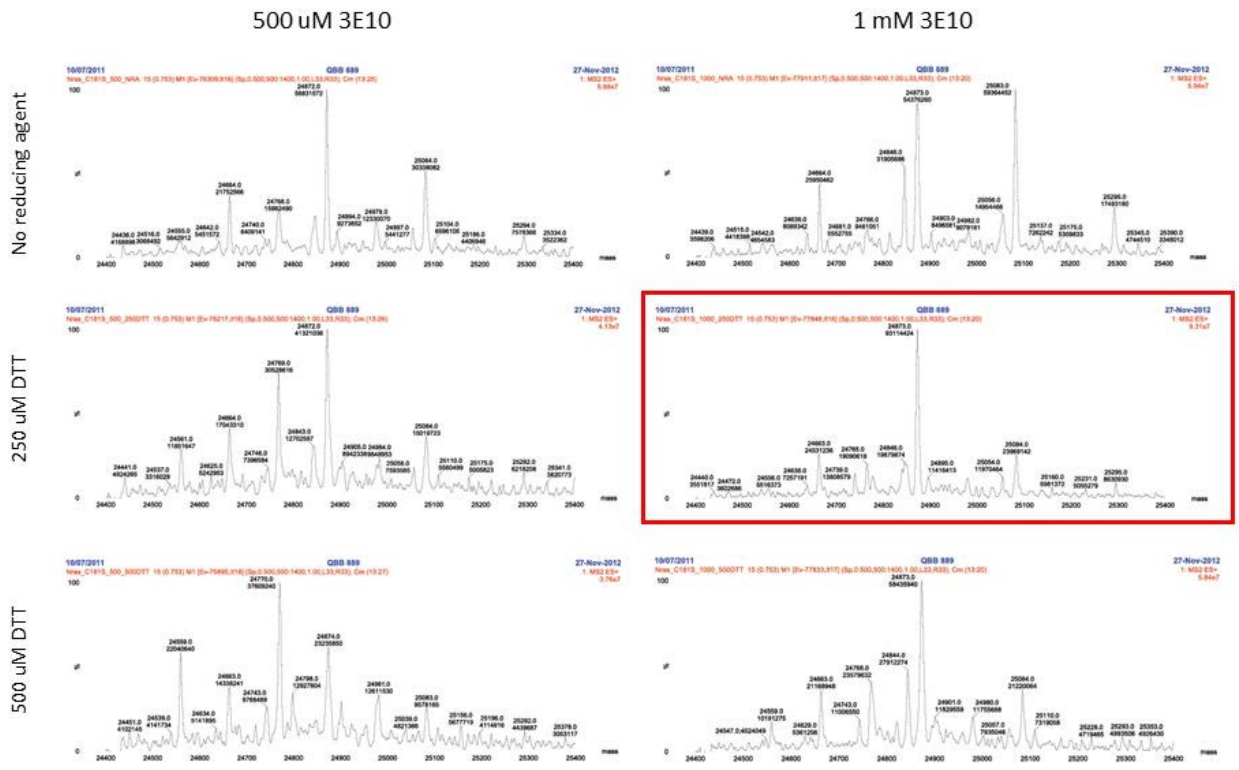

Figure 3.5. Mass spectra of binding conditions for near 100% 3E10-labeling of NRAS

$NRAS^{G12V,C181S}$ was separated into 2 mg aliquots and concentrated to 4 µM, then incubated overnight with either 500 µM or 1 mM 3E10 and the shown concentration of reducing agent (DTT) before mass spec runs to assess compound binding.

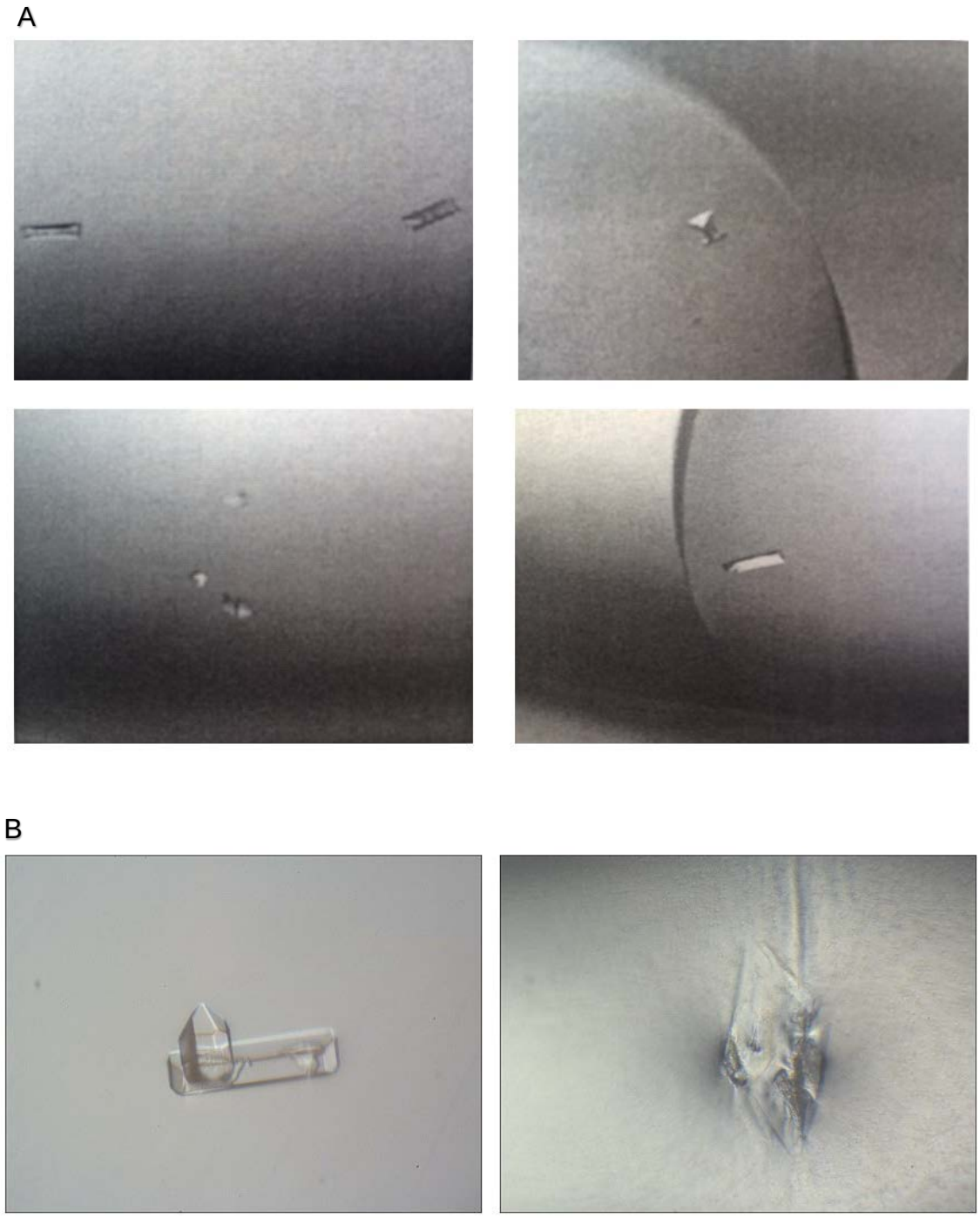

Figure 3.6. NRAS^{G12V,C181S}-3E10 protein crystals

(A) Small crystals (10-40 microns) observed in an optimization screen around JCSG Core Suite III A10 (30% v/v PEG 200, 0.1 M CAPS pH 10.5, 0.2 M $AmSO_4$). (10x)
(B) Large crystals (60-120 microns observed 8 months after seeding small crystals from reservoir solution: 0.18 M $AmSO_4$, 0.1 M CAPS pH 10.4, 28% PEG 200. (20x)

CHAPTER 4.

POTENTIAL MECHANISMS FOR WILD TYPE SUPPRESSION OF ONCOGENIC RAS SIGNALING

4.1 INTRODUCTION

Tumors driven by oncogenic Ras often show loss of heterozygosity, suggesting that the wild-type allele may suppress optimal growth. The strongest suppression phenotypes are elicited when wild type Ras is co-expressed with mutant Ras of the cognate isoform, while weaker suppressive effects are observed from alternative wild-type Ras isoforms that are present[42]. Considering the potential for wild type inhibition of oncogenic Ras signaling by dimerization, these findings support a preference for self-dimerization among molecules of the same isoform. If wild type Ras competes with oncogenic Ras molecules in dimers, then a lower dimerized fraction would be observed in the cells retaining wild type Ras expression. If full-length Ras must be GTP-bound for the C-termini to interact in dimers, then wild type Ras could not compete with the oncogenic form in dimers in the starved state and a significant reduction in the fraction of oncogenic molecules dimerized would only be observed in the stimulated cells retaining wild type Ras expression.

Evidence points to WT inhibition of oncogenic Ras being specific to each isoform consistent with our finding that the C-terminus, containing the hypervariable region, is sufficient for Ras dimerization (unpublished data). Although the guanine nucleotide binding domain is not required for Ras dimerization, there is still the possibility that this region may interfere with dimerization in the GDP-bound state and interference may be relieved by exchange for GTP. Considering that Ras acts as a dose-sensitive rheostat[64], it is likely that wild type Ras inhibits tumor development by reducing the pro-growth signaling from oncogenic Ras.

Alternatively, there is the potential explanation that wild type and oncogenic Ras differentially regulate the major effector pathways in active signaling. We hypothesized that recusing Rasless MEFs with either wild type or oncogenic Ras variants would allow

for direct interrogation of signaling output through transcriptional network analysis in the MAPK and PI3K pathways.

4.2 RESULTS

4.2.i. TIRF-PALM imaging of KRAS G12D plasma membrane organization in a Rasless background

We determined that a likely mechanism for wild type suppression of oncogenic KRAS is the direct physical interaction of the two KRAS variants in the PM[Fig. 4.1]. In order to gather insight into the organization of oncogenic KRAS in the cell membrane and the potential for wild type KRAS to affect the segregation or clustering of the proteins, we used a superresolution approach known as photoactivation localization microscopy (PALM) and the $KRAS^{lox}$ MEFs. These MEFs were either left in normal growth conditions or treated with tamoxifen for 10 days until all Ras expression was lost. Equal numbers of these cells, before and after loss of the endogenous KRAS alleles, were infected with lentivirus for transduction of photoactivatable (PA)-mCherry tagged KRAS G12D. The membrane organization of the individual oncogenic KRAS proteins can then be assessed, with or without the influence of the endogenous wild type form, by total internal reflection (TIRF)-PALM imaging of the plasma membrane on the surface of glass chamber slides. We found that KRAS is fairly evenly distributed throughout the plasma membrane though increasingly concentrated at the edges of the projections of cells[Fig. 4.2a]. Though the cell morphologies differ dependent on where the endogenous KRAS is retained, there is no apparent difference in the general distribution of the tagged oncogenic proteins. The transduced $KRAS^{lox}$ cells are flatter and display more thin projections while the transduced Rasless cells are longer and more three-dimensional with less contact inhibition[Fig. 4.2a].

4.2.ii. Wild type KRAS displays a minor disruption of oncogenic KRAS clustering in the plasma membrane

Closer analysis was performed to quantify the extent of oligomerization or cluster formation of oncogenic KRAS proteins in the PM, as well as the potential for wild type KRAS to impact this measure though their association. Ripley's K function was used to test for spatial randomness of the distribution of the tagged molecules in the PM and it was determined to be non-random through a preference for dimer formation, though some high order oligomers were also observed. Comparing the degree of dimerization observed in the Rasless versus $KRAS^{lox}$ background, we measure that there is around a 25% decrease in the proportion of the dimerized to monomeric KRAS that is detected when the wildtype form is present versus the proportion observed in the Rasless cells (15-20% versus 20-25% dimerized). This was measured across several cells of each genotype, all expressing at a protein density of approximately 30 molecules/μm^2, and the difference just reached statistical significance[Fig. 4.2b-c]. This analysis was performed with the Rasless MEFs starved and the $KRAS^{lox}$ MEFs EGF-stimulated, under the expectation that the wild type form may require stimulation for GTP-loading and interaction with the active oncogenic form. It is possible that a significantly greater degree of dimerization would be observed in the Rasless background if these cells were stimulated, considering that ligand-mediated dimerization of upstream growth factor receptors (RTKs) may bring KRAS into dimers by interaction with RTK-recruited GEFs.

Immunoblotting was used to measure the relative expression of the exogenous oncogenic and endogenous wild type KRAS in the lines, as well as their basal and stimulated downstream signaling output. Using a KRAS antibody to detect blot expressed forms on the same blot, we observed approximately equal expression levels in the $KRAS^{lox}$ background and confirmed equal exogenous expression and no wild type KRAS in the

Rasless background[Fig. 4.3]. Though basal (starved) KRAS signaling in the PI3K and MAPK pathways was slightly elevated in the $KRAS^{lox}$ background, in normal serum growth conditions, both effector pathways display significantly higher activation when wild type KRAS is not present[Fig. 4.3]. This supports the idea that wild type KRAS negatively contributes to PI3K and MAPK signaling output in the context of oncogenic KRAS signaling. As expected, EGF stimulation can activate the wild type KRAS to contribute to the signaling output of oncogenic KRAS, though the oncogenic form on its own is not strongly affected.

4.2.iii. Comparison of wild type to oncogenic (G12V) expression profiles across isoforms displays isoform-independent differences in gene regulation

In order to assess whether wild type and oncogenic Ras may separately regulate downstream genes in the PI3K and MAPK pathways, we individually reconstituted MEFs with the three isoforms most commonly implicated in human cancers *KRAS4B, KRAS4A and NRAS* in either wild type or the G12V oncogenic variant. First, we aimed to confirm that the wild type forms display a greater degree of responsiveness to upstream signals in their gene regulation within the major Ras effector pathways. Secondly, we sought to determine whether the basal signaling of the oncogenic form may better sustain transcriptional networks downstream of PI3K and MAPK activation than basal wild type signaling, where we would expect little Ras activity. If this holds true, we would expect stimulation of the wild type Ras driven cells to remove a large degree of the difference in effector gene regulation observed in direct comparison with the transcriptional output of oncogenic Ras driven cells. There is also the possibility that the wild type and oncogenic forms may display divergent effector responses to stimulation at the level of transcriptional regulation.

Using quantitative PCR arrays focused on the major Ras effectors, MAPK and PI3K, we performed wild type to G12V comparisons across the three isoforms. Though this analysis disregards potential for Ras isoform-specific signaling differences, our aim was to first identify similarly regulated genes across isoforms displaying significant differences between in simulation responsiveness between wild type and oncogenic forms. The focus panel of genes related to the PI3K and MAPK were uniformly analyzed across our lines using the Qiagen RT^2 Profiler PCR Arrays (*SABiosciences*) shown below.

Table 4.1. PI3K array gene table

Symbol	Gene Bank	Description
Adar	NM_019655	Adenosine deaminase, RNA-specific
Akt1	NM_009652	Thymoma viral proto-oncogene 1
Akt2	NM_007434	Thymoma viral proto-oncogene 2
Akt3	NM_011785	Thymoma viral proto-oncogene 3
Apc	NM_007462	Adenomatosis polyposis coli
Bad	NM_007522	BCL2-associated agonist of cell death
Btk	NM_013482	Bruton agammaglobulinemia tyrosine kinase
Casp9	NM_015733	Caspase 9
Ccnd1	NM_007631	Cyclin D1
Cd14	NM_009841	CD14 antigen
Cdc42	NM_009861	Cell division cycle 42 homolog (S. cerevisiae)

Cdkn1b	NM_009875	Cyclin-dependent kinase inhibitor 1B
Chuk	NM_007700	Conserved helix-loop-helix ubiquitous kinase
Csnk2a1	NM_007788	Casein kinase 2, alpha 1 polypeptide
Ctnnb1	NM_007614	Catenin (cadherin associated protein), beta 1
Eif2ak2	NM_011163	Eukaryotic translation initiation factor 2-alpha kinase 2
Eif4b	NM_145625	Eukaryotic translation initiation factor 4B
Eif4e	NM_007917	Eukaryotic translation initiation factor 4E
Eif4ebp1	NM_007918	Eukaryotic translation initiation factor 4E binding protein 1
Eif4g1	NM_001005331	Eukaryotic translation initiation factor 4, gamma 1
Elk1	NM_007922	ELK1, member of ETS oncogene family
Fasl	NM_010177	Fas ligand (TNF superfamily, member 6)
Fkbp1a	NM_008019	FK506 binding protein 1a
Fos	NM_010234	FBJ osteosarcoma oncogene
Foxo1	NM_019739	Forkhead box O1
Foxo3	NM_019740	Forkhead box O3
Mtor	NM_020009	Mechanistic target of rapamycin (serine/threonine kinase)
Gja1	NM_010288	Gap junction protein, alpha 1
Grb10	NM_010345	Growth factor receptor bound protein 10

Grb2	NM_008163	Growth factor receptor bound protein 2
Gsk3b	NM_019827	Glycogen synthase kinase 3 beta
Hras1	NM_008284	Harvey rat sarcoma virus oncogene 1
Hspb1	NM_013560	Heat shock protein 1
Igf1	NM_010512	Insulin-like growth factor 1
Igf1r	NM_010513	Insulin-like growth factor I receptor
Ilk	NM_010562	Integrin linked kinase
Irak1	NM_008363	Interleukin-1 receptor-associated kinase 1
Irs1	NM_010570	Insulin receptor substrate 1
Itgb1	NM_010578	Integrin beta 1 (fibronectin receptor beta)
Jun	NM_010591	Jun oncogene
Map2k1	NM_008927	Mitogen-activated protein kinase kinase 1
Mapk1	NM_011949	Mitogen-activated protein kinase 1
Mapk14	NM_011951	Mitogen-activated protein kinase 14
Mapk3	NM_011952	Mitogen-activated protein kinase 3
Mapk8	NM_016700	Mitogen-activated protein kinase 8
Mtcp1	NM_010839	Mature T-cell proliferation 1
Myd88	NM_010851	Myeloid differentiation primary response gene 88

Nfkb1	NM_008689	Nuclear factor of kappa light polypeptide gene enhancer in B-cells 1, p105
Nfkbia	NM_010907	Nuclear factor of kappa light polypeptide gene enhancer in B-cells inhibitor, alpha
Pabpc1	NM_008774	Poly(A) binding protein, cytoplasmic 1
Pak1	NM_011035	P21 protein (Cdc42/Rac)-activated kinase 1
Pdgfra	NM_011058	Platelet derived growth factor receptor, alpha polypeptide
Pdk1	NM_172665	Pyruvate dehydrogenase kinase, isoenzyme 1
Pdk2	NM_133667	Pyruvate dehydrogenase kinase, isoenzyme 2
Pdpk1	NM_011062	3-phosphoinositide dependent protein kinase 1
Pik3ca	NM_008839	Phosphatidylinositol 3-kinase, catalytic, alpha polypeptide
Pik3cg	NM_020272	Phosphoinositide-3-kinase, catalytic, gamma polypeptide
Pik3r1	NM_001024955	Phosphatidylinositol 3-kinase, regulatory subunit, polypeptide 1 (p85 alpha)
Pik3r2	NM_008841	Phosphatidylinositol 3-kinase, regulatory subunit, polypeptide 2 (p85 beta)
Prkca	NM_011101	Protein kinase C, alpha
Prkcb	NM_008855	Protein kinase C, beta
Prkcz	NM_008860	Protein kinase C, zeta
Pten	NM_008960	Phosphatase and tensin homolog
Ptk2	NM_007982	PTK2 protein tyrosine kinase 2
Ptpn11	NM_011202	Protein tyrosine phosphatase, non-receptor type 11

Rac1	NM_009007	RAS-related C3 botulinum substrate 1
Raf1	NM_029780	V-raf-leukemia viral oncogene 1
Rasa1	NM_145452	RAS p21 protein activator 1
Rbl2	NM_011250	Retinoblastoma-like 2
Rheb	NM_053075	Ras homolog enriched in brain
Rhoa	NM_016802	Ras homolog gene family, member A
Rps6ka1	NM_009097	Ribosomal protein S6 kinase polypeptide 1
Rps6kb1	NM_028259	Ribosomal protein S6 kinase, polypeptide 1
Shc1	NM_011368	Src homology 2 domain-containing transforming protein C1
Sos1	NM_009231	Son of sevenless homolog 1 (Drosophila)
Srf	NM_020493	Serum response factor
Tcl1	NM_009337	T-cell lymphoma breakpoint 1
Tirap	NM_054096	Toll-interleukin 1 receptor (TIR) domain-containing adaptor protein
Tlr4	NM_021297	Toll-like receptor 4
Tollip	NM_023764	Toll interacting protein
Tsc1	NM_022887	Tuberous sclerosis 1
Tsc2	NM_011647	Tuberous sclerosis 2
Wasl	NM_028459	Wiskott-Aldrich syndrome-like (human)
Ywhah	NM_011738	Tyrosine 3-monooxygenase/tryptophan 5-monooxygenase activation protein, eta

Table 4.2. MAPK array gene table

Symbol	Gene Bank	Description
Araf	NM_009703	V-raf murine sarcoma 3611 viral oncogene homolog
Atf2	NM_009715	Activating transcription factor 2
Ccna1	NM_007628	Cyclin A1
Ccna2	NM_009828	Cyclin A2
Ccnb1	NM_172301	Cyclin B1
Ccnb2	NM_007630	Cyclin B2
Ccnd1	NM_007631	Cyclin D1
Ccnd2	NM_009829	Cyclin D2
Ccnd3	NM_007632	Cyclin D3
Ccne1	NM_007633	Cyclin E1
Cdc42	NM_009861	Cell division cycle 42 homolog (S. cerevisiae)
Cdk2	NM_016756	Cyclin-dependent kinase 2
Cdk4	NM_009870	Cyclin-dependent kinase 4
Cdk6	NM_009873	Cyclin-dependent kinase 6
Cdkn1a	NM_007669	Cyclin-dependent kinase inhibitor 1A (P21)
Cdkn1b	NM_009875	Cyclin-dependent kinase inhibitor 1B

Cdkn1c	NM_009876	Cyclin-dependent kinase inhibitor 1C (P57)
Cdkn2a	NM_009877	Cyclin-dependent kinase inhibitor 2A
Cdkn2b	NM_007670	Cyclin-dependent kinase inhibitor 2B (p15, inhibits CDK4)
Cdkn2c	NM_007671	Cyclin-dependent kinase inhibitor 2C (p18, inhibits CDK4)
Cdkn2d	NM_009878	Cyclin-dependent kinase inhibitor 2D (p19, inhibits CDK4)
Chuk	NM_007700	Conserved helix-loop-helix ubiquitous kinase
Col1a1	NM_007742	Collagen, type I, alpha 1
Creb1	NM_133828	CAMP responsive element binding protein 1
Crebbp	NM_001025432	CREB binding protein
Dlk1	NM_010052	Delta-like 1 homolog (Drosophila)
E2f1	NM_007891	E2F transcription factor 1
Egfr	NM_007912	Epidermal growth factor receptor
Egr1	NM_007913	Early growth response 1
Elk1	NM_007922	ELK1, member of ETS oncogene family
Ets1	NM_011808	E26 avian leukemia oncogene 1, 5' domain
Ets2	NM_011809	E26 avian leukemia oncogene 2, 3' domain
Fos	NM_010234	FBJ osteosarcoma oncogene
Grb2	NM_008163	Growth factor receptor bound protein 2

Hras1	NM_008284	Harvey rat sarcoma virus oncogene 1
Hspa5	NM_022310	Heat shock protein 5
Hspb1	NM_013560	Heat shock protein 1
Jun	NM_010591	Jun oncogene
Kcnn1	NM_032397	Potassium intermediate/small conductance calcium-activated channel, subfamily N, member 1
Kras	NM_021284	V-Ki-ras2 Kirsten rat sarcoma viral oncogene homolog
Ksr1	NM_013571	Kinase suppressor of ras 1
Map2k1	NM_008927	Mitogen-activated protein kinase kinase 1
Lamtor3	NM_019920	Late endosomal/lysosomal adaptor, MAPK and MTOR activator 3
Map2k2	NM_023138	Mitogen-activated protein kinase kinase 2
Map2k3	NM_008928	Mitogen-activated protein kinase kinase 3
Map2k4	NM_009157	Mitogen-activated protein kinase kinase 4
Map2k5	NM_011840	Mitogen-activated protein kinase kinase 5
Map2k6	NM_011943	Mitogen-activated protein kinase kinase 6
Map2k7	NM_011944	Mitogen-activated protein kinase kinase 7
Map3k1	NM_011945	Mitogen-activated protein kinase kinase kinase 1
Map3k2	NM_011946	Mitogen-activated protein kinase kinase kinase 2
Map3k3	NM_011947	Mitogen-activated protein kinase kinase kinase 3

Map3k4	NM_011948	Mitogen-activated protein kinase kinase kinase 4
Map4k1	NM_008279	Mitogen-activated protein kinase kinase kinase kinase 1
Mapk1	NM_011949	Mitogen-activated protein kinase 1
Mapk10	NM_009158	Mitogen-activated protein kinase 10
Mapk11	NM_011161	Mitogen-activated protein kinase 11
Mapk12	NM_013871	Mitogen-activated protein kinase 12
Mapk13	NM_011950	Mitogen-activated protein kinase 13
Mapk14	NM_011951	Mitogen-activated protein kinase 14
Mapk3	NM_011952	Mitogen-activated protein kinase 3
Mapk6	NM_015806	Mitogen-activated protein kinase 6
Mapk7	NM_011841	Mitogen-activated protein kinase 7
Mapk8	NM_016700	Mitogen-activated protein kinase 8
Mapk8ip1	NM_011162	Mitogen-activated protein kinase 8 interacting protein 1
Mapk8ip2	NM_021921	Mitogen-activated protein kinase 8 interacting protein 2
Mapk8ip3	NM_013931	Mitogen-activated protein kinase 8 interacting protein 3
Mapk9	NM_016961	Mitogen-activated protein kinase 9
Mapkapk2	NM_008551	MAP kinase-activated protein kinase 2
Mapkapk5	NM_010765	MAP kinase-activated protein kinase 5

Max	NM_008558	Max protein
Mef2c	NM_025282	Myocyte enhancer factor 2C
Mknk1	NM_021461	MAP kinase-interacting serine/threonine kinase 1
Mos	NM_020021	Moloney sarcoma oncogene
Myc	NM_010849	Myelocytomatosis oncogene
Nfatc4	NM_023699	Nuclear factor of activated T-cells, cytoplasmic, calcineurin-dependent 4
Nras	NM_010937	Neuroblastoma ras oncogene
Pak1	NM_011035	P21 protein (Cdc42/Rac)-activated kinase 1
Rac1	NM_009007	RAS-related C3 botulinum substrate 1
Raf1	NM_029780	V-raf-leukemia viral oncogene 1
Rb1	NM_009029	Retinoblastoma 1
Sfn	NM_018754	Stratifin
Smad4	NM_008540	MAD homolog 4 (Drosophila)
Trp53	NM_011640	Transformation related protein 53

Comparing expression profiles at 6 h after either serum starvation or stimulation with serum and added growth factors, we observed a greater number effector genes displaying a significant difference in expression level in the wild type Ras MEF lines[Fig. 4.4]. Particularly in the PI3K array, there was no overlap in the significant simulation responsive genes between the wild type and oncogenic Ras lines[Fig.4.4]. This provides initial evidence that normal and oncogenic Ras on their own respond to upstream signals by generating different output. While the stimulation-responsive PI3K pathway genes in the wild type lines (e.g. down: *CDKN1B, TSC1*; up: *SHP2, JUN*) promote cell cycle, the stimulation-responsive genes in the oncogenic lines (e.g. down: *FOXO3, RBL2*; up: *SRF*) prevent apoptosis[Fig. 4.4]. MAPK pathway gene expression is not strongly affected by stimulation in the oncogenic Ras lines. The MAPK array genes that are stimulation responsive with significance across the wild type but not oncogenic Ras lines (e.g. down: *JIP1, JIP3, CDKN2D*; up: *MAP2K3, ETS1, MYC*) largely act in the JNK signaling pathway and promote cell cycle and survival over apoptosis[Fig. 4.4].

Directly comparing expression between the wild type and oncogenic Ras lines in either the starved or stimulated state allows for the assessment of differences in transcriptional regulation generated in either condition[Fig. 4.5]. In the starved state, we observe that the oncogenic and wild type Ras lines differentially regulate MAPK family genes involved in the stress response for survival. Notably, in the stimulated but not the starved state, the wild type Ras lines display significantly higher expression of growth promoting *IGF1, RAC1, CCNB1 and CCNB2*. This highlights the possibility that wild type and oncogenic Ras subvert the stress response and promote progression through mitosis relying on different sets of effector molecules in the major pathways.

4.2. iv. Oncogenic allele-specific differential regulation of KRAS effector genes

As we uncovered broad, isoform-independent differences between oncogenic and wild type Ras transcriptional output in the major effector pathways, we focused in on the most common isoform in cancer, KRAS4B, to analyze the two most prevalent mutations, G12D and G12V, for possible differences in comparison to the wild type and Rasless MEF profiles. Rasless MEFs reconstituted with KRAS G12D where treated as previously described and RNA samples were collected for expression analysis on PI3K and MAPK PCR arrays. This analysis was mirrored using Rasless MEFs with no reconstitution as a control for Ras-independent expression.

As expected, we observed a dramatic difference in the expression of Ras effector genes in the KRAS4B-driven cells versus the Rasless cells and these expression differences generally moved in the same direction across the allelic variants. The few genes that were differentially regulated between wild type and oncogenic KRAS variants in different directions from the Rasless level most often changed this directionality dependent on stimulation. On the PI3K and MAPK arrays, there were a total of 36 genes that displayed at least a two-fold difference between wild type and either oncogenic variant in either the starved or stimulated state[Fig. 4.6]. Most of these differences were observed in both conditions. There were also many significant expression differences observed between effector genes regulated by the G12D and G12V oncogenic KRAS alleles. For example, the CDK inhibitor and tumor suppressor *CDKN2B* (p15) is dramatically further downregulated in the KRAS G12D line in both conditions relative to the level in the KRAS G12V line. Another interesting finding was that the *Myc* oncogene, which also has tumor suppressive roles[65], is about 4-fold higher expressed in the G12V over G12D driven MEFs, under both conditions. Also potentially differentiating the signaling output of these two oncogenic KRAS variants, the G12D line upregulates the PLC effector Protein Kinase

C beta (*PRKCB*) while the G12V line oppositely downregulates *PRKCB* relative to the Rasless expression level.

4.3 DISCUSSION

There is mounting evidence that wild type Ras has tumor suppressive potential in the context of oncogenic Ras signaling in cancer[40-42, 66]. Whether this occurs primarily through direct interaction in heterodimers or via divergent downstream signaling and transcriptional regulation remains unclear. We display that the presence of wild type KRAS can affect the level of oncogenic KRAS dimerization observed in the plasma membrane. Under normal growth conditions, the major effector readouts of pAKT and pERK are suppressed by the presence of wild type KRAS in MEFs expressing the oncogenic G12D form at a similar level.

Comparing the signaling output of the KRAS variants at the level of transcriptional regulation, we observe distinct networks activated by the wild type and oncogenic forms. Though it is not surprising that the oncogenic form regulates fewer genes in a stimulation-dependent manner, we did not expect that there would be such distinct sets of genes regulated by the wild type and oncogenic forms. This novel finding supports the idea that wild type Ras may inhibit oncogenic Ras signaling through a separate, antagonistic transcriptional network. Closer analysis, including overexpression and knockout analysis, focused on particular genes shown to be differentially regulated will provide a better understanding of where there may be potential to harness the inhibitory effectors of wild type Ras to potentially dampen the oncogenic signal below the thresholds for tumor initiation and maintenance.

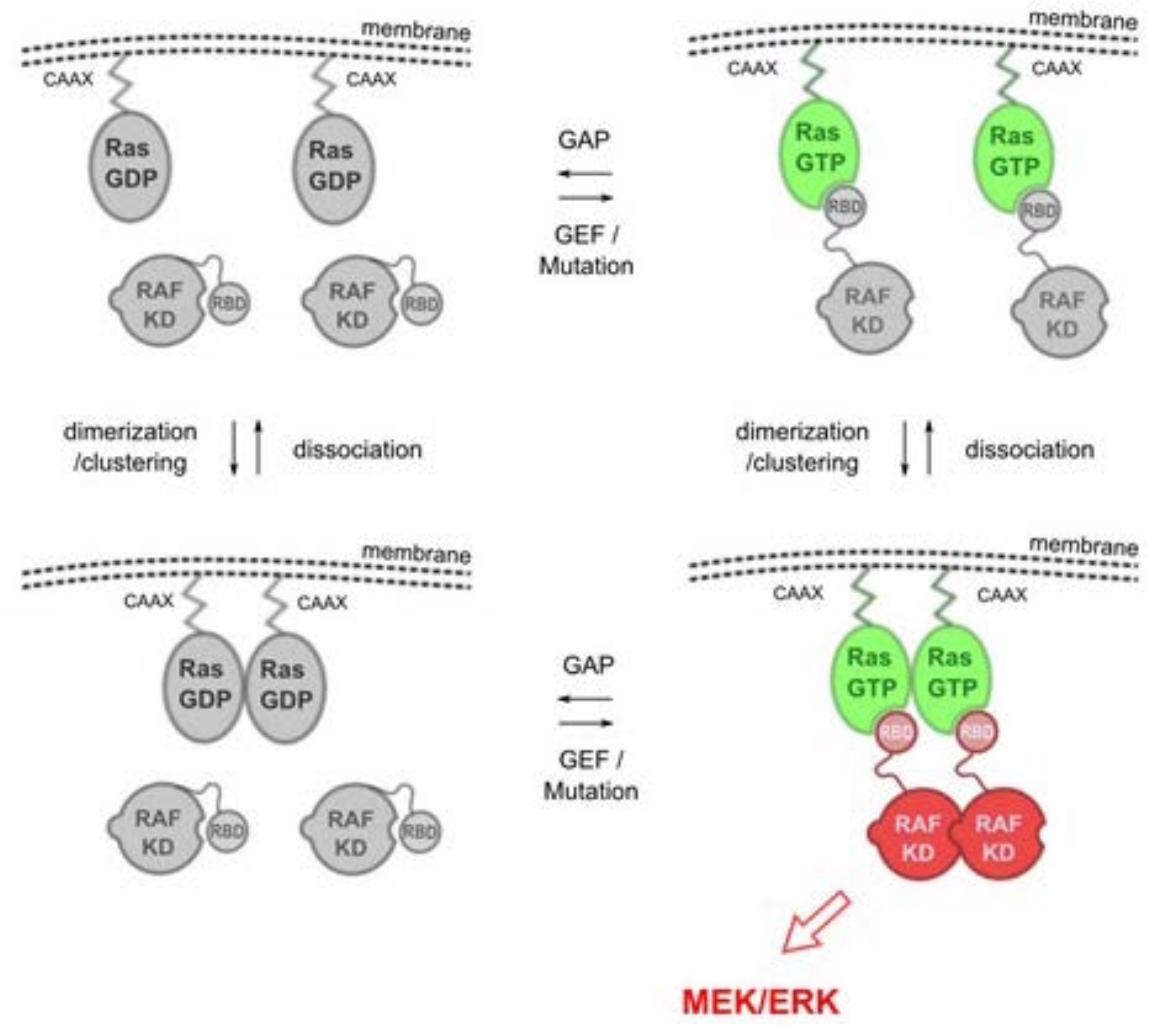

Figure 4.1. Proposed Ras dimerization model for MAPK signaling following Ras activation

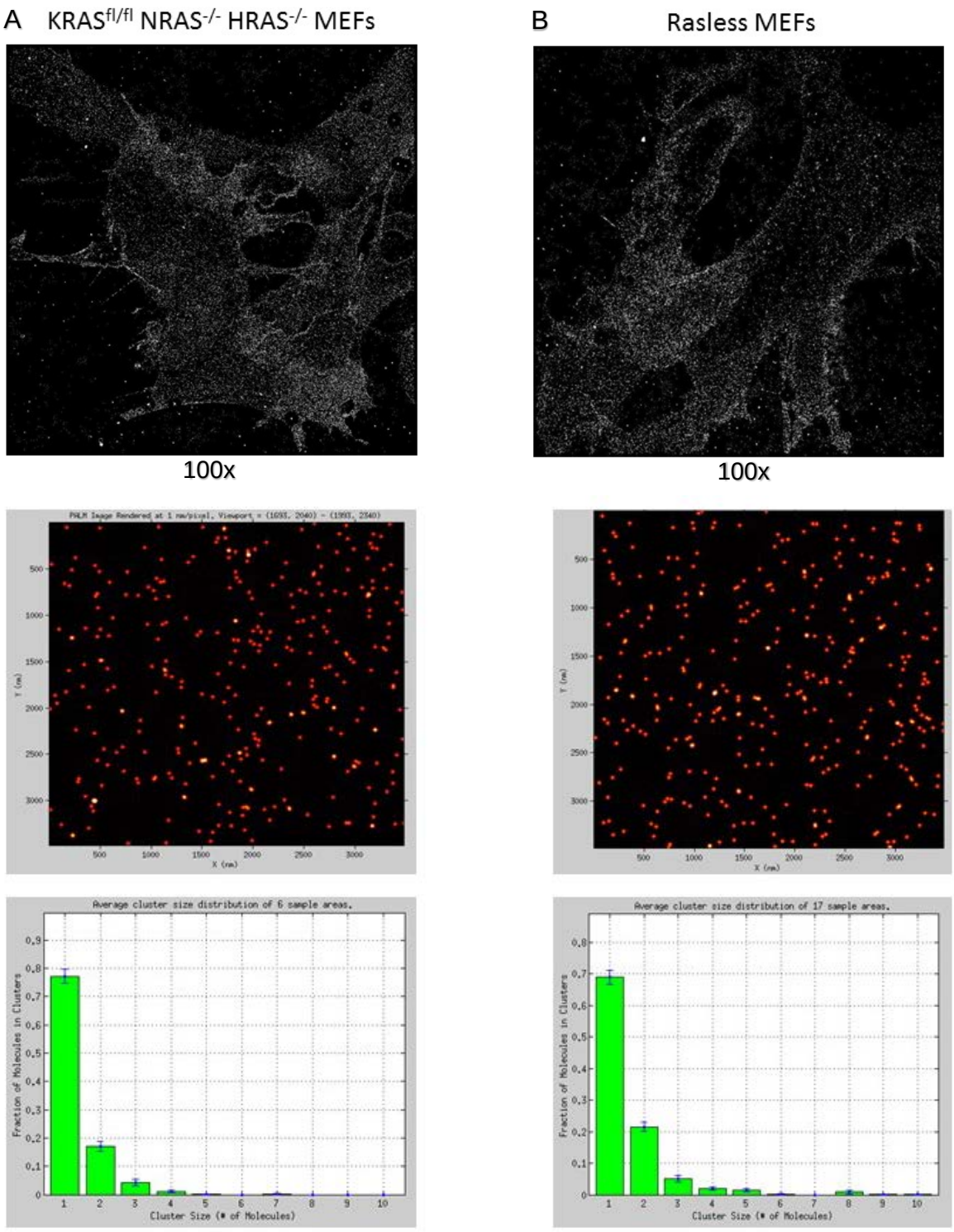

Figure 4.2. Superresolution imaging comparison of KRAS G12D membrane organization and clustering in MEFs before and after loss of wild type alleles

PAmCherry-KRAS G12D PALM images and quantification of clustering in $KRAS^{lox}$ (A) or Rasless (B) background.

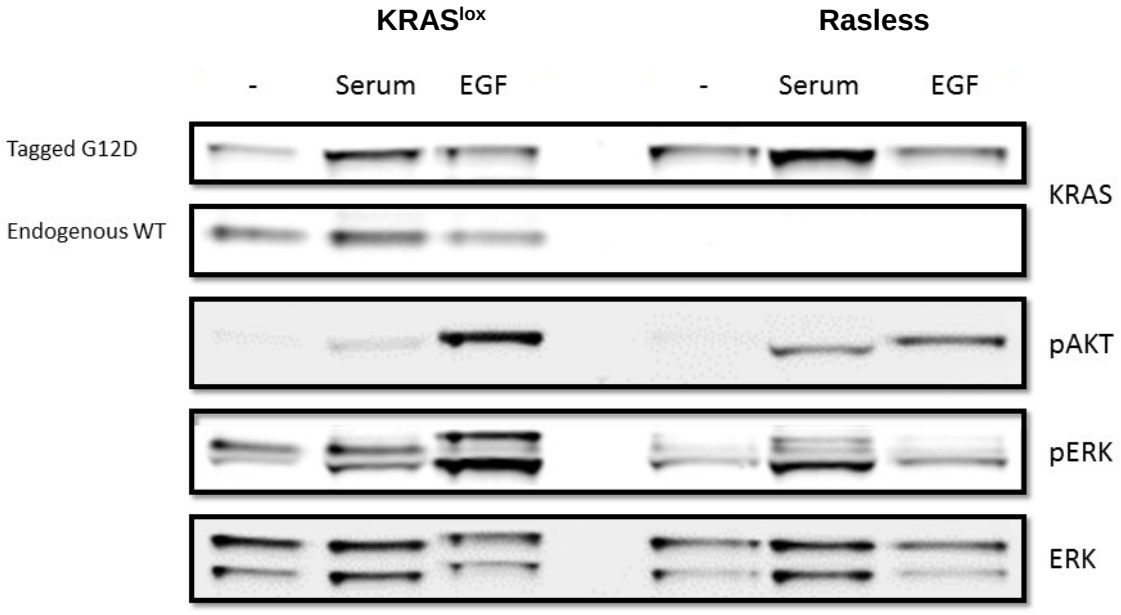

Figure 4.3. Loss of wild type KRAS alleles affects stimulation-dependent signaling of KRAS G12D transgenic MEFs

Western blot analysis of PI3K and MAPK effector signaling (pAKT S473, pERK, ERK) and KRAS expression in the PAmCherry-KRAS G12D transduced MEFs used for imaging.

PI3K Arrays



MAPK Arrays

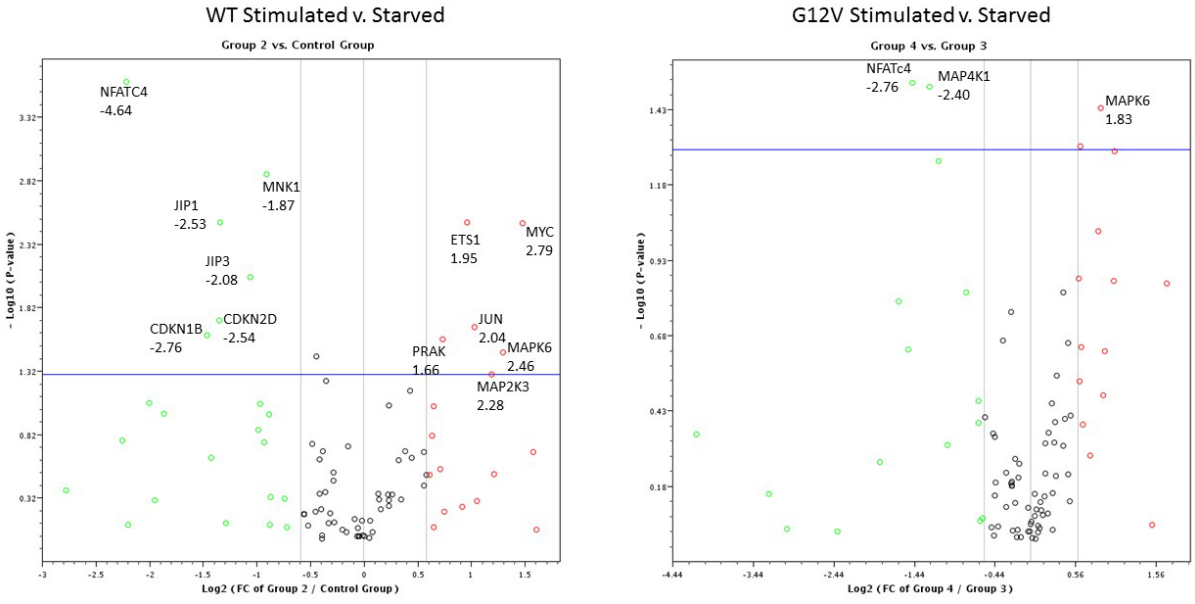

Figure 4.4. Stimulation-responsive expression changes of PI3K and MAPK pathway genes across Ras isoforms in wild type and oncogenic forms

Volcano plots displaying PI3K and MAPK pathway genes with differential expression dependent on growth conditions (green: higher starved, red: higher stimulated), across Ras isoforms (NRAS, KRAS4A and KRAS4B), either all WT or all G12V.

PI3K Arrays

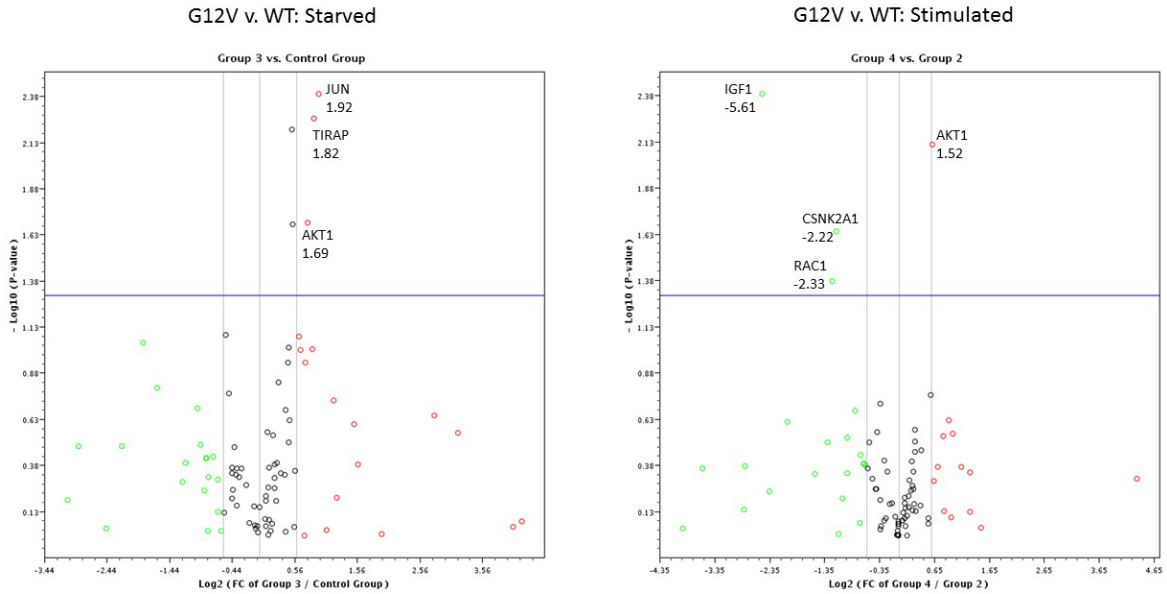

MAPK Arrays

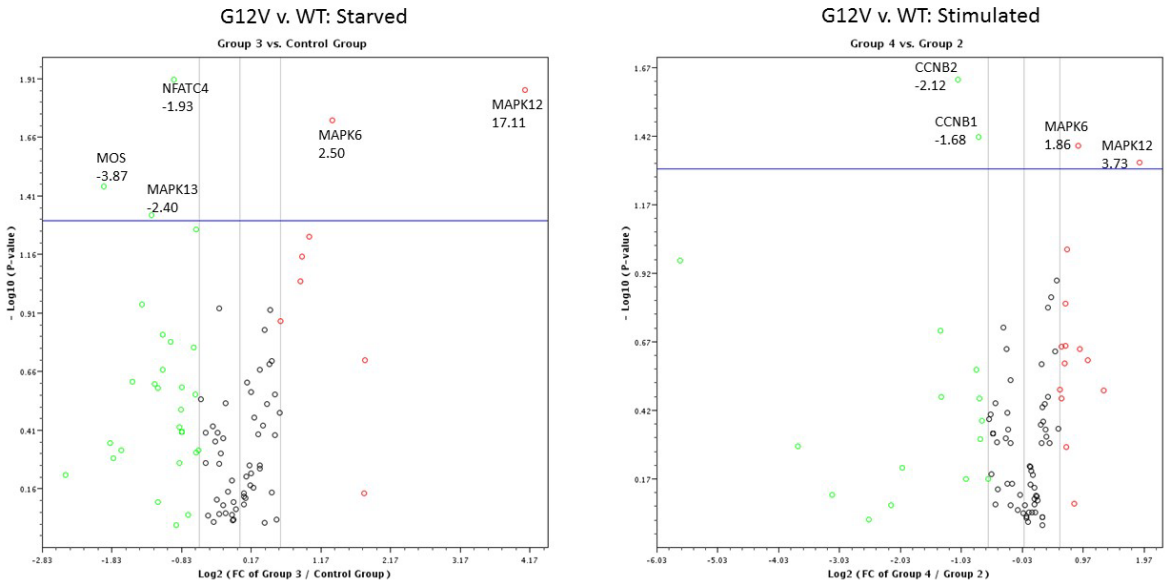

Figure 4.5. Oncogenic and wild type Ras produce significant differences in regulation of PI3K and MAPK pathway genes whether starved or stimulated

Volcano plots displaying PI3K and MAPK pathway genes with differential expression dependent on KRAS status (green: higher in wild type, red: higher in G12V), across Ras isoforms (NRAS, KRAS4A and KRAS4B), either all starved or all stimulated.

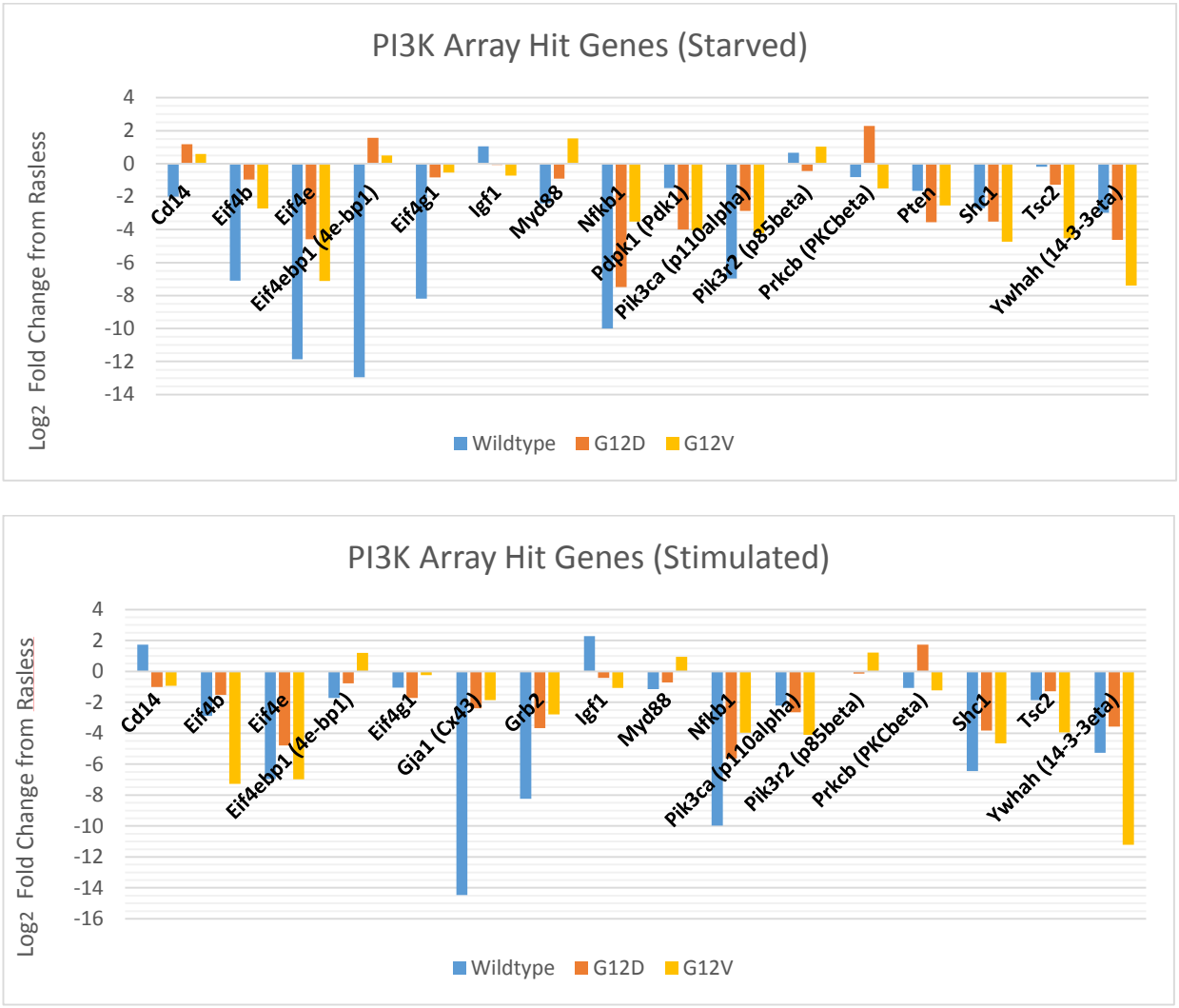

Figure 4.6. PI3K array genes showing over 2-fold differential expression between wild type and G12D or G12V KRAS4B MEFs

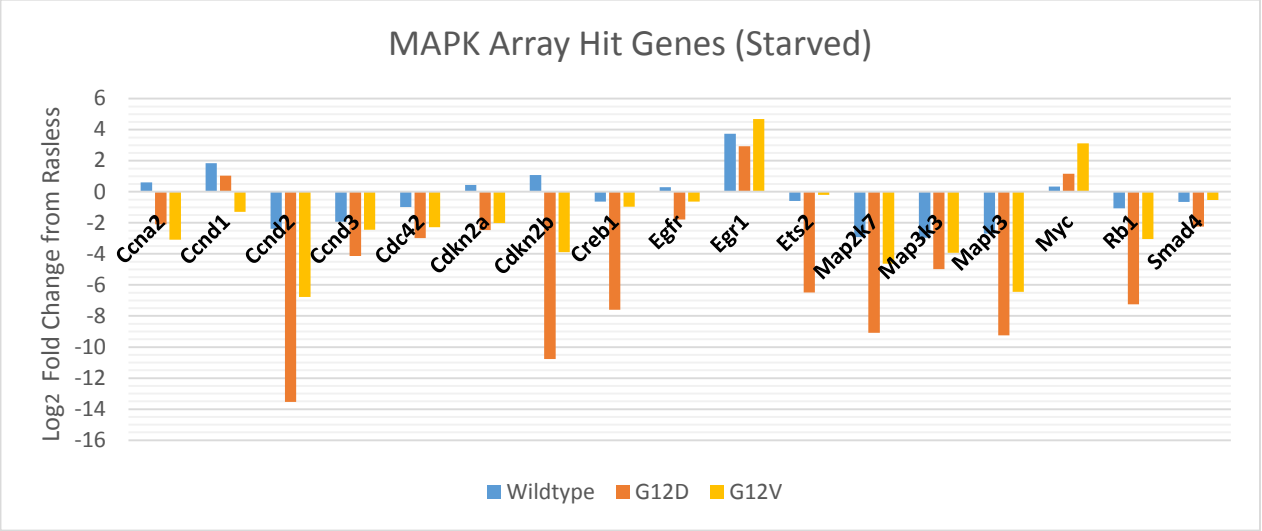

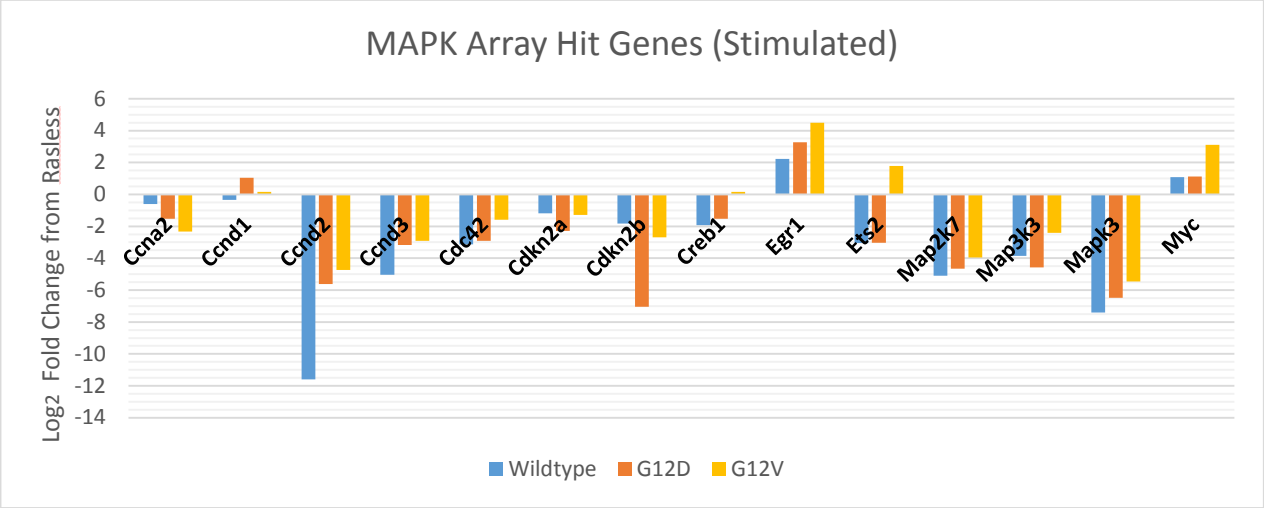

Figure 4.7. MAPK array genes showing over 2-fold differences in expression between wild type and G12D or G12V KRAS4B MEFs

CHAPTER 5.

ONCOGENIC KRAS MUTANTS RETAIN DEPENDENCE ON NUCLEOTIDE EXCHANGE AND LINK EGFR-PLC POSITIVE FEEDBACK SIGNALING TO MAPK ACTIVATION

5.1 INTRODUCTION

Ras proteins are critical switches in mitogenic signaling[1]. When in the active GTP-bound state, Ras proteins bind signaling effectors at the plasma membrane, resulting in their activation[2-5]. Of the three major Ras isoforms (*H-, N- and K-RAS*), the *KRAS* gene is most commonly mutated, a tumor-driving event occurring in 25-30% of human cancers[6, 7]. *KRAS* is most frequently point mutated at glycine 12 of the P-loop, producing an amino acid switch to aspartic acid, valine, cysteine or other products in minor frequencies. Interestingly, particular mutations are linked to certain tissue types[43]. Similarly, mutation of *NRAS* or, more rarely, *HRAS* are also linked to tissue type, though mutation of the catalytic residue glutamine 61 is very common (62% of *NRAS*, 36% of *HRAS* and 2% of *KRAS* mutations) in these genes[43]. The majority of glutamine 61 mutations produce an amino acid switch to histidine, leucine or arginine[43]. The variation in distribution of missense mutations observed in each cancer type implies significant functional differences in the signaling outputs of Ras variants.

Although oncogenic Ras mutants have long been viewed as constitutively active, differences in stability of the mutants in the GTP-bound state are linked to differences in oncogenic potential and patient survival[44, 45]. Mechanistically, mutation at G12 blocks entry of the arginine finger of GTPase activating proteins (GAPs), rendering these Ras variants insensitive to GAP-mediated inactivation and left with varied residual intrinsic GTPase activity[28]. Mutation at Q61 disrupts the transition state for GTP hydrolysis producing a constant “on state” [46]. Though it has be thought that oncogenesis by either of these mechanisms nullifies the role of recruitment of Ras guanine-nucleotide exchange factors (GEFs) in growth factor-induced Ras activation, definitive investigation of residual and alternative effects of upstream signals on Ras mutant proteins has been obscured by

the persistent activities of the remaining wild type allele and other Ras isoforms. Moreover, potential differences in oncogenic signaling between the various Ras mutants may be hidden by secondary genetic alterations particular to the cell lines or tumor samples under comparison. Our approach uses an isogenic system to compare the direct signaling effects of the major Ras oncogenes in the absence of other Ras proteins. The reversible proliferation phenotype of Rasless cells is the pleiotropic result of interplay among pro- and anti-proliferative, and stress-response pathways[67] that may be differentially invoked by distinct Ras variants.

The major effector proteins bound by GTP-loaded Ras are Raf, PI3K and RalGDS. Though PI3K and RalGDS can be activated by Ras-independent mechanisms in growth factor signaling, Ras is required to couple upstream signals to Raf and downstream MAPK activation[54, 55]. Furthermore, it has been shown that only constitutive activation of Raf, MEK and ERK kinases downstream of Ras can bypass the requirement for Ras proteins in proliferative signaling[56]. As all evidence has indicated that the MAPK cascade is essential for the growth effects of Ras in cancer, we focused on this pathway to read out the differences in output between Ras variants.

In this study we focus on the most commonly mutated cancer driver *KRAS* and demonstrate that significant differences can be observed between KRAS mutants at the levels of nucleotide exchange and connection of CRAF activation to downstream MAPK components. Phospholipase C (PLC) upregulates MAPK signaling by generating diacylglycerol (DAG) and inositol trisphosphate (IP3), activating PKC and calcium signaling. MAPK output downstream of mutant KRAS proteins displays differences in sensitivity to perturbation of PLC signaling. Using the “Rasless” MEF model[Fig. 5.1] to probe for unique dependencies of KRAS variants, we display that upstream receptor tyrosine kinase (RTK) signaling and the requirement for a second signal following GTP

loading of KRAS can be exploited to target MAPK hyperactivation in KRAS-driven cells characterized by particular mutation. Furthermore, PLC-Ca^{2+} signaling to ion channels potentiates the MAPK signal from KRAS variants in a differentially RTK-dependent manner.

5.2 RESULTS

5.2.i. Oncogenic KRAS mutants respond to growth factors

To assess differences in MAPK signaling between Ras alleles in a "Rasless" background, we started with the previously described $KRAS^{lox}$ MEFs[56, 61]. Treatment of these cells with 4-OHT for two weeks results in complete loss of Ras protein, through CRE-ER-mediated K-Ras excision. Loss of KRAS was confirmed by Western blot analysis[Fig. 5.3a], and by cell cycle arrest in the G1 phase, as reported previously [56]. These Rasless MEFs require Ras for MAPK activation[55]. To confirm the complete loss of Ras signaling in the Rasless MEFs, the cells were stimulated with EGF after serum-starvation and levels of pEGFR, pCRAF, pMEK, pAKT and pERK were measured. As expected, the Rasless MEFs are growth factor responsive, as measured by pEGFR and pAKT, but completely deficient in producing a MAPK response[Fig. 5.3a]. Rasless cells do express detectable levels of pERK. This basal MAPK signal was uanaffected by EGF stimulation, or by blocking PI3K signaling, though MEK inhibition eliminated Ras-independent pERK completely[Fig. 5.3a]. Reconstitution of Rasless MEFs with any of the wild type Ras isoforms (HRAS, NRAS, KRAS4A, KRAS4B) restored proliferation by re-sensitizing the cells to growth factor activation of MAPK signaling. The magnitude and kinetics of EGF signaling and the negative feedback response were similar across the Ras isoforms under direct comparison over a time course of EGF treatment following serum starvation[Fig. 5.3b].

Stable MEF lines derived from Rasless cells and driven by individual KRAS oncogenes were used to compare MAPK signaling generated by the three most common oncogenic KRAS mutants: G12D, G12V and G12C[Fig. 5.2]. To our surprise, all three oncogenic KRAS-driven lines displayed transient ERK activation in response to growth factor stimulation, peaking around 15 min of EGF treatment and returning to near basal levels by 1 h[Fig. 5.3c]. We then extended our analysis to include the rarely observed but more GTPase-deficient codon 61 mutants: Q61L and Q61R. While expression of the G12D form in Rasless cells results in restoration of sensitivity to EGF stimulation in the MAPK pathway, the codon 61 mutants did not respond at all to growth factor stimulation using pERK as the primary readout[Fig. 5.3d].

We set out to determine whether GTP loading of the KRAS proteins is the mechanism by which growth factors activate the MAPK pathway. Though it has been previously shown that oncogenic Ras has some potential for upstream stimulation[18, 19], it remains unclear whether this is true of all Ras mutants or if there is a range in the degree that oncogenic Ras-driven cells retain growth factor dependence. As EGFR ligand binding promotes CRAF oligomerization and activation at the membrane in a Ras-GTP dependent manner[20], EGF could promote MAPK signaling by increasing GTP loading with upstream activation of Ras, by activating downstream components of the MAPK pathway, or both.

To assess whether GTP loading of the varied KRAS mutants occurs in response to upstream RTK activation, we stimulated MEFs expressing KRAS G12C, G12D, G12V, Q61L or Q61R with EGF for 0, 5, 15 or 60 minutes following serum starvation, and measured Ras-GTP levels at each time point. Notably, the codon 12 mutants display substantial increases in GTP-bound KRAS immediately following EGFR activation while the codon 61 mutants do not[Fig. 5.4a-b]. The sensitivity of codon 12 mutants yields

transient ERK activation while the insensitive codon 61 mutants display no MAPK response downstream of stability active KRAS[Fig. 5.4a]. Further, the KRAS G12C MEF line displays a reduction to near basal KRAS activity by 60 min of treatment due to loss of pEGFR by negative feedback[Fig. 5.4a-b]. The dependence on sustained EGFR activation for maximal KRAS-GTP stability of the G12C mutant indicates that the protein possesses residual GTPase function acting as a significant deactivation force.

To evaluate the key functional difference between oncogenic KRAS mutants, we determined their intrinsic rates of GTP hydrolysis using purified proteins. The GTPase impairment of the mutant KRAS proteins we analyzed spans from the least catalytically active Q61R (about 160-fold slower than wild type) to the most active G12C (about 2.8-fold slower than wild type)[Fig. 5.4c]. These dramatic differences in enzymatic activity in vitro correlated with the extent that acute EGF stimulation increases the GTP-bound KRAS fraction and the durability of activation in MEF lines harboring matching KRAS mutations[Fig. 5.4a-c]. Though the Q61L mutant only displays about 2.4% of the GTP hydrolysis activity of wild type KRAS and appears constitutively activated in our MEF model, the finding that Q61R mutation confers a protein with only about one-fourth of the remaining intrinsic activity of KRAS Q61L may begin to explain the differences in tumor initiation potential between these two mutants when signaling alongside wild type KRAS[21], where the degree of competition may depend on the GTPase rate differential.

To determine whether the KRAS mutants are exclusively sensitive to EGFR activation or also dependent on other expressed RTKs, we briefly stimulated the codon 12 mutant MEFs with FGF and measured Ras-GTP levels before and after washing out the FGF for 1 h. FGF also stimulated nucleotide exchange for GTP-loading of KRAS codon 12 mutants, supporting investigation of the common mechanism of SOS recruitment to

phosphorylated RTKs as an explanation for oncogenic KRAS activation by growth factor signaling.

5.2.ii. GTP-loading of mutant KRAS in response to receptor tyrosine kinase signaling is SOS1-mediated

All activated growth factor receptors upstream of Ras contain homologous docking sites for Grb2, facilitating Ras-GEF recruitment[51]. In normal EGFR signaling, following ligand binding and autophosphorylation, Grb2 bound to the cytosolic Ras-GEF SOS1 is recruited to pY1068 and other phospho-sites on EGFR for catalysis of guanine-nucleotide exchange[68]. Constitutive membrane localization of SOS1 is sufficient for Ras activation[51]. Using full-length SOS1 fused with the H-Ras C-terminal tail (SOS-F), we assessed the effects of overexpression of membrane-localized SOS-F. As a control, we used a point mutant of SOS-F that lacks a functional CAAX box and is unable to localize to the plasma membrane (SOS-F*)[69]. We tested these SOS constructs on MEFs expressing the most intrinsically-active mutant, KRAS G12C and on the most GTPase-deficient KRAS Q61R. In KRAS G12C MEFs grown in serum and transfected with the SOS1 expression constructs, SOS-F produces approximately 3-fold greater Ras activation as measured by Ras-GTP pulldown assay and quantified using LICOR Image Studio™[Fig. 5.5a]. In KRAS Q61R MEFs, membrane localization of SOS1 has no effect, even with addition of EGF after serum starvation[Fig. 5.5b]. Conversely, transfection with siRNA depleting SOS1 in the KRAS G12C MEFs results in the loss of GTP loading (2% versus 23% increase in active KRAS fraction) in response to EGF stimulation[Fig. 5.5c]. These data support the idea that the most common oncogenic KRAS mutants retain significant intrinsic GTPase activity and can be further activated by growth-factor mediated SOS recruitment.

5.2.iii. Phorbol esters increase MAPK output by activating GTP-loading on mutant KRAS and by downstream signaling

EGFR activation in SOS1-depleted KRAS G12C MEFs still produces a MAPK signaling response at the basal level of KRAS activation, suggesting that another EGFR effector contributes to MAPK hyperactivation in a Ras-dependent manner[Fig. 5.5c]. Directly downstream of EGFR, phosphorylation of PLCγ regulates hydrolysis of phosphatidylinositol 4,5-bisphosphate (PIP2), forming the secondary messengers inositol triphosphate (IP3) and diacylglycerol (DAG) to trigger calcium flux and PKC activation. There is evidence that PLC and calcium signaling downstream of growth factor receptors requires active Ras, as it can be inhibited by Sprouty in competition with SOS1[25]. We hypothesized that a PLC-mediated signal downstream of EGFR could contribute to MAPK activation in the KRAS mutant MEF lines. KRAS-GTP binds CRAF at the plasma membrane where activated PKC can phosphorylate CRAF at S338 and induce kinase activity on the immediate downstream effector MEK[26]. PKC is also known to phosphorylate S181 of KRAS 4B in promoting oncogenic signaling[27]. Using PMA, a PKC agonist and potent tumor promoter, we find that increasing PKC activity amplifies MAPK signaling in KRAS G12C MEFs by stimulating GTP loading of KRAS and by phosphorylation of CRAF at activation site S338[Fig. 5.6a-b].

Inhibition of either PLC or PKC prior to growth factor stimulation of KRAS-driven cells reduces KRAS-GTP accumulation and downstream ERK activation[19]. There is also evidence that activators of PKC may increase SOS activity by direct phosphorylation[28] or generating a binding site for the SH2 domain of Grb2-SOS at the membrane for EGFR-independent KRAS activation[29]. We find that GTP loading of KRAS G12C in response to PMA is SOS1 dependent, as SOS1 knockdown results in a loss of KRAS-GTP and

impaired MAPK induction in response to PMA[Fig. 5.6c-d]. Though oncogenic KRAS holds an elevated level of CRAF at the membrane producing the basal MAPK signal, without recruitment of additional CRAF to the membrane in the SOS1-deficient PMA response, there is no S338 phosphorylation and weakened downstream MAPK activation in response to the tumor promoter[Fig. 5.6c].

5.2.iv. KRAS 4B variants display a differential requirement for PLC in MAPK activation

While there is evidence that calcium flux enhances signaling from active Ras[70-73], the extent that oncogenic KRAS mutants retain dependency on PLC-generated calcium signals is unclear. By briefly treating our MEF lines with either PLC inhibitor U73122 or PLC agonist m3M3FBS, we can assess the KRAS status-dependent differences in sensitivity to PLC modulators in MAPK signaling. We find that PLC inhibition reduces basal the MAPK signal in G12 but not Q61 mutants[Fig. 5.7]. MAPK signaling is not greatly affected by inhibition or activation of PLC in wildtype KRAS MEFs[Fig. 5.7], suggesting that PLC-Ca^{2+}-MAPK signaling may depend on active Ras.

To determine the extent that PLC inhibition blocks the KRAS-dependent response to stimulation, MEFs pretreated with DMSO or the PLC inhibitor U73122 were briefly stimulated with EGF or PMA, then MAPK signaling responses were assessed by western blot. These treatments produced no effect on the weak Ras-independent MAPK signal in Rasless MEFs[Fig. 5.8a]. Evaluating the effects on oncogenic KRAS signaling, PLC inhibition impairs the basal MAPK signal and blocks responsiveness to growth factor or phorbol ester stimulation[Fig. 5.8a]. A striking exception appears in the ability of KRAS G12D MEFs to respond to PMA stimulation when PLC is inhibited[Fig. 5.8a]. Additionally, the basal pERK signal from wild type KRAS is significantly less affected by loss of PLC

activity than observed with the oncogenic mutants[Fig. 5.8a]. Human pancreatic ductal carcinoma (PDAC) lines also display the KRAS genotype-linked differences in the PLC-dependence of MAPK responses to PMA observed in the MEF model[Fig. 5.8b]. Using the same PDAC lines in complete media, increasing concentration of PLC inhibitor results in significant reduction of MAPK signaling specifically in the KRAS G12V-driven KP-3 cells[Fig. 5.9].

5.2.v. Requirement for PLC in phorbol ester-induced CRAF-MAPK signaling complexes differs between oncogenic KRAS mutants

While valine or cysteine at codon 12 of KRAS yields a PLC-dependent MAPK response to PMA stimulation, mutation to aspartic acid yields a PLC-independent MAPK response[Fig. 5.8a,c]. Conformational differences between the KRAS mutant proteins provide a possible explanation for differences in their recruitment of regulatory proteins to signaling complexes, though the role of PLC in this level of regulation is unclear. To address this question, we looked for differences between the KRAS G12C and G12D MEFs in PLC regulation of KRAS and CRAF complexes. MAPK signaling between these two KRAS mutants diverges when comparing the PMA-stimulated cells after pre-treatment with either PLC inhibitor or a non-targeting analog. PLC inhibition blocks the PMA-induced MAPK signal in KRAS G12C but not G12D MEFs, though KRAS activation status is unaffected regardless of the mutation[Fig. 5.8c].

Using a Ras-specific antibody for immunoprecipitation of KRAS proteins in the MEF lysates, we observe a loss of binding to the MAPK signal promoting-scaffold KSR1 with PLC inhibition[Fig. 5.8d]. KRAS G12C shows a significantly greater affinity for KSR1 and PLC inhibitor decreases binding to a similar level to that of KRAS G12D treated with

the inactive analog, associated with a reduction of similar magnitude in KRAS-bound pMEK[Fig. 5.8d]. Immunoprecipitation of CRAF and immunoblotting for proteins known to regulate CRAF phosphorylation status suggests that KRAS G12D may remain PMA-responsive by evading PP2A regulation following PLC inhibition. When PP2A structural subunit A is recruited to CRAF following loss of PLC activity, CRAF is dephosphorylated at S338 while inactivation by S259 phosphorylation is maintained[Fig. 5.8e]. In suppression of mitogenic signals, PP2A is known to regulate Ras signaling in G2 to promote quiescence and normal G1 length[74]. Our findings suggest that the threshold for this effect of PP2A may vary depending on the particular KRAS mutant participating in PP2A recruitment to MAPK signaling complexes.

5.2.vi. Activation of PLC-responsive channel TMEM16A triggers MEK-ERK signaling in an EGFR-dependent manner

Downstream of PLC signaling, calcium flux activates membrane-bound sensors to induce specific membrane-bound metalloproteases (ADAMs) for EGFR-ligand shedding[34]. TMEM16A (i.e. ANO1) is a critical component of calcium-responsive chloride channels[35-37]. The TMEM16A gene is amplified in many human cancer types and its product has been shown to couple with the IP3 receptor, activate EGFR and induce MAPK[38, 39]. TMEM16A up-regulation plays roles in growth, migration and apoptosis, varying in cancers dependent on MAPK signaling[40, 41]. For these reasons, we investigated a potential key role for TMEM16A in connecting the EGFR-PLC-Ca^{2+} signaling axis to the MAPK responses potentiating active KRAS in the MEF lines.

In Rasless cells, pharmacologic activation of TMEM16A with the compound Eact[42] after serum-starvation is sufficient to induce phosphorylation of PLCγ at

S1248[Fig. 5.10a], an activation site known to be regulated by EGFR signaling[43]. Though this suggests that TMEM16A activation is sufficient for initiation of a Ras-independent autocrine-loop in EGFR signaling, there is no MAPK response in the absence of KRAS[Fig. 5.10a]. After reconstitution with wild type KRAS, Eact is sufficient to induce MAPK signaling in the MEFs[Fig. 5.10b]. As the Eact response is completely lost when the cells are pretreated with erlotinib, the mechanism of activation in these cells is RTK-dependent[Fig. 5.10b]. We observed that this TMEM16A-EGFR-MAPK response is largely mediated by activation of KRAS in a positive feedback loop that potentiates mutant signaling[Fig. 5.12]. Knockdown of TMEM16A activates MAPK through disruption of negative regulation of EGFR, as this increase in signal is lost with erlotinib[Fig. 5.10c]. In KRAS G12D MEFs, we observe an increase of approximately 11% in the KRAS-GTP/total KRAS ratio and induction of downstream MAPK signaling after brief TMEM16A activation using Eact[Fig. 5.10d]. Pretreatment with either SOS1 siRNA or erlotinib reduces active KRAS and MAPK response to Eact[Fig. 5.10d]. Moreover, combination of these two methods of upstream KRAS blockade completely removes the KRAS activation response to Eact and strongly impairs MAPK signaling of KRAS G12D MEFs[Fig. 5.10d].

Given the potential for this mechanism of MAPK activation in human cancer as a KRAS genotype-specific route of signaling dependent on extent of sensitivity to EGFR, we treated a KRAS wild type, codon 12-mutant and codon 61-mutant cancer cell lines with a titration of Eact after pretreatment with either DMSO or erlotinib. Consistent with our findings on KRAS status-dependent EGFR sensitivity in the MEF model, KRAS wild type BxPC-3 cells display a clear EGFR-dependent dose-response to Eact, KRAS codon 12-mutant PDAC-08-13 cells display a dampened but largely EGFR-dependent response and KRAS codon 61-mutant Hs766T cells display a dose-dependent MAPK response to Eact that is disconnected from EGFR activity[Fig. 5.11a-c]. We confirm that oncogenic KRAS

mutants display significant differences in their reliance on upstream signals for MAPK activation in cancer signaling.

5.3 DISCUSSION

KRAS proteins function as key membrane-bound nodes for the nucleation of protein complexes in which many additional regulators of MAPK signal transduction may bind. Both differences in protein structure between KRAS mutants and in their GTPase activities may affect the signaling networks that KRAS regulates. These differences between the mutant proteins may potentially be exploited to target KRAS variants dependent on particular second signals for their MAPK output. Recognizing the requirement for a second signal following GTP-loading of KRAS provides an opportunity to target KRAS mutant cancers that have proven elusive in effective therapy [7].

The major Ras isoforms are necessary for growth signaling through the MAPK pathway[56]. Rasless MEFs reconstituted with wild type Ras display restored EGF sensitivity with similar response kinetics regardless of the Ras isoform. This suggest that localization differences between the isoforms due to differences in their post-transcriptional modification do not have a major effect on access to upstream signals and GAP-mediated negative feedback. For this reason, we focused on comparisons within KRAS mutant signaling rather than across isoforms, though there is evidence that the same mutation in different isoforms may confer different levels of tumorigenicity. For example, NRAS Q61R and KRAS G12D but not NRAS G12D are sufficient to produce melanomas, possibly due to differences in stability of the active GTP-bound state[45].

In previous studies examining the basic signaling functions of Ras oncogenes in various cancer models, the oncogenic output has been obscured by the assortment of Ras

signals in the model system, displaying a combinatorial signal output. Using Ras-knockout MEFs as the isogenic background for this study has granted a unique opportunity to determine the sensitivities of particular mutants to upstream signals as can only be accurately measured in a Rasless backround. Most notably, we provide evidence that differences in the intrinsic GTPase activity of KRAS mutants can be observed by measuring GTP-loading in response to growth factor stimulation. Ostrem et al. have developed compounds which use the mutant cysteine of KRAS G12C to allosterically alter the native nucleotide preference to favor GDP over GTP[63]. Together with our finding that the KRAS G12C mutant relies on SOS-mediated guanine nucleotide exchange to maintain activation, these results support the testing of G12C-specific compounds regulating nucleotide preference in combination with upstream RTK inhibition to promote accumulation of the protein in the inactive GDP-bound state. Additionally, our finding that the loss of SOS1 combined with EGFR inhibition reduces KRAS activation and MAPK output in KRAS G12D-driven cells displays the potential value of small molecules that bind KRAS and inhibit SOS-mediated activation[31] for combination therapies targeting the most common KRAS mutation.

In the oncogenic KRAS context, it has been unclear whether PKC signaling potentiates active KRAS directly by further increasing GTP-loading or downstream by kinase activity in the MAPK cascade. While there is clear evidence that CRAF phosphorylation is a key second step in signaling downstream of active Ras[73], the assessment of direct KRAS activation has been difficult. Although phorbol esters may induce PKC-dependent SOS phosphorylation to increase GEF activity independent of EGFR[75], we do not detect an electrophoretic mobility shift in SOS1 in response to PMA. The most likely mechanism for engagement of SOS1 by PMA-activated PKC is direct

membrane recruitment through PKC autophosphorylation generating a binding site for the SH2 domain of the SOS1 adaptor protein Grb2[76].

PLC mediates MAPK signal transduction through PKC and calcium signaling[52]. KRAS mutants differentially recruit the regulatory phosphatase PP2A in signaling complexes that can be modulated by PLC inhibition, producing differences in MAPK sensitivity. Scaffolds facilitate the dynamic behavior of Ras-MAPK signaling[3, 4, 77]. KSR1 has been shown to be a necessary link in Ras-Raf signaling, regulating oncogenic Ras engagement with MAPK[2, 5]. KSR1 and KSR2 both interact with components of the MAPK cascade though KSR2 is not expressed in MEFs[78, 79]. On KSR scaffolds, CRAF is subject to phosphoregulation which desensitizes CRAF to stimuli until hyperphosphorylation is relieved by PLC-responsive PP2A activity[3, 4]. We suspect that the differences in levels of KSR1 binding observed between KRAS mutants may be due to allosteric effects amplified from the amino acid substitution in the active site.

Following PLC-mediated calcium flux, TMEM16A activation cooperates with KRAS in a positive feedback loop through EGFR activation, connecting active CRAF to MEK and ERK[Fig. 5.12]. As IP3R activity is sufficient to promote EGFR signaling in *C. elegans*, this response to calcium flux performs as a highly conserved mechanism for growth signaling[80]. Following stimulation, calcium flux activates the ADAMs family of membrane metalloproteases for shedding of various EGFR ligands[81]. Human cancers commonly invoke this autocrine EGFR response to ionic flux[81, 82]. Consistent with our finding that TMEM16A activation in PDAC lines triggers MAPK signaling in a variably EGFR-dependent manner by strength of KRAS mutation, others have shown that mutant KRAS can activate ADAM17 for autocrine EGFR signaling necessary for pancreatic tumor growth[83]. Furthermore, the combination of erlotinib with the mainstay treatment for

advanced pancreatic cancer, gemcitabine, has demonstrated statistically significantly improved survival in a phase III clinical trial[84].

Here, we show that mutant KRAS proteins possess distinct biochemical properties affecting their activation status and requirements for maximal MAPK signaling. We show that the most common KRAS driver mutations in human cancer do not result in complete loss of sensitivity to upstream growth factor signaling in SOS-mediated activation and cooperative downstream signaling. Since recent efforts have revealed druggable pockets in Ras in which small molecules can modulate SOS activity[85, 86], the discovery that KRAS mutants display varied levels of reliance on SOS for modulation of their activity in response to growth promoters may predict patient subsets that would be responsive to these KRAS-targeted approaches. Additionally, we have found that particular KRAS variants display a requirement for PLC signaling in generating MAPK signaling responses. By both EGFR-dependent and -independent mechanisms, calcium signaling to TMEM16A reduces the threshold for activation of MAPK by KRAS. These avenues present potential opportunities to exploit the particular dependencies of cancers characterized by their KRAS mutation. As RTK inhibitors are commonly used in cancer therapy, but generally with the exclusion of KRAS mutant patients, the greater implication of this study is that closer analysis of the upstream dependencies of particular KRAS mutants may allow for the effective use of available inhibitors of growth factor signaling. Combination therapies on both sides of RAS in RTK signaling may result in significant blocks to MAPK feedback and show clinical benefits.

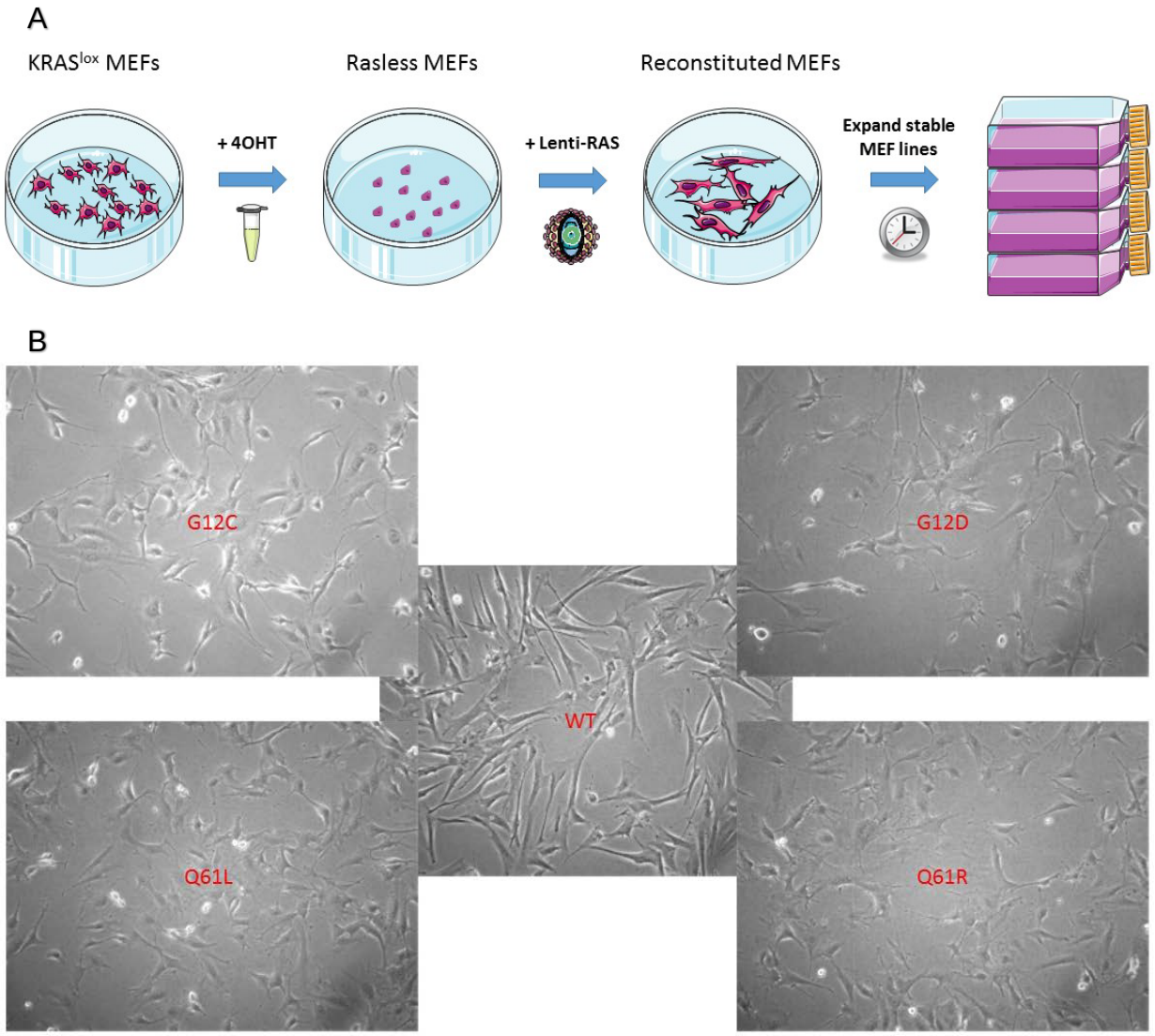

Figure 5.1. Generating MEF lines for comparison of Ras variants without background

(A) Basic schematic model for generation of MEF lines expressing single Ras variants from KRAS^{lox} MEFs through an intermediate Rasless cell state, using proliferation as the primary readout for loss and gain of Ras function.

(B) 16x images of KRAS4B reconstituted MEF lines (WT, G12C, G12D, Q61L, Q61R).

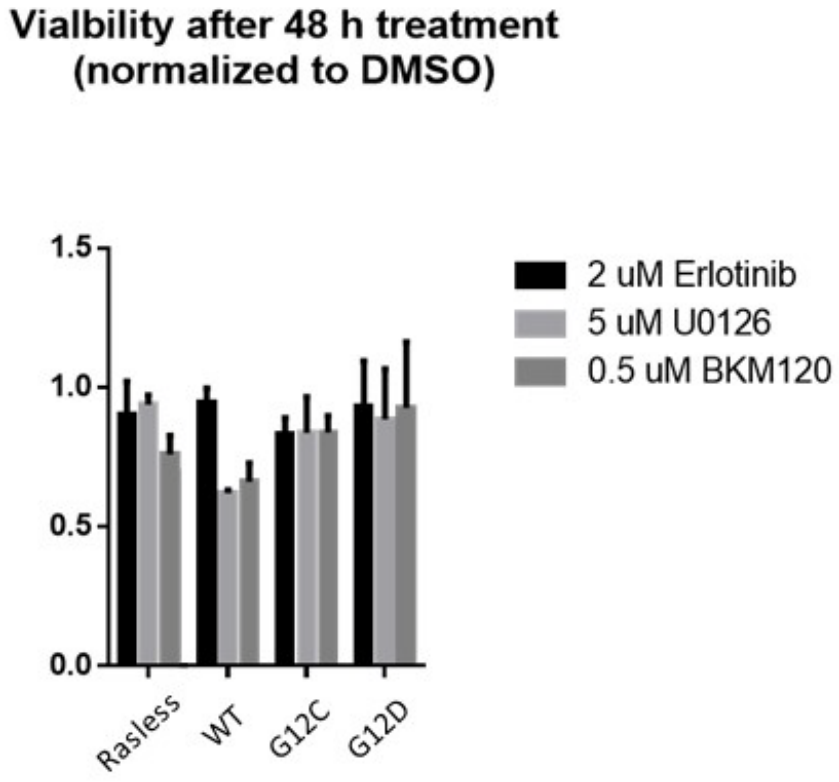

Figure 5.2. Comparing effects of EGFR-Ras signaling inhibitors by KRAS genotype

Histogram of MTS assay reads normalized to DMSO treatment within each MEF line after 48 h with 2 μM EGFR inhibitor erlotinib, 5 μM MEK inhibitor U0126 or 0.5 μM PI3K inhibitor BKM120. (error bars represent 95% confidence limits)

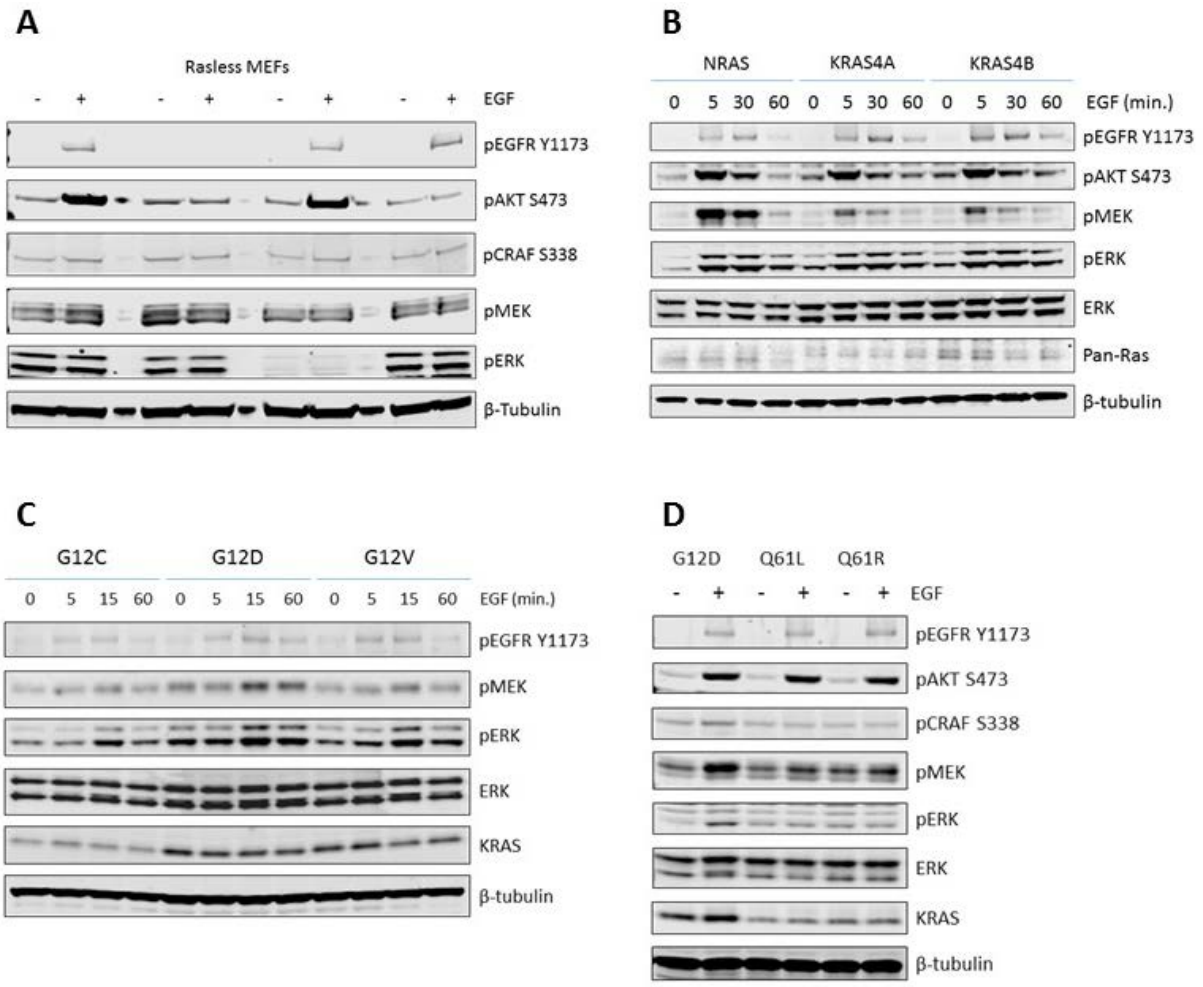

Figure 5.3. MEF lines display Ras-dependent EGFR-MAPK signaling responses

(A) Western blot analysis of EGFR, AKT, CRAF, MEK and ERK activation in Rasless cells after 6 h complete serum starvation with addition of 1 μM erlotinib (EGFRi), 20 μM U0126 (MEKi), 1 μM BKM120 (PI3Ki) or DMSO during the final hour of starve, followed by a 5 min stimulation with 30 ng/mL EGF. β-Tubulin expression served as a loading control.

(B) Western blot analysis of EGFR, AKT, MEK and ERK activation, total ERK levels and Ras expression in MEF lines driven by wild type NRAS, KRAS 4A or KRAS 4B after 4 h complete serum starvation and stimulation for 0, 5, 30 or 60 min with 30 ng/mL EGF. β-Tubulin expression served as a loading control.

(C) Western blot analysis of MEK and ERK activation, total ERK levels and KRAS expression in MEF lines driven by KRAS G12C, G12D or G12V after 4 h complete serum starvation and stimulation for 0, 5, 15 or 60 min with 50 ng/mL EGF. β-Tubulin expression served as a loading control.

(D) Western blot analysis of oncogenic [G12D/Q61L/Q61R] KRAS-induced MAPK activation in response to stimulation with 50 ng/mL EGF for 10 min a following 6 h of complete serum starvation in MEFs lacking endogenous Ras. β-Tubulin expression served as a loading control.

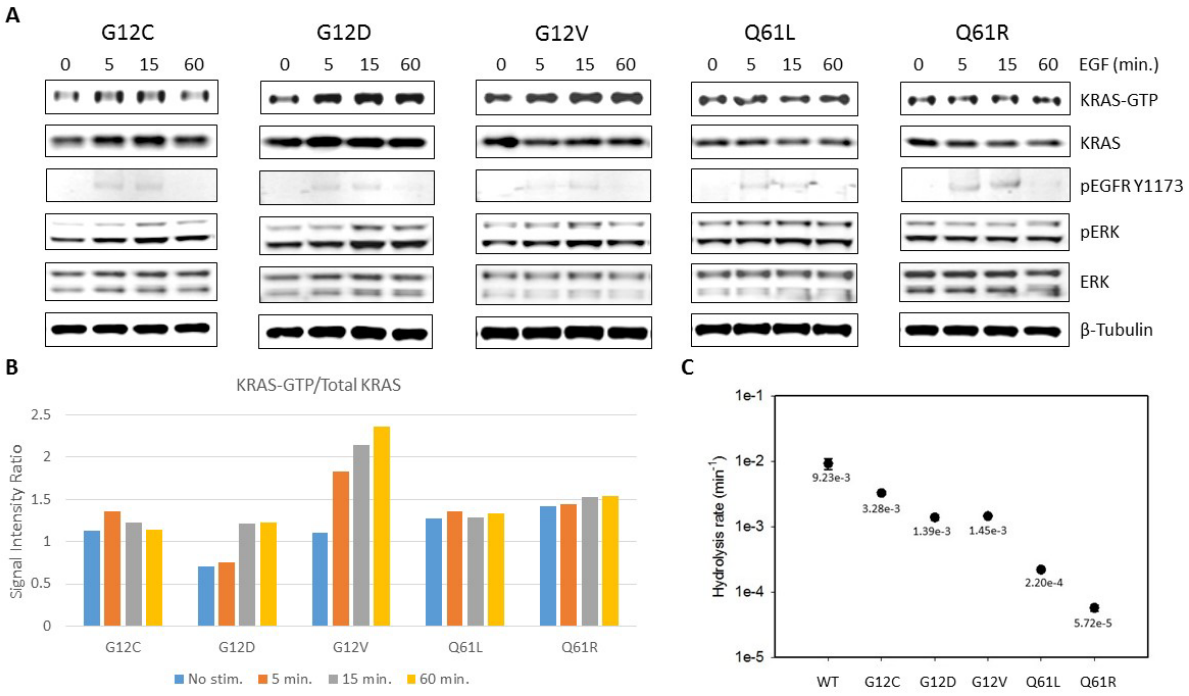

Figure 5.4. Oncogenic KRAS mutants display differences in their persisting dependency on EGFR signaling for GTP loading and MAPK signaling

(A) Western blot analysis of KRAS-GTP fractions precipitated from KRAS G12C, G12D, G12V, Q61L or Q61R MEFs using Raf-RBD beads and total KRAS, pERK and total ERK in 5% of the input lysates used for the Ras activity assay. Cells were harvested after treatment with 50 ng/mL EGF for 0, 15, 30 or 60 min following 6 h of complete serum starvation. β-Tubulin expression served as a loading control.

(B) LICOR Image Studio™ quantification of the ratio of KRAS-GTP levels to total KRAS levels from the western blot analysis in (A) is depicted in a histogram.

(C) Plot displaying the intrinsic rates of GTP hydrolysis calculated for purified KRAS proteins. (Mean rates calculated from 3-6 measurements, error bars indicate 95% confidence limits)

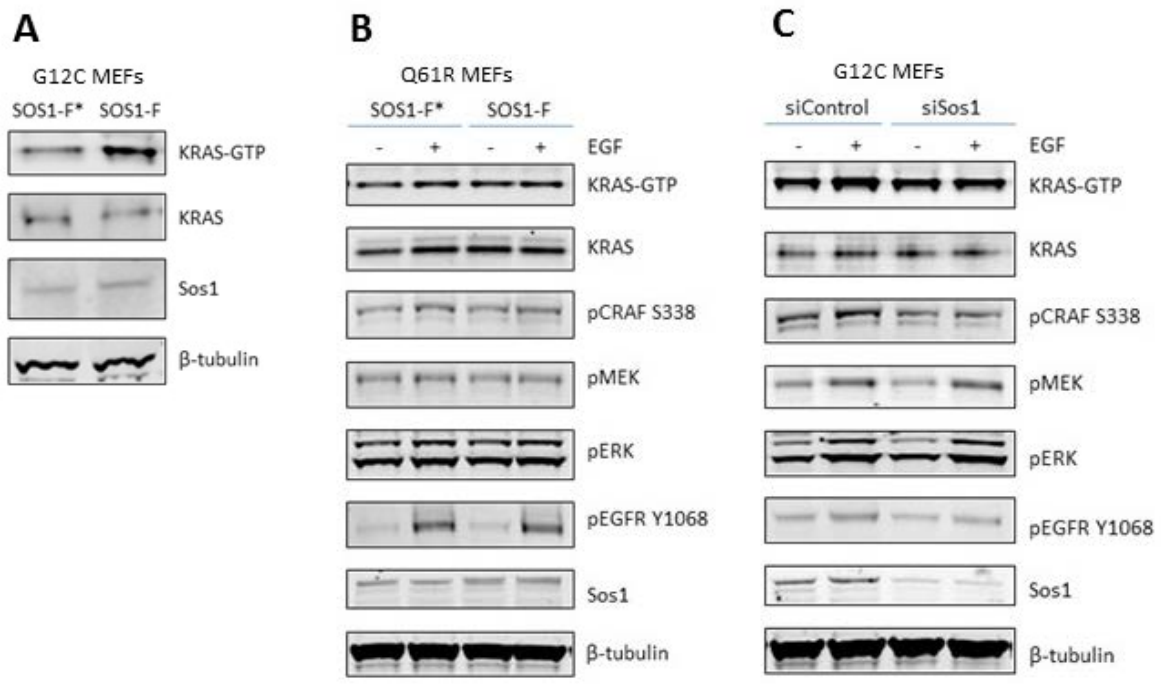

Figure 5.5. GTP loading of oncogenic KRAS in response to growth factors is SOS1-mediated

(A) Western blot comparison of the KRAS response to expression of cytosolic SOS1-F* or membrane-localized SOS1-F 32 h after transfection in the presence of serum, using KRAS G12C MEFs. SOS1 expression was also assessed and β-tubulin expression served as a loading control.

(B) Western blot analysis of KRAS activation and MAPK signaling in KRAS Q61R MEFs after 32 h expression of either SOS1-F* or SOS1-F ending in 4 h of complete serum starvation, with or without a 10 min EGF stimulation at 50 ng/mL. SOS1 expression was also assessed and β-tubulin expression served as a loading control.

(C) Western blot analysis of KRAS activation and MAPK signaling in KRAS G12C MEFs 52 h after transfection with siRNA targeting endogenous SOS1 or a control GFP-targeting siRNA. Cells were switched to serum-free media for the final 4 h then treated with 50 ng/mL EGF or left untreated. Knockdown efficiency was assessed by SOS1 protein expression levels and β-tubulin expression served as a loading control.

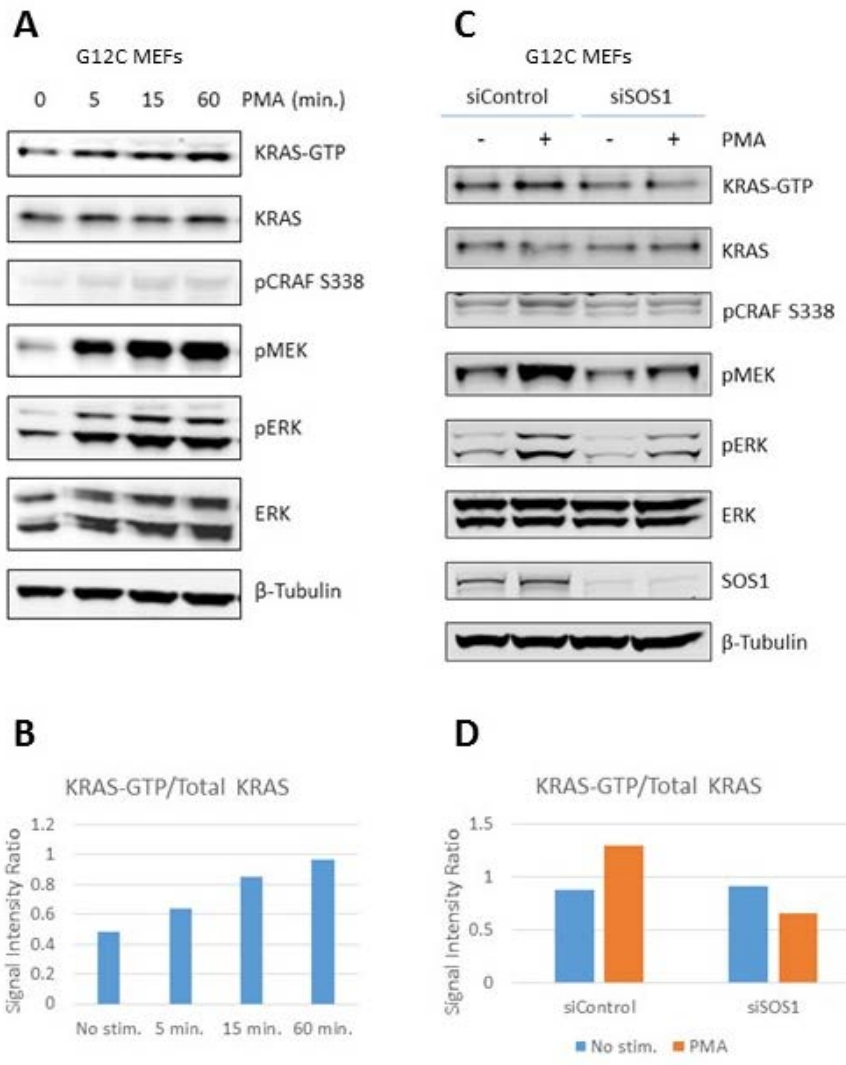

Figure 5.6. Phorbol esters amplify MAPK signaling upstream and downstream of oncogenic KRAS

(A) Western blot analysis of KRAS activation and MAPK signaling in KRAS G12C after 4 h of complete serum starvation before harvesting cells or 5, 15 or 60 min treatment with 200 ng/mL PMA. β-Tubulin expression served as a loading control.

(B) LICOR Image Studio™ quantification of the ratio of KRAS-GTP levels to total KRAS levels from the western blot analysis in (A) is depicted in a histogram.

(C) Western blot analysis of KRAS G12C activation, MAPK signaling and SOS1 knockdown after transfection for 48 h with non-targeting control siRNA or SOS1 siRNA and 4 h of complete serum starvation followed by a 15 min treatment with DMSO or 200 ng/mL PMA. β-Tubulin expression served as a loading control.

(D) LICOR Image Studio™ quantification of the ratio of KRAS-GTP levels to total KRAS levels from the western blot analysis in (C) is depicted in a histogram.

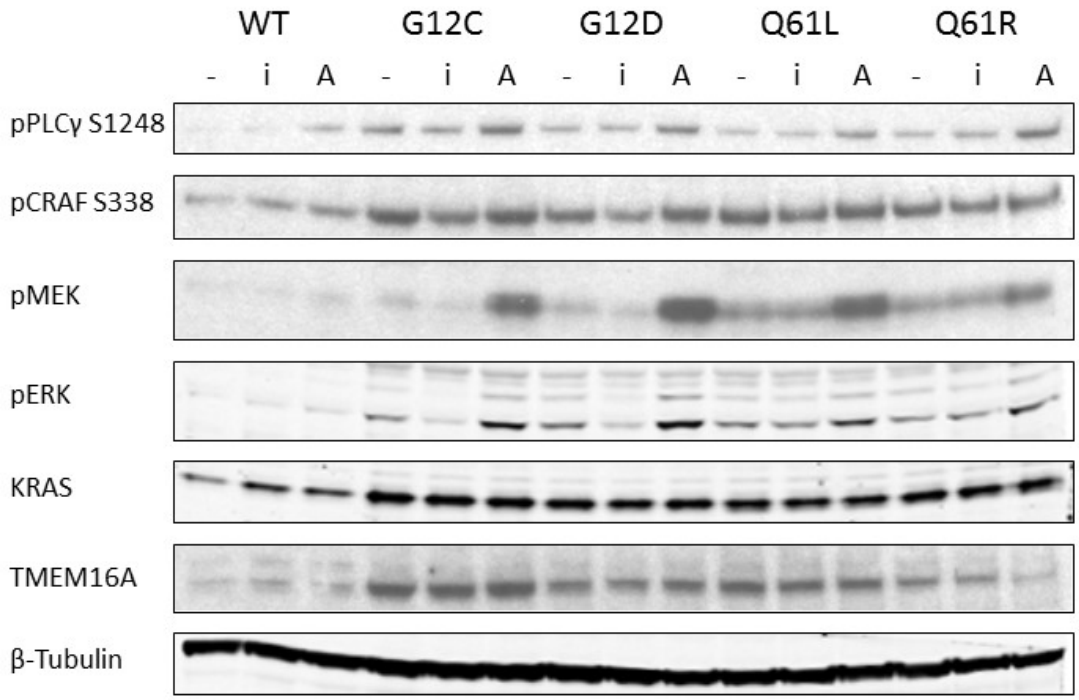

Figure 5.7. KRAS mutants display different levels of dependence on PLC signaling for MAPK output

Western blot analysis of PLC-MAPK signaling in KRAS [WT/G12C/G12D/Q61L/Q61R] MEF lines after 4 h of complete serum starvation before a 10 min treatment with DMSO, 2 μM U73122 PLC inhibitor or 25 μM m3M3FBS PLC activator. β-Tubulin expression served as a loading control.

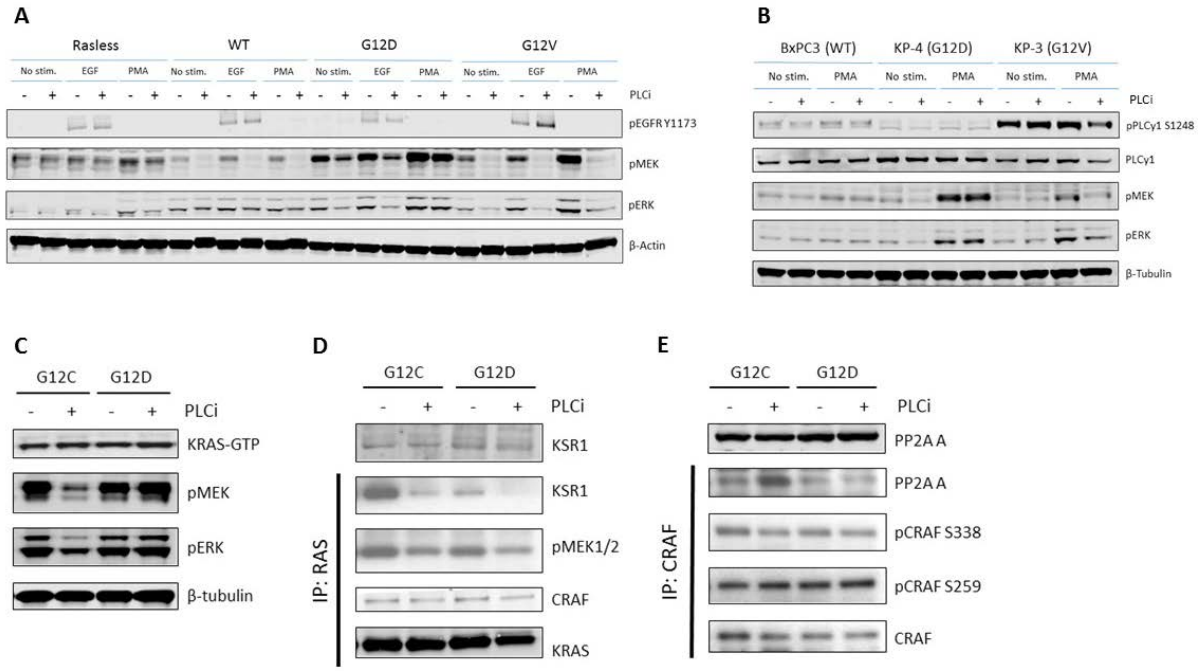

Figure 5.8. KRAS mutants display different levels of dependence on PLC activity for MAPK output downstream of PKC signaling

(A) Western blot analysis of MAPK signaling in Rasless, KRAS wild type, G12D and G12V MEF lines after 4 h of complete serum starvation and 15 min pretreatment with either DMSO or 5 μM U73122 PLC inhibitor, followed by 15 min without stimulation or treated with 50 ng/mL EGF or 200 ng/mL PMA. β-Actin expression served as a loading control.

(B) Western blot analysis of PLC-MAPK signaling in KRAS wild type-, G12D- and G12V-driven PDAC lines after 4 h complete serum starvation and 10 min pretreatment with either PLC inhibitor (U73122) or a non-targeting analog (U73343) at 5 μM, ending with or without 10 min PMA stimulation at 200 ng/mL. β-Tubulin expression served as a loading control.

(C) Western blot analysis of MAPK signaling after 4 h serum starve, 5 min pretreatment with either non-targeting U73343 or PLC inhibitor U73122 and 15 min stimulation with 200 ng/mL PMA, comparing KRAS G12C and G12D MEFs.

(D) Immunoprecipitation and western blot analysis of levels of KRAS interaction with KSR1, active MEK and CRAF in response to the treatment described in (C). KRAS protein detection after immunoprecipitation served as a control for pulldown efficiency.

(E) Immunoprecipitation and western blot analysis of CRAF interaction with PP2A A and phosphoregulation at CRAF S338 and S259 in response to the treatment described in (C). Total CRAF protein detection after immunoprecipitation served as a control for pulldown efficiency.

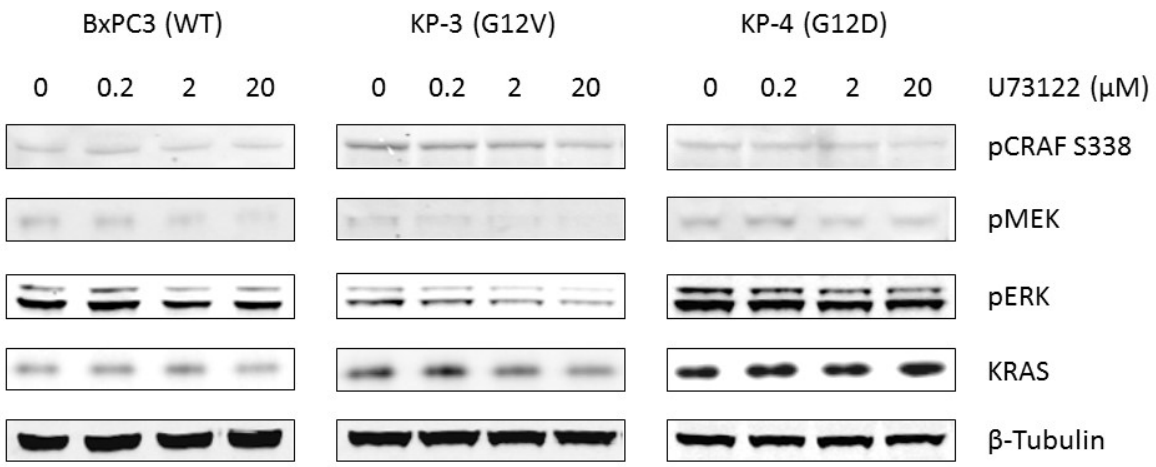

Figure 5.9. Human PDAC cell lines display KRAS mutation status-dependent differences in MAPK sensitivity to PLC inhibition

Western blot analysis of pCRAF S338, pMEK and pERK sensitivity to increasing doses of U73122 (0, 0.2, 2 or 20 μM) for 20 min, comparing BxPC3 (KRAS wild type), KP-3 (KRAS G12V) and KP-4 (KRAS G12D) cells in complete media. KRAS expression levels are also displayed. β-Tubulin expression served as a loading control.

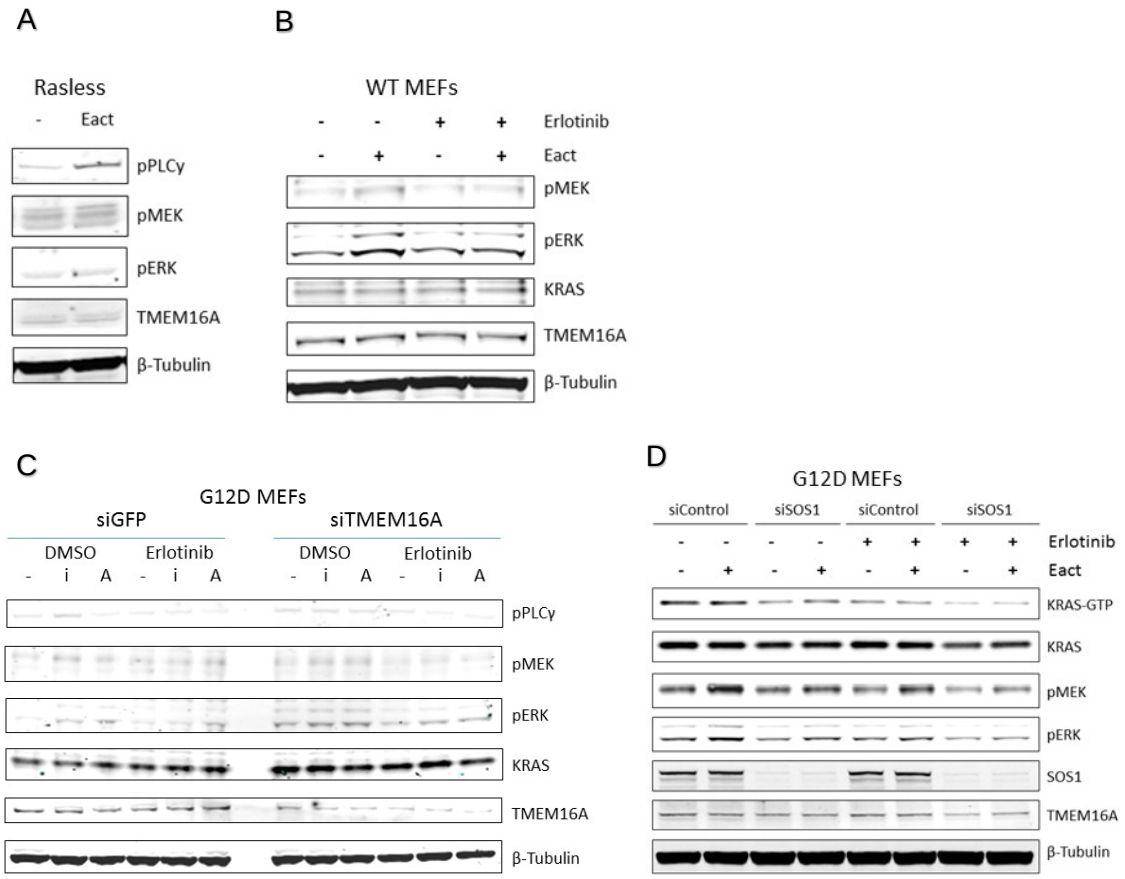

Figure 5.10. Calcium-responsive TMEM16A activity connects the PLC response to EGFR-induced KRAS dependent MAPK signaling

(A) Western blot analysis of pPLCγ, pMEK, pERK and TMEM16A expression in Rasless MEFs treated for 10 min with 10 μM Eact TMEM16A activator after 4 h of complete serum starvation. β-Tubulin expression served as a loading control.

(B) Western blot analysis of pMEK, pERK, KRAS and TMEM16A expression in wild type KRAS MEFs treated for 10 min with 10 μM Eact TMEM16A activator after 4 h of complete serum starvation, with or without 2 μM erlotinib pretreatment during the final hour of the starve. β-Tubulin expression served as a loading control.

(C) Western blot analysis of pPLCγ, pMEK, pERK, KRAS and TMEM16A expression after TMEM16A knockdown by transfection for 48 h with non-targeting GFP siRNA or TMEM16A siRNA and 4 h of complete serum starvation, with or without 2 μM erlotinib pretreatment during the final hour, followed by a 15 min treatment with 10 μM Eact (A), 10 μM T16inh-A01 (i) or DMSO. β-Tubulin expression served as a loading control.

(D) Western blot analysis of KRAS activity, MAPK signaling and SOS knockdown after a 48 h treatment with either non-targeting or SOS1-specific siRNA, followed by a 4 h serum starvation with DMSO or 2 μM erlotinib added for the final hour before a 10 min treatment with 10 μM Eact TMEM16A activator. β-Tubulin expression served as a loading control.

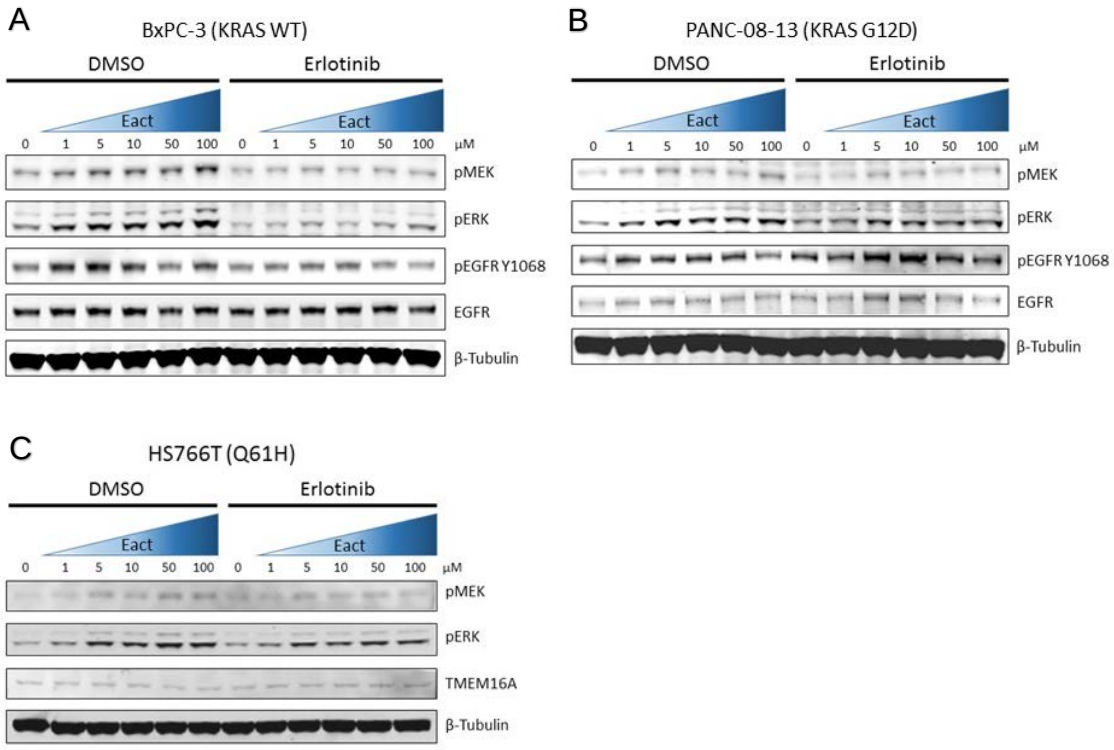

Figure 5.11. Human cancer cell lines display a KRAS genotype-specific EGFR dependence in MAPK activation with increasing doses of TMEM16A activator

(A) Western blot analysis of the BxPC-3 PDAC MAPK response to increasing doses of Eact (0, 1, 5, 10, 50 or 100 µM) for 10 min after 4 h of complete serum starvation, with or without 2 µM erlotinib pretreatment during the final hour of the starve. β-Tubulin expression served as a loading control.

(B) Western blot analysis of the PANC-08-13 PDAC MAPK response to increasing doses of Eact (0, 1, 5, 10, 50 or 100 µM) for 10 min after 4 h of complete serum starvation, with or without 2 µM erlotinib pretreatment during the final hour of the starve. β-Tubulin expression served as a loading control.

(C) Western blot analysis of pMEK, pERK and TMEM16A levels in HS766T (KRAS Q61H) PDAC cells treated with increasing doses of Eact (0, 1, 5, 10, 50 or 100 µM) for 10 min after 4 h of complete serum starvation, with or without 2 µM erlotinib pretreatment during the final hour of the starve. β-Tubulin expression served as a loading control.

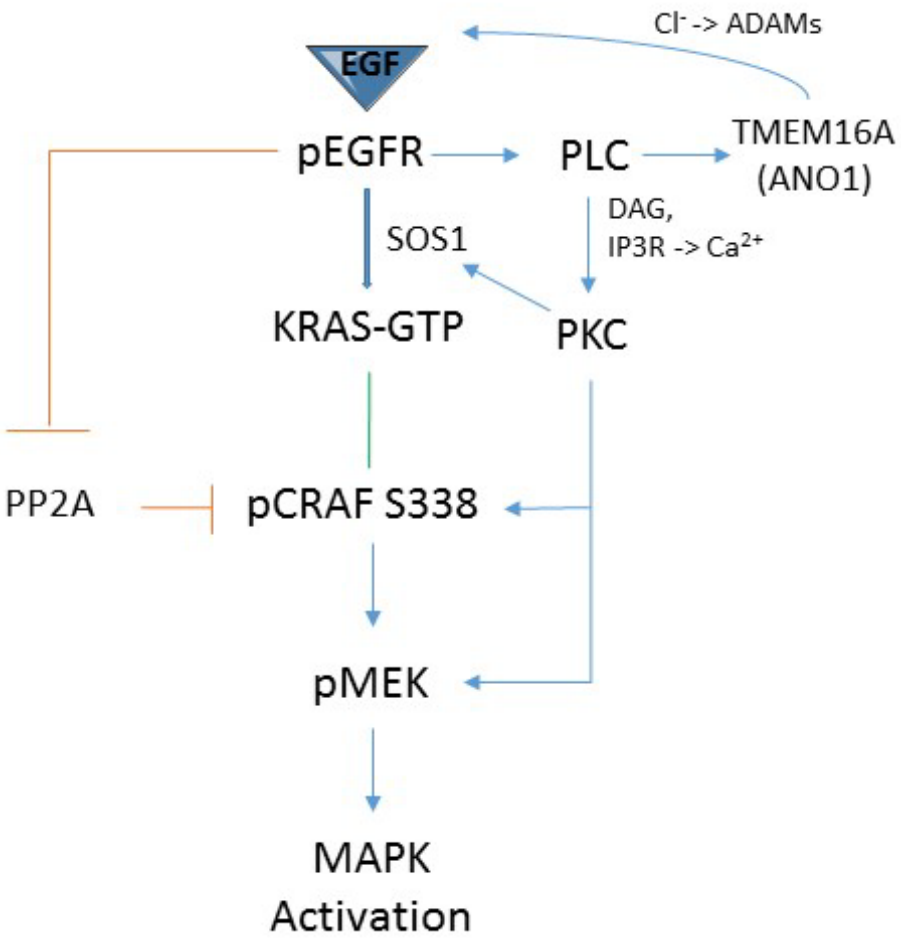

Figure 5.12. Positive feeback mechanism for oncogenic signaling

Schematic mechanism for the role of the EGFR-PLC-Ca^{2+}-TMEM16A signaling axis in KRAS-dependent MAPK signaling.

BIBLIOGRAPHY

1. Cully, M. and J. Downward, *SnapShot: Ras Signaling.* Cell, 2008. **133**(7): p. 1292-1292 e1.
2. Downward, J., *KSR: a novel player in the RAS pathway.* Cell, 1995. **83**(6): p. 831-4.
3. Ory, S., et al., *Protein phosphatase 2A positively regulates Ras signaling by dephosphorylating KSR1 and Raf-1 on critical 14-3-3 binding sites.* Curr Biol, 2003. **13**(16): p. 1356-64.
4. Raabe, T. and U.R. Rapp, *Ras signaling: PP2A puts Ksr and Raf in the right place.* Curr Biol, 2003. **13**(16): p. R635-7.
5. Therrien, M., et al., *KSR, a novel protein kinase required for RAS signal transduction.* Cell, 1995. **83**(6): p. 879-88.
6. Fernandez-Medarde, A. and E. Santos, *Ras in cancer and developmental diseases.* Genes Cancer, 2011. **2**(3): p. 344-58.
7. Stephen, A.G., et al., *Dragging ras back in the ring.* Cancer Cell, 2014. **25**(3): p. 272-81.
8. Ahmadian, M.R., et al., *Individual rate constants for the interaction of Ras proteins with GTPase-activating proteins determined by fluorescence spectroscopy.* Biochemistry, 1997. **36**(15): p. 4535-41.
9. Ahmadian, M.R., et al., *Structural fingerprints of the Ras-GTPase activating proteins neurofibromin and p120GAP.* Journal of molecular biology, 2003. **329**(4): p. 699-710.
10. Baker, R., et al., *Site-specific monoubiquitination activates Ras by impeding GTPase-activating protein function.* Nature structural & molecular biology, 2013. **20**(1): p. 46-52.
11. Berthiaume, L.G., *Insider information: how palmitoylation of Ras makes it a signaling double agent.* Science's STKE : signal transduction knowledge environment, 2002. **2002**(152): p. pe41.
12. Bivona, T.G. and M.R. Philips, *Ras pathway signaling on endomembranes.* Current opinion in cell biology, 2003. **15**(2): p. 136-42.
13. Caloca, M.J., J.L. Zugaza, and X.R. Bustelo, *Exchange factors of the RasGRP family mediate Ras activation in the Golgi.* The Journal of biological chemistry, 2003. **278**(35): p. 33465-73.
14. Clyde-Smith, J., et al., *Characterization of RasGRP2, a plasma membrane-targeted, dual specificity Ras/Rap exchange factor.* The Journal of biological chemistry, 2000. **275**(41): p. 32260-7.
15. Downward, J., *Targeting RAS signalling pathways in cancer therapy.* Nature reviews. Cancer, 2003. **3**(1): p. 11-22.
16. Fehrenbacher, N., D. Bar-Sagi, and M. Philips, *Ras/MAPK signaling from endomembranes.* Molecular oncology, 2009. **3**(4): p. 297-307.
17. Forbes, S.A., et al., *The Catalogue of Somatic Mutations in Cancer (COSMIC).* Current protocols in human genetics / editorial board, Jonathan L. Haines ... [et al.], 2008. **Chapter 10**: p. Unit 10 11.
18. Forbes, S.A., et al., *COSMIC: mining complete cancer genomes in the Catalogue of Somatic Mutations in Cancer.* Nucleic acids research, 2011. **39**(Database issue): p. D945-50.
19. Jaumot, M., et al., *The linker domain of the Ha-Ras hypervariable region regulates interactions with exchange factors, Raf-1 and phosphoinositide 3-kinase.* The Journal of biological chemistry, 2002. **277**(1): p. 272-8.
20. Jura, N., et al., *Differential modification of Ras proteins by ubiquitination.* Molecular cell, 2006. **21**(5): p. 679-87.
21. Karnoub, A.E. and R.A. Weinberg, *Ras oncogenes: split personalities.* Nature reviews. Molecular cell biology, 2008. **9**(7): p. 517-31.
22. Leon, J., I. Guerrero, and A. Pellicer, *Differential expression of the ras gene family in mice.* Molecular and cellular biology, 1987. **7**(4): p. 1535-40.
23. Matallanas, D., et al., *Differences on the inhibitory specificities of H-Ras, K-Ras, and N-Ras (N17) dominant negative mutants are related to their membrane microlocalization.* The Journal of biological chemistry, 2003. **278**(7): p. 4572-81.

24. Mitin, N., K.L. Rossman, and C.J. Der, *Signaling interplay in Ras superfamily function.* Current biology : CB, 2005. **15**(14): p. R563-74.
25. Mor, A. and M.R. Philips, *Compartmentalized Ras/MAPK signaling.* Annual review of immunology, 2006. **24**: p. 771-800.
26. Omerovic, J., A.J. Laude, and I.A. Prior, *Ras proteins: paradigms for compartmentalised and isoform-specific signalling.* Cellular and molecular life sciences : CMLS, 2007. **64**(19-20): p. 2575-89.
27. Sasaki, A.T., et al., *Ubiquitination of K-Ras enhances activation and facilitates binding to select downstream effectors.* Science signaling, 2011. **4**(163): p. ra13.
28. Scheffzek, K., et al., *The Ras-RasGAP complex: structural basis for GTPase activation and its loss in oncogenic Ras mutants.* Science, 1997. **277**(5324): p. 333-8.
29. Wolfman, A., *Ras isoform-specific signaling: location, location, location.* Science's STKE : signal transduction knowledge environment, 2001. **2001**(96): p. pe2.
30. Yang, M.H., et al., *Regulation of RAS oncogenicity by acetylation.* Proceedings of the National Academy of Sciences of the United States of America, 2012. **109**(27): p. 10843-8.
31. Sun, Q., et al., *Discovery of small molecules that bind to K-Ras and inhibit Sos-mediated activation.* Angew Chem Int Ed Engl, 2012. **51**(25): p. 6140-3.
32. Prior, I.A. and J.F. Hancock, *Ras trafficking, localization and compartmentalized signalling.* Semin Cell Dev Biol, 2012. **23**(2): p. 145-53.
33. Gysin, S., et al., *Therapeutic strategies for targeting ras proteins.* Genes Cancer, 2011. **2**(3): p. 359-72.
34. Willumsen, B.M., et al., *The p21 ras C-terminus is required for transformation and membrane association.* Nature, 1984. **310**(5978): p. 583-6.
35. Rocks, O., et al., *An acylation cycle regulates localization and activity of palmitoylated Ras isoforms.* Science, 2005. **307**(5716): p. 1746-52.
36. Roy, S., et al., *Individual palmitoyl residues serve distinct roles in H-ras trafficking, microlocalization, and signaling.* Mol Cell Biol, 2005. **25**(15): p. 6722-33.
37. Bivona, T.G., et al., *PKC regulates a farnesyl-electrostatic switch on K-Ras that promotes its association with Bcl-XL on mitochondria and induces apoptosis.* Mol Cell, 2006. **21**(4): p. 481-93.
38. Inder, K., et al., *Activation of the MAPK module from different spatial locations generates distinct system outputs.* Mol Biol Cell, 2008. **19**(11): p. 4776-84.
39. Chiu, V.K., et al., *Ras signalling on the endoplasmic reticulum and the Golgi.* Nat Cell Biol, 2002. **4**(5): p. 343-50.
40. Bremner, R. and A. Balmain, *Genetic changes in skin tumor progression: correlation between presence of a mutant ras gene and loss of heterozygosity on mouse chromosome 7.* Cell, 1990. **61**(3): p. 407-17.
41. Zhang, Z., et al., *Wildtype Kras2 can inhibit lung carcinogenesis in mice.* Nat Genet, 2001. **29**(1): p. 25-33.
42. To, M.D., et al., *Interactions between wild-type and mutant Ras genes in lung and skin carcinogenesis.* Oncogene, 2013. **32**(34): p. 4028-33.
43. Pylayeva-Gupta, Y., E. Grabocka, and D. Bar-Sagi, *RAS oncogenes: weaving a tumorigenic web.* Nat Rev Cancer, 2011. **11**(11): p. 761-74.
44. Ihle, N.T., et al., *Effect of KRAS oncogene substitutions on protein behavior: implications for signaling and clinical outcome.* J Natl Cancer Inst, 2012. **104**(3): p. 228-39.
45. Burd, C.E., et al., *Mutation-Specific RAS Oncogenicity Explains N-RAS Codon 61 Selection in Melanoma.* Cancer Discov, 2014.
46. Krengel, U., et al., *Three-dimensional structures of H-ras p21 mutants: molecular basis for their inability to function as signal switch molecules.* Cell, 1990. **62**(3): p. 539-48.

47. Hynes, N.E. and H.A. Lane, *ERBB receptors and cancer: the complexity of targeted inhibitors.* Nat Rev Cancer, 2005. **5**(5): p. 341-54.
48. Tebbutt, N., M.W. Pedersen, and T.G. Johns, *Targeting the ERBB family in cancer: couples therapy.* Nat Rev Cancer, 2013. **13**(9): p. 663-73.
49. Ebi, H., et al., *Receptor tyrosine kinases exert dominant control over PI3K signaling in human KRAS mutant colorectal cancers.* J Clin Invest, 2011. **121**(11): p. 4311-21.
50. Yarden, Y. and M.X. Sliwkowski, *Untangling the ErbB signalling network.* Nat Rev Mol Cell Biol, 2001. **2**(2): p. 127-37.
51. Aronheim, A., et al., *Membrane targeting of the nucleotide exchange factor Sos is sufficient for activating the Ras signaling pathway.* Cell, 1994. **78**(6): p. 949-61.
52. Dougherty, M.K., et al., *Regulation of Raf-1 by direct feedback phosphorylation.* Mol Cell, 2005. **17**(2): p. 215-24.
53. Schubbert, S., K. Shannon, and G. Bollag, *Hyperactive Ras in developmental disorders and cancer.* Nat Rev Cancer, 2007. **7**(4): p. 295-308.
54. Ferro, E. and L. Trabalzini, *RalGDS family members couple Ras to Ral signalling and that's not all.* Cell Signal, 2010. **22**(12): p. 1804-10.
55. Drosten, M., et al., *Loss of p53 induces cell proliferation via Ras-independent activation of the Raf/Mek/Erk signaling pathway.* Proc Natl Acad Sci U S A, 2014. **111**(42): p. 15155-60.
56. Drosten, M., et al., *Genetic analysis of Ras signalling pathways in cell proliferation, migration and survival.* EMBO J, 2010. **29**(6): p. 1091-104.
57. Bergo, M.O., et al., *Absence of the CAAX endoprotease Rce1: effects on cell growth and transformation.* Mol Cell Biol, 2002. **22**(1): p. 171-81.
58. Fiordalisi, J.J., et al., *High affinity for farnesyltransferase and alternative prenylation contribute individually to K-Ras4B resistance to farnesyltransferase inhibitors.* J Biol Chem, 2003. **278**(43): p. 41718-27.
59. Serafimova, I.M., et al., *Reversible targeting of noncatalytic cysteines with chemically tuned electrophiles.* Nat Chem Biol, 2012. **8**(5): p. 471-6.
60. Dursina, B., et al., *Identification and specificity profiling of protein prenyltransferase inhibitors using new fluorescent phosphoisoprenoids.* J Am Chem Soc, 2006. **128**(9): p. 2822-35.
61. Urosevic, J., et al., *Using cells devoid of RAS proteins as tools for drug discovery.* Mol Carcinog, 2009. **48**(11): p. 1038-47.
62. Cox, A.D., C.J. Der, and M.R. Philips, *Targeting RAS Membrane Association: Back to the Future for Anti-RAS Drug Discovery?* Clin Cancer Res, 2015. **21**(8): p. 1819-27.
63. Ostrem, J.M., et al., *K-Ras(G12C) inhibitors allosterically control GTP affinity and effector interactions.* Nature, 2013. **503**(7477): p. 548-51.
64. Tian, T., et al., *Plasma membrane nanoswitches generate high-fidelity Ras signal transduction.* Nat Cell Biol, 2007. **9**(8): p. 905-14.
65. Nilsson, J.A. and J.L. Cleveland, *Myc pathways provoking cell suicide and cancer.* Oncogene, 2003. **22**(56): p. 9007-21.
66. Staffas, A., et al., *Wild-type KRAS inhibits oncogenic KRAS-induced T-ALL in mice.* Leukemia, 2015. **29**(5): p. 1032-40.
67. Azrak, S.S., et al., *Reversible, interrelated mRNA and miRNA expression patterns in the transcriptome of Rasless fibroblasts: functional and mechanistic implications.* BMC Genomics, 2013. **14**: p. 731.
68. Rojas, M., S. Yao, and Y.Z. Lin, *Controlling epidermal growth factor (EGF)-stimulated Ras activation in intact cells by a cell-permeable peptide mimicking phosphorylated EGF receptor.* J Biol Chem, 1996. **271**(44): p. 27456-61.

69. Roose, J.P., et al., *Unusual interplay of two types of Ras activators, RasGRP and SOS, establishes sensitive and robust Ras activation in lymphocytes.* Mol Cell Biol, 2007. **27**(7): p. 2732-45.
70. Bivona, T.G., et al., *Phospholipase Cgamma activates Ras on the Golgi apparatus by means of RasGRP1.* Nature, 2003. **424**(6949): p. 694-8.
71. Kupzig, S., S.A. Walker, and P.J. Cullen, *The frequencies of calcium oscillations are optimized for efficient calcium-mediated activation of Ras and the ERK/MAPK cascade.* Proc Natl Acad Sci U S A, 2005. **102**(21): p. 7577-82.
72. Yoshiki, S., et al., *Ras and calcium signaling pathways converge at Raf1 via the Shoc2 scaffold protein.* Mol Biol Cell, 2010. **21**(6): p. 1088-96.
73. Marais, R., et al., *Requirement of Ras-GTP-Raf complexes for activation of Raf-1 by protein kinase C.* Science, 1998. **280**(5360): p. 109-12.
74. Naetar, N., et al., *PP2A-Mediated Regulation of Ras Signaling in G2 Is Essential for Stable Quiescence and Normal G1 Length.* Mol Cell, 2014. **54**(6): p. 932-45.
75. Rubio, I., et al., *Ras activation in response to phorbol ester proceeds independently of the EGFR via an unconventional nucleotide-exchange factor system in COS-7 cells.* Biochem J, 2006. **398**(2): p. 243-56.
76. Kawakami, Y., et al., *A Ras activation pathway dependent on Syk phosphorylation of protein kinase C.* Proc Natl Acad Sci U S A, 2003. **100**(16): p. 9470-5.
77. Cullis, J., et al., *The RhoGEF GEF-H1 is required for oncogenic RAS signaling via KSR-1.* Cancer Cell, 2014. **25**(2): p. 181-95.
78. Dougherty, M.K., et al., *KSR2 is a calcineurin substrate that promotes ERK cascade activation in response to calcium signals.* Mol Cell, 2009. **34**(6): p. 652-62.
79. Fernandez, M.R., M.D. Henry, and R.E. Lewis, *Kinase suppressor of Ras 2 (KSR2) regulates tumor cell transformation via AMPK.* Mol Cell Biol, 2012. **32**(18): p. 3718-31.
80. Clandinin, T.R., J.A. DeModena, and P.W. Sternberg, *Inositol trisphosphate mediates a RAS-independent response to LET-23 receptor tyrosine kinase activation in C. elegans.* Cell, 1998. **92**(4): p. 523-33.
81. Britschgi, A., et al., *Calcium-activated chloride channel ANO1 promotes breast cancer progression by activating EGFR and CAMK signaling.* Proc Natl Acad Sci U S A, 2013. **110**(11): p. E1026-34.
82. Shiwarski, D.J., et al., *To "Grow" or "Go": TMEM16A Expression as a Switch between Tumor Growth and Metastasis in SCCHN.* Clin Cancer Res, 2014.
83. Sauter, D.R., et al., *ANO1 (TMEM16A) in pancreatic ductal adenocarcinoma (PDAC).* Pflugers Arch, 2014.
84. Moore, M.J., et al., *Erlotinib plus gemcitabine compared with gemcitabine alone in patients with advanced pancreatic cancer: a phase III trial of the National Cancer Institute of Canada Clinical Trials Group.* J Clin Oncol, 2007. **25**(15): p. 1960-6.
85. Burns, M.C., et al., *Approach for targeting Ras with small molecules that activate SOS-mediated nucleotide exchange.* Proc Natl Acad Sci U S A, 2014. **111**(9): p. 3401-6.
86. Maurer, T., et al., *Small-molecule ligands bind to a distinct pocket in Ras and inhibit SOS-mediated nucleotide exchange activity.* Proc Natl Acad Sci U S A, 2012. **109**(14): p. 5299-304.

Publishing Agreement

It is the policy of the University to encourage the distribution of all theses, dissertations, and manuscripts. Copies of all UCSF theses, dissertations, and manuscripts will be routed to the library via the Graduate Division. The library will make all theses, dissertations, and manuscripts accessible to the public and will preserve these to the best of their abilities, in perpetuity.

Please sign the following statement:

I hereby grant permission to the Graduate Division of the University of California, San Francisco to release copies of my thesis, dissertation, or manuscript to the Campus Library to provide access and preservation, in whole or in part, in perpetuity.

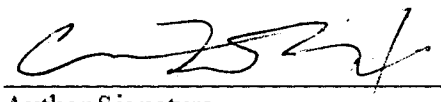

Author Signature

Print Form

8/15/15

Date